Annex 2a

Climate Rationale

to the GCF Funding Proposal

"Building the resilience of Togo's national health system and vulnerable communities to climate-sensitive health outcomes"

19 December 2025

Version 1.0

Submitted by:
Deutsche Gesellschaft für internationale Zusammenarbeit (GIZ) GmbH

Acknowledgements

The LSHTM team would like to thank many colleagues in the Planetary Health Group at the MRC Unit The Gambia at the London School of Hygiene and Tropical Medicine (MRCG @ LSHTM), the Data Science Platform and the Statistics team at MRCG, the Centre on Climate Change and Planetary Health at LSHTM, the Environment and Health Modelling Lab at LSHTM, and the Malaria Atlas Project at the Kids Research Institute Australia / Curtin University for fruitful discussions about this work.

Ethics

Ethical approval for this analysis was reviewed and obtained from the London School of Hygiene & Tropical Medicine - Project ID/Ethics Reference Number: 32854

Table of Contents

List of Figures

List of Tables

Abbreviations

AC	Air Conditioning
AIC	Akaike information criterion
ANC	Antenatal care
AR6	Sixth Assessment Report
BLUPS	Best linear unbiased predictions
CHDH	Compound Hot and Dry Days
CHW	Community Health Worker
CI	Confidence Interval
CHIRPS -	Climate Hazards Group InfraRed Precipitation with Station
CHW	Community Health Worker
CIMP6	Coupled Model Intercomparison Project Phase 6
CVD	Cardiovascular Disease
DALY	Disability Adjusted Life Years
DHIS2	District Health Information System 2
DHS	Demographic Health Survey
DLNM	Distributed Lag Non-linear Model
DTR	Diurnal Temperature Range
ECMWF	European Centre for Medium-Range Weather Forecasts
EHE	Extreme Heat Event
EIR	Entomological Inoculation Rate
ERA5-Land	ECMWF Reanalysis 5th generation - Land
ESA	European Space Agency
GADM	Global Administrative Areas Database
GAM	Generalized additive model
GBD	Global Burden of Disease
GCF	Green Climate Fund
GCM	General Circulation Model
GHG	Green House Gas
GIZ	*Deutsche Gesellschaft für Internationale Zusammenarbeit (GIZ) GmbH*
HMIS	Health Management Information System
HIV	Human Immunodeficiency Virus
HSI	Habitat Suitability Index
HW	Heat Wave
IHME	Institute for Health Metrics and Evaluation
INSEED	*Institut National de la Statistique et des Études Économiques*
IPCC	Intergovernmental Panel on Climate Change
IPT	Intermittent preventive treatment
IRR	Incident Rate Ratio
ISIMIP	Inter-Sectoral Impact Model Intercomparison Project
LLINs	Long Lasting Insecticidal Nets
LMIC	Lower and Middle Income Country
LCMI	Lancet Countdown Malaria Indicator
LTS	Length of Transmission Season
LSHTM	London School of Hygiene and Tropical Medicine
MAP	Malaria Atlas Project
MCDA	Multi Criteria Decision Analysis
MICS	Multiple Indicator Cluster Survey
MIS	Malaria Indicator Survey
MODIS	Moderate Resolution Imaging Spectroradiometer
MSWEP	Multi-Source Weighted-Ensemble Precipitation
MSWX	Multi Source Weather Data
NASA NEX	NASA Earth eXchange (NEX)
NDVI	Normalized Difference Vegetation Index
OR	Odds Ratio
PACF	Partial Autocorrelation Fraction
PAR	Population at Risk
PND	National Development Plan

PNLP	*Programme National de Lutte contre le Paludisme* - National Malaria Control Program
PTB	Preterm Birth
RCP	Representative Concentration Pathway
RGPH-5	*Recensement général de la Population et de l'Habitat - 5*
RH	Relative Humidity
RMSE	Root Mean Square Error
SSA	Sub-Saharan Africa
SSPs	Shared Socioeconomic Pathways
TFR	Total Fertility Rate
VECTRI	Vector-transmission Model
WASH	Water, Sanitation and Hygiene
WCDE	Wittgenstein Centre Data Explorer
WHO	World Health Organisation
WPP	World population prospects
WRA	Women of Reproductive Age
UN	United Nations

1. Executive Summary

Togo is experiencing a warmer climate with more frequent very hot days and heatwaves, alongside heavier rainfall extremes in some regions due to anthropogenic climate change. Current climate change models that forecast future climate conditions indicate these trends will intensify across the country throughout this century (Pörtner & Löschke, 2022).

Following the Intergovernmental Panel on Climate Change (IPCC) AR6 lens of Hazard–Exposure–Vulnerability (H–E–V), climate hazards translate into health risk, influenced by exposure and vulnerability factors (Pörtner & Löschke, 2022). These impacts are not evenly distributed: children under five, pregnant women, older adults, low-income and informal-settlement households, and communities far from functioning health facilities often are more vulnerable. Limited electricity and cooling, weak Water, Sanitation and Hygiene (WASH) services, and long travel times to care can also amplify harms.

The aim of this report is to provide recent, actionable evidence – a Climate Rationale - to help strengthen climate-resilient health programming in Togo by producing subnational H/E/V and composite risk maps, alongside modelled health impacts (burdens/incidence) for priority health outcomes and regions.

The climate rationale, aligned with IPCC AR6 and Green Climate Fund (GCF) guidance, aims to explain why climate change justifies targeted health investments now. By tracing a clear line from evolving climate hazards to population exposure and population and system vulnerabilities, it can be used to help support financing and adaptation / intervention choices that protect high-risk groups, make infrastructure and services more reliable, and yield measurable health gains.

Methods used throughout the report are a combination of evidence synthesis, risk mapping and epidemiological modelling.

Disease case studies are first selected on the basis of key risks emerging from a structured literature review and prioritisation process, incorporating burden of disease and noted regional climate-health associations. Three health outcomes were selected for a subsequent two-stage climate change risk assessment, comprising risk mapping (Stage 1) and epidemiological model development (Stage 2). The three focal health outcomes are:

- malaria,
- diarrhoeal diseases,
- heat-related impacts on maternal/child health (preterm birth).

The three northern regions of Togo – Centrale, Kara, Savanes – were selected as priority regions from the Stage 1 assessment. These regions exhibit the highest climate change and health related risks arising due to the combination of the climatic hazards and changes present in these regions, as well as growing exposure and high levels of vulnerability.

For projecting future climate change risks, climate hazard Information was derived from bias-adjusted CMIP6 daily time series data, with both general (national) and health outcome specific hazards highlighted. To highlight future trends, projections are summarised into a number of relevant time slices that, where appropriate, are compared to a reference baseline period (when discussion long term changes) or to the recent period (to express changes that may occur in the near-term and longer-term relative to present/recent conditions):

- 1981 – 2000: reference baseline,
- 2001 – 2020: recent,
- 2021 – 2040: near-term,
- 2041 – 2060: mid-century.

To contrast potential socio-economic and climate trajectories and assess their influence on projected health impacts, we employ AR6's Shared Socioeconomic Pathways (SSP) framework (Pörtner & Löschke, 2022). For modelling we generate and present results according to two SSPs:

- SSP2-4.5 (middle of the road) and
- SSP5-8.5 (fossil-fuelled development).

We do not explicitly include reference to or compare results to a counterfactual (or no anthropogenic climate change) scenario, an approach increasingly used for attribution studies, as this was considered outside the scope of this study. As such, the reference baseline used here is a temporal baseline, not a no-climate change baseline.

Exposure information is based on age- and sex-stratified human population information from the 2022 national census (RGPH-5) combined with WorldPop projections (INSEED, 2022) (Worldpop, 2020).

Information on vulnerability factors comes from a wide range of datasets on demographic, socio-economic, health system access, infrastructure and housing, and treatment intervention coverage, among others.

A Stage 1 Risk Assessment compiles spatial information on hazards, exposure groups and vulnerability factors that emerge from the literature review. These are combined into indices and overlaid into a composite index to provide an indication of the spatial heterogeneity of climate change risk in Togo for the three health outcomes, highlighting priority regions and population groups for adaptation.

A Stage 2 Risk Assessment develops epidemiological models from health outcome data within Togo itself for each of the three health outcomes. The aim of these more specific analyses is to characterise climate–health associations and project how disease risk may change due to climate change in future. Outputs are expressed as change in incidence, relative risk or attributable fractions, with notes around key uncertainties. It is important to note that this is not a burden quantification study, and we do not analyse mortality (deaths) or morbidity (e.g. DALYs) explicitly.

Currently, there are no recent Togo specific projections available for malaria, diarrhoeal disease or heat-related preterm birth. Results from the current study must therefore be considered a starting point, requiring future development and refinement as improved information is compiled in parallel to existing health and climate change interventions and adaptation.

Our results do however provide some indications of future trends and adaptation requirements. In the case of malaria, climate suitability for transmission appears to have slightly increased in cooler, higher-elevation areas in Plateaux and Centrale in recent decades, while declining elsewhere. Projections suggest this pattern will continue, with gradual long-term declines in incidence in already warm lowland and northern regions, but potential increases in higher-elevation zones across the centre of the country as they warm towards more suitable thermal conditions. For diarrhoeal disease, the models indicate an overall long-term decline in climate-driven risk associated with warmer conditions and shifts in rainfall patterns, although wetter months remain a key driver of transmission. In both cases, however, projections are uncertain, confidence intervals are relatively wide, and there are clear indications of changing seasonality. This implies that climate-driven increases in risk will still occur locally and during particular periods of the year, even if national-scale trends point to modest net declines.

For heat-related preterm births, the signal is more unequivocal: increases in extreme heat will almost certainly increase the fraction of preterm births attributable to climate change in the coming decades. This will place additional pressure on maternal and neonatal health services, particularly in hotter and more vulnerable regions where cooling, antenatal care and obstetric services are already constrained.

Adaptation interventions are therefore required to offset these risks and to prevent climate change from eroding progress in child and maternal health. Extreme events are likely not only to contribute directly to ill health and disease outbreaks, but also to disrupt prevention and treatment services. Enhancing access to care, strengthening routine surveillance and early warning, and undertaking targeted WASH upgrades and preparedness in high-risk settings will be central to climate risk reduction. Electrification and reliable cooling for vulnerable households and health facilities, together with heat–health plans in antenatal and child health services, should become adaptation priorities for heat-related conditions.

Overall, this Climate Rationale provides an initial, Togo-specific, evidence base linking evolving climate hazards to exposure and vulnerability for three priority health outcomes. It delivers subnational hazard, exposure and vulnerability maps, composite risk indices and the first national projections of climate-sensitive health risks for malaria, diarrhoeal disease and heat-related preterm birth. These results should be interpreted as conservative estimates of the climate signal under “all else equal” assumptions,

not as full forecasts of future burden. Nonetheless, they offer a practical foundation for climate-resilient health planning: helping to identify priority regions and populations, refine the timing and targeting of interventions, and guide investments by government and partners, including the Green Climate Fund. With continued data strengthening and iterative refinement, this evidence can support a transition from reactive crisis response towards proactive, climate-smart health systems that protect the most vulnerable in Togo as the climate continues to change.

2. Introduction

Projected climate change impacts are expected to intensify globally over coming decades, with perturbations of sufficient magnitude to undermine both livelihoods and human habitability (Alize le Roux, 2025). The increasing frequency and severity of extreme climatic events such as heatwaves, floods, and droughts are anticipated to contribute directly and indirectly to elevated mortality, reduced quality of life, diminished labour productivity, and decreased agricultural yields, with potentially persistent macroeconomic consequences (Romanello et al., 2024). Moreover, climate change is likely to modify the spatiotemporal distribution of key vector-borne and water-borne pathogens. These impacts will be disproportionately concentrated in Lower/Middle Income Countries (LMICs), including in Sub-Saharan Africa (SSA), despite their minimal contribution to global greenhouse gas emissions (Alize le Roux, 2025). The region's adaptive capacity is constrained by a limited evidence base on the health impacts of climate change, thereby hindering the formulation and implementation of effective climate adaptation and mitigation strategies.

Some work has already examined the potential effects on health of climate change in Togo and examining which areas may be most vulnerable to climate related disease in the future. In 2019, an assessment of climate change-related risks and vulnerabilities in the health sector in Togo was published (Schmuck, 2019). This risk assessment included three climate vulnerable diseases - malaria, meningitis, and respiratory infections. For these three conditions, impact chains were generated to visualise their relationship to key climate hazards. The assessment then quantified current and future risk by identifying and measuring indicators for both hazard and vulnerability factors using indicator-based methods and earlier-generation (CMIP5) climate data. Other relevant efforts include sectoral climate profiles, health surveillance analyses, and WASH/energy access mappings that highlighted north–south disparities and urban service gaps (GIZ, 2024).

Development of the Concept Note to the Funding Proposal "Building the resilience of Togo's national health system and vulnerable communities to climate-sensitive health outcomes" was supported by a Pre-feasibility study and a Preliminary Climate Rationale for Togo (Annex 2 – Feasibility Study). These documents established the importance of (i) climate variability for malaria seasonality, (ii) extreme rainfall and drainage failures for diarrhoeal disease, and (iii) heat exposure for maternal and neonatal risks.

The present Climate Rationale builds on earlier work by updating the evidence base through an extensive literature review, assessment of a wider range of health outcomes, and the application of epidemiological models to project changes in climate-sensitive health outcomes among vulnerable groups in Togo under multiple climate change scenarios. It examines the risk of climate-sensitive health outcomes and provides the analytical foundation for proposed adaptation activities designed to reduce climate-related impacts on health.

Drawing on the concepts and definitions of the Intergovernmental Panel on Climate Change (IPCC), and following specific guidance and requirements from GIZ, the report analyses how climate hazards, population exposure and underlying vulnerabilities interact to affect three selected climate-sensitive health outcomes. Epidemiological models are then used to project potential future impacts under different climate scenarios. The rationale is organised around impact chains, which help visualise the relationships between climate hazards and their downstream health consequences.

The report is structured into four main sections: Background, Methodological approach, Results and Adaptation recommendations.

3. Background

3.1 Country context

Togo is a West African country with a diverse climate and geography. It borders Ghana to the West, Burkina Faso to the North and Benin to the East. To the South Togo has 55km of coastline stretching along the Gulf of Guinea in the Atlantic Ocean (Figure 1A). Togo has a diverse landscape, which includes coastal plains, plateaus in the central regions and the Atakora Mountain range spanning from the southwest to northeast of the country.

According to the National Institute of Statistics and Economic and Demographic Studies (INSEED) census data (INSEED, 2022), Togo had a total population of 8.4 million as of 2022, spread across five administrative level 1 regions: Maritime, Plateaux, Centrale, Kara, and Savanes. These administrative regions are further subdivided at the second level into 39 prefectures, and at the third-level into 394 cantons. The nation's capital of Lome is located in the Maritime Region, the most densely populated region, with a population of 2.2 million (INSEED, 2022).

Figure 1 - A) Togo topography, B) Togo population density

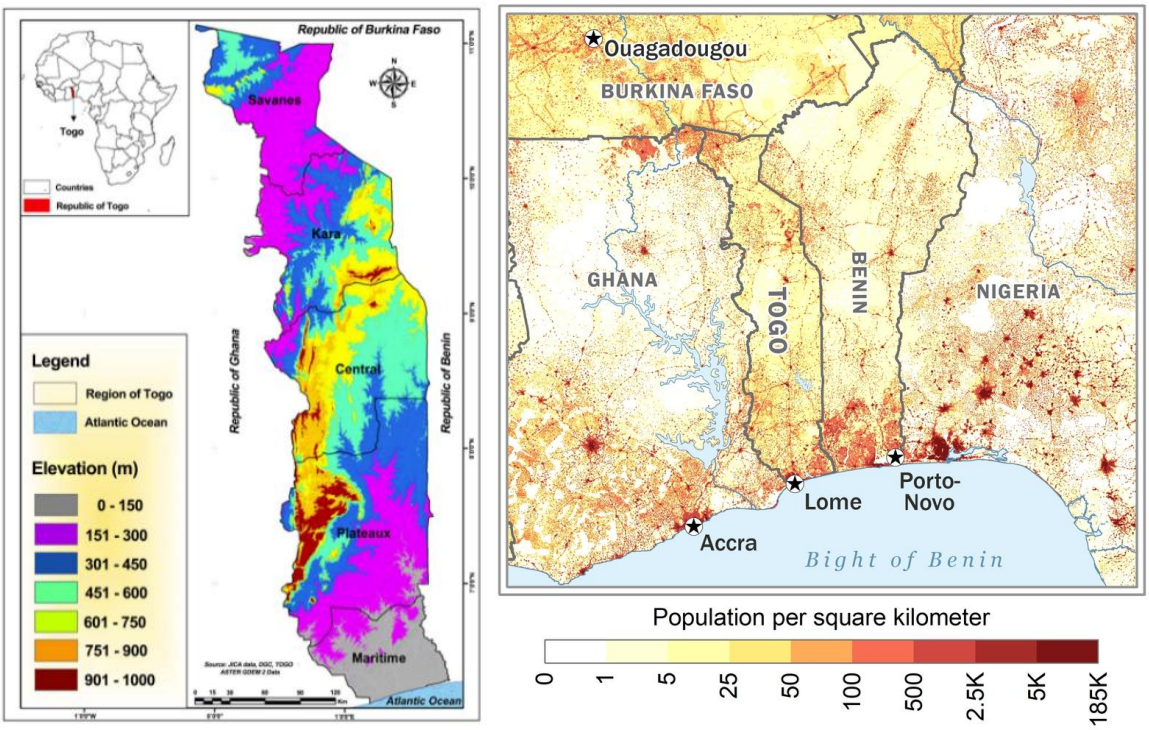

(The World Factbook, 2025)

Togo is designated as a Low Income Country, with the poverty rate (where poverty is defined at the National Poverty Line by the World Bank (World Bank Group, 2024)) in 2021 at 43.8%. While poverty rates are significantly higher in rural areas compared to urban areas, Togo has experienced an overall decline in poverty of 1.7% nationally since 2018 (World Bank Group, 2024).

3.2 Climate context

Togo lies entirely within the Tropical Savannah climate zone (Köppen-Geiger classification) (Figure 2), and is characterised by generally hot conditions year round (mean annual Tmin = ~22.0C, T = ~27.4, Tmax = ~32.8) and seasonal fluctuations in rainfall (~1200mm annually; >80% falling in the wet season from May - October) (World Bank Group, 2025) .

Figure 2 - Köppen-Geiger climate zone classification. Togo falls within the Tropical Savannah zone (Aw).

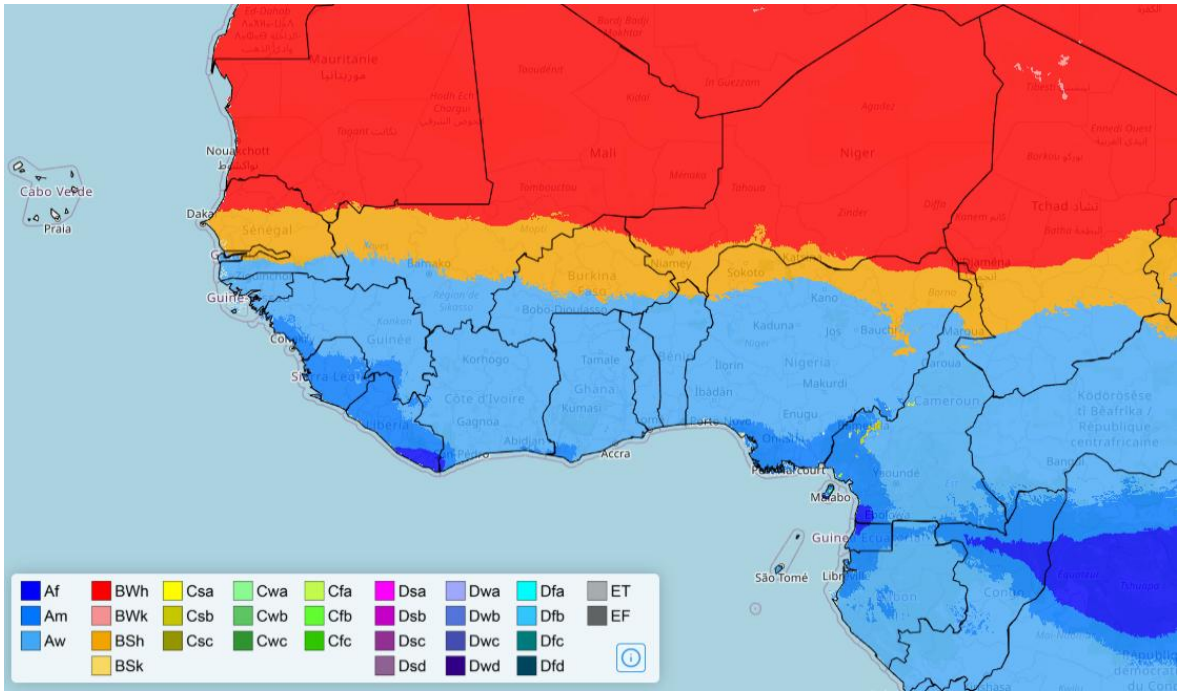

(Beck et al., 2023)

The country's geography gives rise to additional north-south and elevational climatic gradients, ranging from humid coastal/Guinea savanna in the south to drier Sudan–Sahel zones in the north. The northern regions of Togo show a unimodal rainfall pattern (~May–Oct) and a long dry season influenced by Harmattan winds (Dec–Feb). Temperatures are highest during this period, with frequent hot days and heatwaves late in the dry season. The Centrale region is a transition zone with one dominant rainy season (Apr–Oct) and high variability inter-annually. The southern Maritime and Plateaux regions exhibit a bimodal rainfall pattern with long rains (Mar–Jul) and short rains (Sep–Nov) periods (MERF, 2018). The Togo Mountain range lies in the central region of the country, stretching from southwest to northeast and rising to almost 1000m (Figure 1A), creating an area of elevated rainfall and generally cooler temperatures that confound simple comparisons of regional averages.

Precipitation in Togo is highly variable, both annually and between years. A study using data from weather stations across Togo reported that between 1961 and 2001 the annual precipitation in Togo has decreased at 80% of the weather stations, with this reduction being more pronounced in the southern regions (Djaman, 2017).

Togo is also affected by drought (periods of high temperatures and low rainfall), heatwave and flooding events. For example, in 1942, 1976 and 1982 three major droughts have collectively impacted over 500,000 people in Togo (MERF, 2018). Currently the highest risk of drought in Togo is faced by the Savanes, Kara and Maritime regions (MERF, 2018). Floods also impact Togo, causing damage to infrastructure and significant loss to life. Between 1925 and 2018 more than 60 flooding events were recorded (CREWS, 2025).

Togo is directly impacted by climate change, which affects climate hazards including future temperature, precipitation, flooding, heatwaves and humidity. These projected changes are analysed and described in detail in the Results section of this report.

3.3 Health context

The life expectancy at birth in Togo was 63.9 (62.9-65) years in 2021, which was 7.5 years below the global average of 71.4. This life expectancy is however increasing, having improved by 7.8 years since 2000 (World Health Organization, 2025c).

As shown in Figure 3, in 2023 the leading burden of disease in Togo, measured in Disability Adjusted Life Years (DALYs), were neonatal disorders, diarrhoeal diseases and malaria, respectively. For children under 5 years of age, neonatal disorders had the highest burden of disease, followed by diarrhoeal diseases and malaria (Institute for Health Metrics and Evaluation, 2023).

Figure 3 - Global Burden of Disease statistics for Togo. Left) Deaths per 100,000 population per year; right) Disability Adjusted Life Years (DALYs) per 100,000 population per year

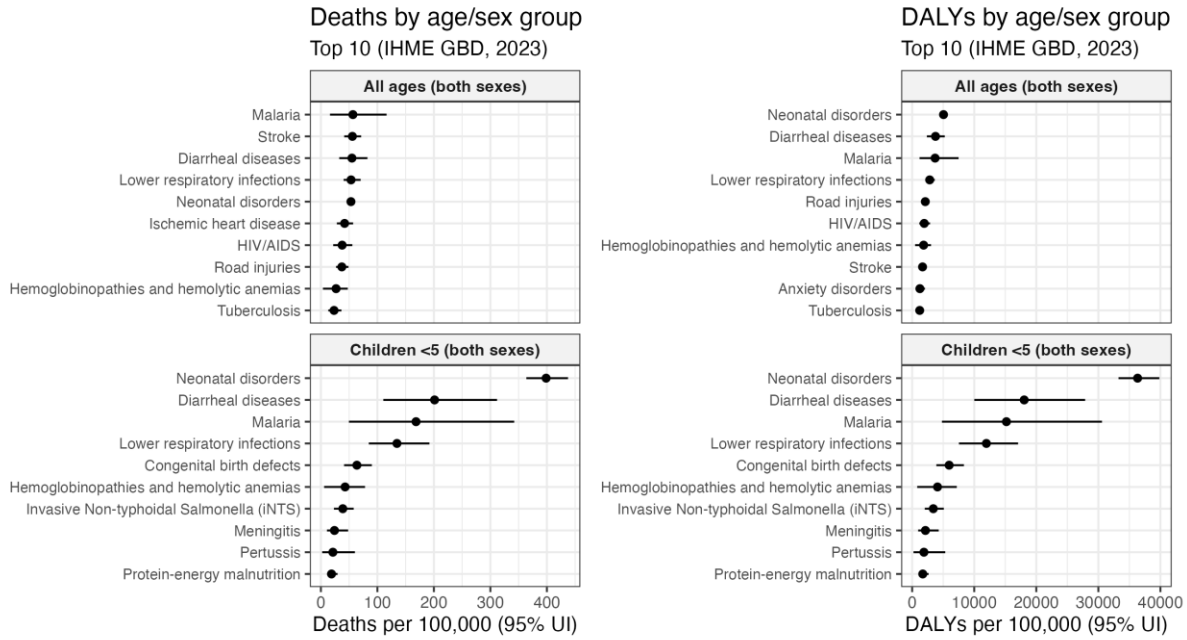

(Figure constructed from data provided by IHME GBD, 2023)

The healthcare system in Togo is structured into three distinct levels: the peripheral level, the intermediate level, and the central level (Figure 4) (Republic Togolaise, 2017).

Figure 4 - Pyramidal organisation of Togo's health system

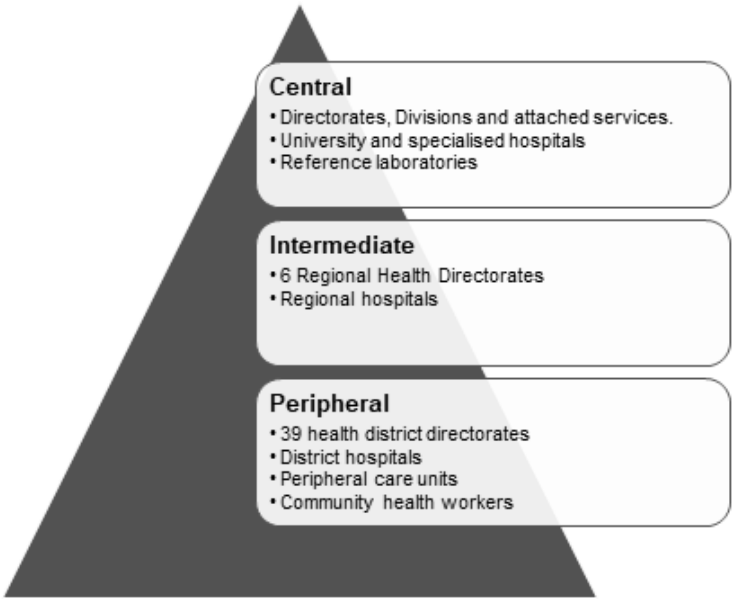

(Republic Togolaise, 2017)

Regionally, the distribution of healthcare facilities is uneven, with the highest density of facilities located in the greater Lomé area and in the Maritime region more broadly (Exchange, 2025). The distance to the nearest health care facility is highly heterogeneous, with implications for travel time when seeking health care.

Togo has a very low density of health professionals compared to population, with just 3.15 health professionals per 10,000 inhabitants. This is far below the World Health Organization (WHO) recommended target of 23 per 10,000 (GIZ, 2021). There is also a large domestic private health expenditure at 67.7% of total health expenditure, which negatively impacts the populations which are already most vulnerable (WBG, 2022). Overall, the health sector in Togo lacks integration of climate change data to inform future health policy, planning and adaptation. There is a general lack of capacity and preparedness for the impacts that climate change will have on health care provision and outcomes such as WASH services and essential drugs for diseases including malaria and diarrhoea, which are currently inadequate (GIZ; U. N. C. s. F. World Health Organization, 2025).

4. Methodological approach

4.1 IPCC Concepts and Definitions

The definitions and concepts used in this document follow the Sixth Assessment Report (AR6) of IPCC's Working Group II (Pörtner & Löschke, 2022). Following the framework presented in the report, risk of climate change related impacts on human and natural systems is conceptualised as the interaction of climate hazards, exposure and vulnerability factors.

Following the framework from the IPCC AR6 report, these concepts have the following definitions:

Hazard: natural or human induced physical event or trend that may cause loss of life, injury or other health impacts, as well as damage and loss to property, infrastructure, livelihoods, service provision, ecosystems and environmental resources.

Exposure: presence of people, livelihoods, species or ecosystems, environmental functions, services, and resources, infrastructure, or economic, social or cultural assets in places and settings that could be adversely affected.

Vulnerability: propensity or predisposition to be adversely affected. Vulnerability encompasses a variety of concepts and elements including: sensitivity or susceptibility to harm, and lack of capacity to cope and adapt.

The interaction between these inter-related factors is summarized in

Figure 5 below, taken from the IPCC (Pörtner & Löschke, 2022).

As illustrated in the graphic, hazard, exposure and vulnerability all interact to create risk. In this framework, each domain must be considered when aiming to understand different risks for different populations.

Figure 5 - Interaction between Hazard, Exposure and Vulnerability

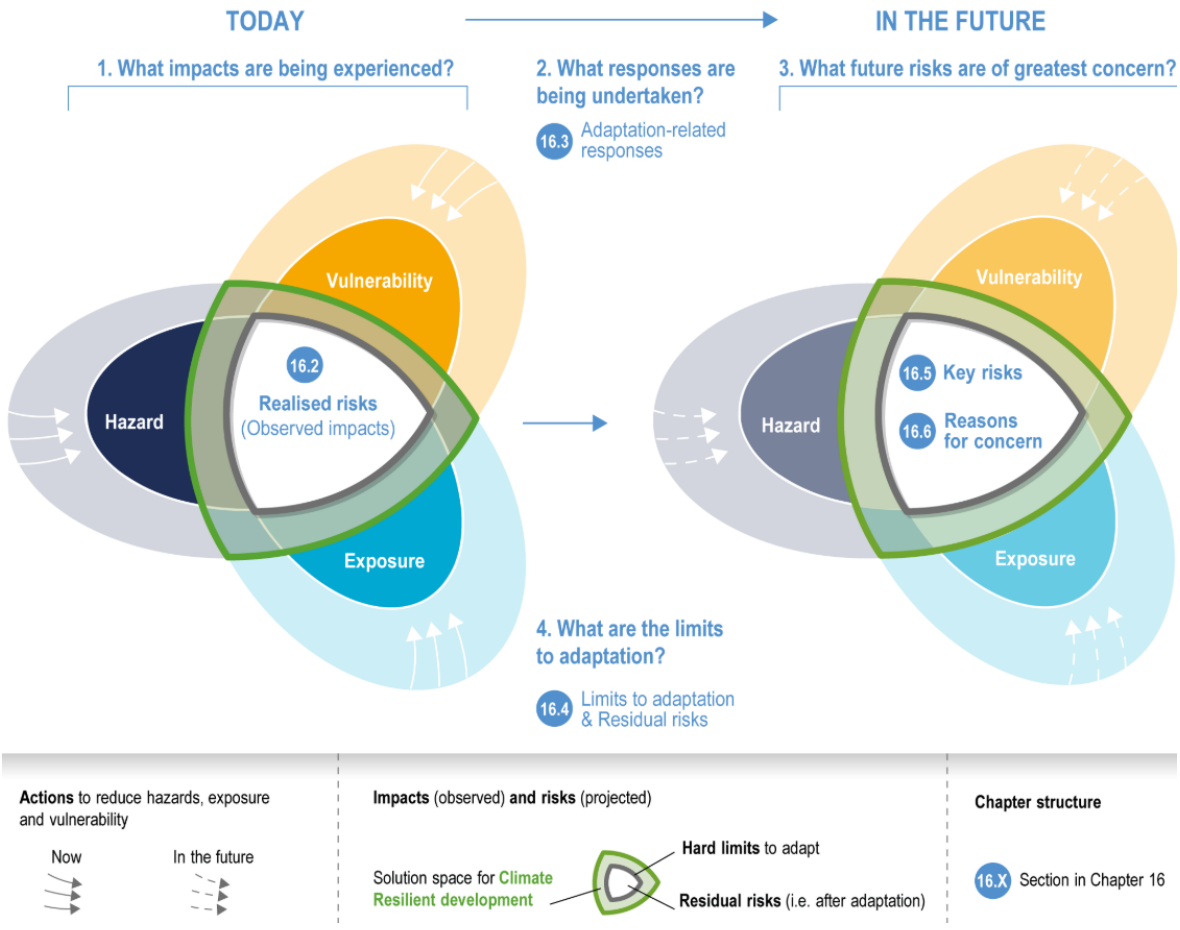

(Pörtner & Löschke, 2022)

4.2 Risk assessment framework and Impact Chains

The most recent GIZ Climate Risk Sourcebook published in 2023 provides guidance on the process of assessing the theoretical concept of risk and incorporates concepts and findings from the IPCC sixth assessment report (Zebisch et al., 2023). For a climate-health risk assessment, this means defining the climate hazard(s), defining the exposed population(s) and characterising the key vulnerability factors for each health impact. Subsequently, future risk can be considered by projecting how these underlying components of risk change or respond in the face of a changing climate.

Impact chains, as specified in the GIZ climate risk sourcebook, are context-specific, typically stakeholder co-developed conceptual models that map the causal path from key climate hazards through exposure and vulnerability to final impacts. Impact chains are used in this report to structure the descriptions of key hazards, vulnerabilities and exposures associated with select climate-sensitive health risks. However, more often they are used to inform and prioritise 'indicators' for semi-quantitative risk assessment. Here, we adopt them to illustrate the factors incorporated into the preliminary risk assessment (Stage 1) and epidemiological models (Stage 2) for each health outcome. Impact chains cannot capture all the information around risk drivers and are instead intended to highlight the key factors for consideration given the context.

Figure 6 below, from the GIZ Climate Risk Sourcebook, outlines the general structure for the development of impact chains.

Figure 6 - Impact chain structure from 2023 GIZ Climate Risk Sourcebook The structure of the impact chain relates to the IPCC AR6 concepts using the same definitions of climate related hazards, exposure and vulnerability

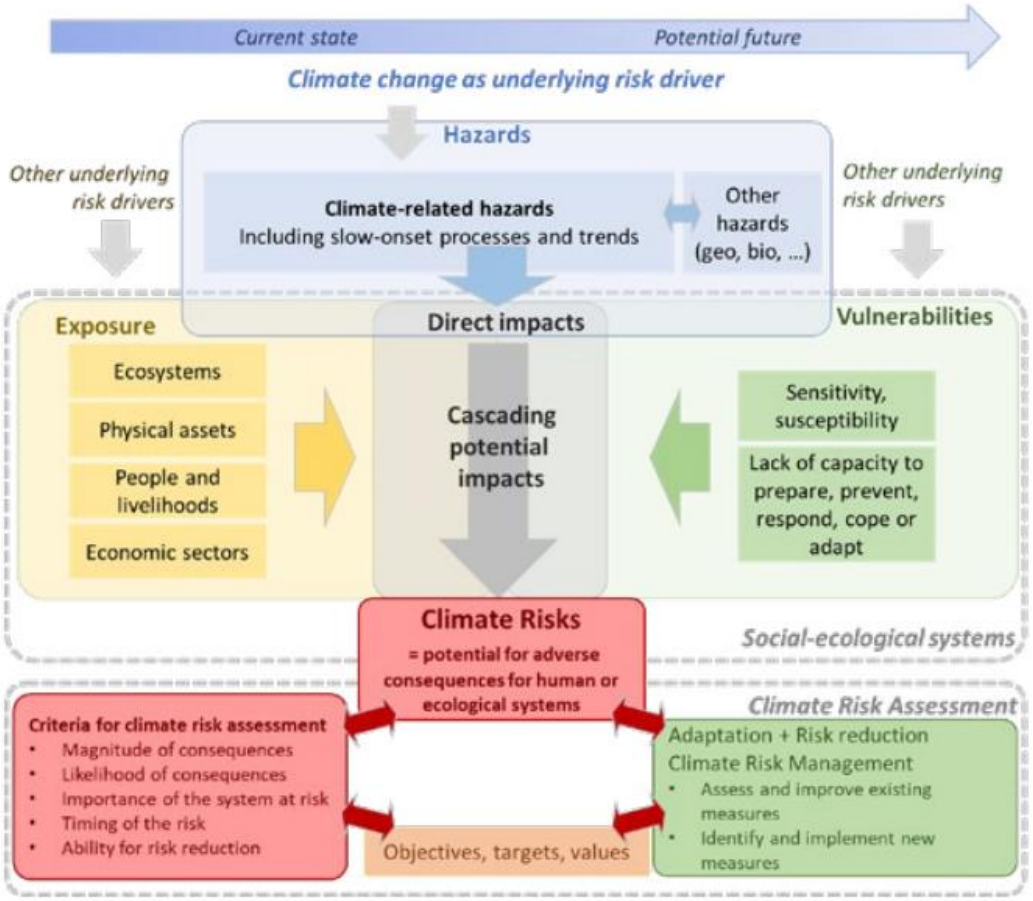

(source (Zebisch et al., 2023)).

4.3 Health outcomes

A key aspect of this study was to identify relevant climate-sensitive health outcomes for Togo and understand how they may be impacted by climate change. For the purposes of this report, three key climate-sensitive health outcomes were selected on the basis of a comprehensive systematic literature review and prioritisation process.

4.3.1 Literature review

A literature review was conducted to identify previous research on climate-sensitive health outcomes that are or will become particularly relevant to Togo. The purpose of this review was to identify climate-sensitive health outcomes with a body of evidence supporting the relationship between climate hazard and disease in countries that share a similar location and climate to Togo. This helps to identify diseases which are important to the area, and which have a strong link to climate hazards. The review aims to

identify the number of studies per health outcome, and which climate hazards these diseases are linked to. A systematic approach following gold standard Cochrane guidelines was followed[1].

The search strategy used keywords around diseases, health, climate change and climate hazards (e.g., temperature, rainfall, flooding, drought and so on). The full search strategy is presented in Appendix 1. For inclusion, studies had to be conducted in Togo or other countries that were both in the West Africa Region (as defined by the UN (United Nations Office for West Africa and the Sahel, 2025)) and were predominantly in the same climate zone as Togo - the tropical savannah (Aw) as defined in the Köppen Geiger classification based on constrained CMIP6 projections (Beck et al., 2023). Eligible countries were Togo, Benin, Nigeria, Ghana, Ivory coast, Guinea, Guinea-Bissau and Burkina Faso. These are shown in the map at**Error! Reference source not found.**.

Studies were included if they quantified the relationship between one or more climate hazards and one or more health outcomes. Both a specific climate hazard and a health outcome or disease outcome was necessary for inclusion. Studies were excluded if they were qualitative, animal studies or focused on air-pollution as this was not considered as a climate hazard due to the complex relationship between climate, emissions, pollution and air-pollution.

The search was run across the following databases: Medline, Embase, Global-health, Africa-wide information, GreenFILE, Web of Science and Scopus. See Appendix 1 for number of results per database. Covidence software was used to coordinate review stages. After initial deduplicating this yielded 6599 papers to screen by title and abstract. The search was run on 27th of August 2025, with no restriction on publication date.

Two independent reviewers screened each title and abstract to evaluate if studies should proceed to full text screening. Disagreements were resolved by discussion between the two independent reviewers, with a third reviewer contributing if a decision could not be reached by the initial reviewers. Full-text review was then carried out again by two independent reviewers. Full-text versions of articles that met the inclusion criteria were retained for further assessment. The PRISMA diagram (**Error! Reference source not found.**) below shows how many texts were screened and included/excluded at each section of the literature review.

[1] with the exception of being unable to lodge a review protocol in the Cochrane Library for peer review before starting the review, due to time constraints in delivering our results.

Figure 7 - PRISMA flow diagram for literature review

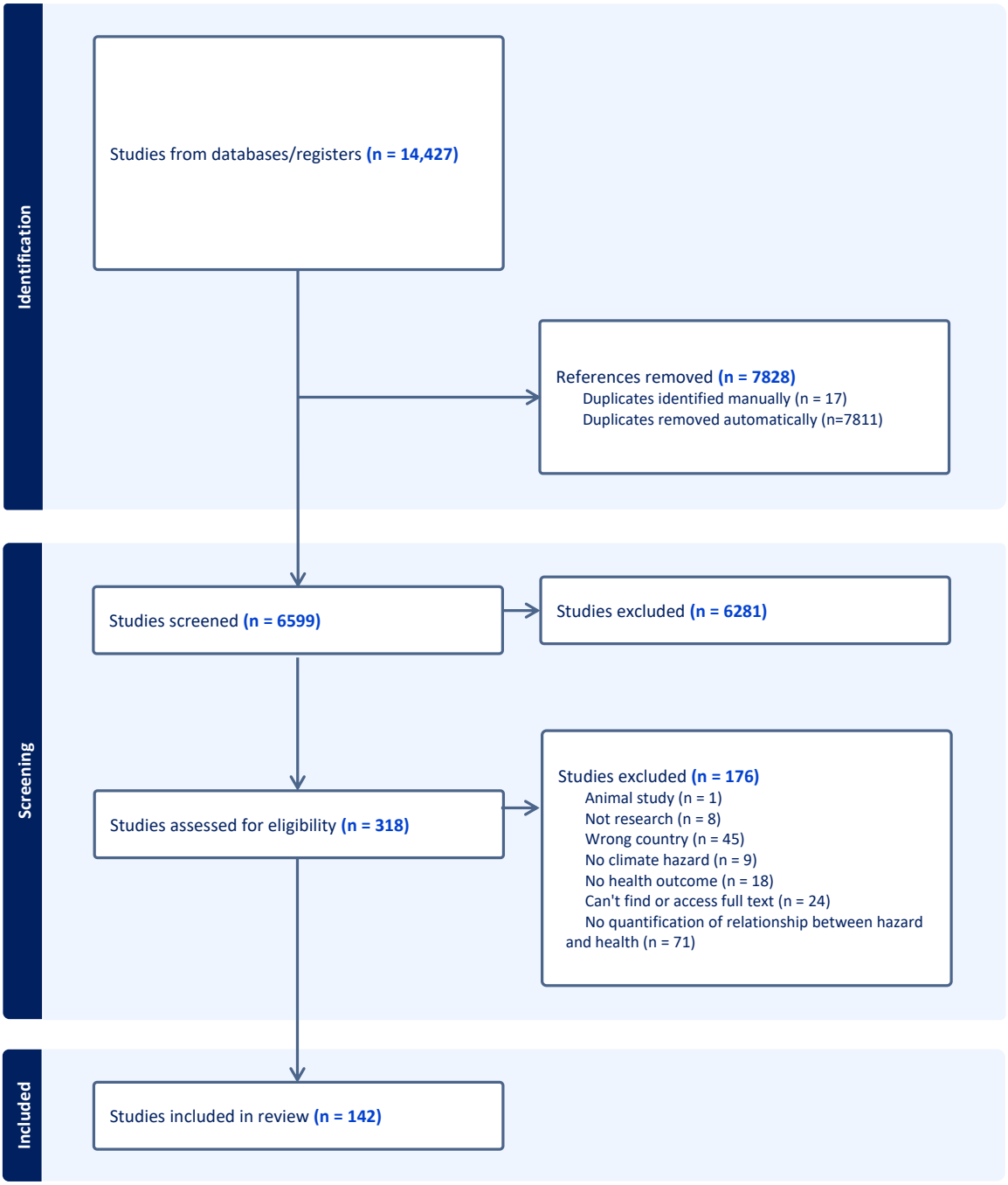

(Source: Own elaboration)

The results of the literature review highlight climate-sensitive health outcomes with the largest body of research quantifying the relationship between climate hazards and health outcomes in West Africa that share the same or similar climatic characteristics as Togo. These diseases, along with the climate hazards they are related to, are summarized in Table 1 below[2]:

[2] The total numbers in the "number of studies" column sum to more than 142 (the total number of studies included in the review), as several of the studies included multiple health outcomes

Table 1 - Number of studies identified in literature review

Disease	Climate Hazard(s)	Number of studies
Malaria	Temperature, precipitation, humidity, seasons	50
Diarrhoeal Disease (any)	Precipitation, seasons, temperature, humidity, flooding	21
Malnutrition (including stunting)	Precipitation, temperature,	13
Meningitis	Humidity, temperature, season,	13
Adverse perinatal and neonatal outcomes: Neonatal mortality/stillbirth/preterm birth/low birth weight	Temperature, humidity	12
Mortality	Precipitation, temperature, flooding, drought, season, humidity	10
Other Respiratory Disease	Temperatures, humidity, windspeed	8
COVID-19	Temperature, humidity	7
Measles	Precipitation, temperature, humidity	4
Schistosomiasis	Precipitation, temperature	4
Dengue Fever	Temperature, precipitation, humidity	3
Mental Health	Drought	3
Other Cardiovascular Disease (CVD)	Temperature, season	2
Other (diseases with only one paper)	Precipitation, temperature, season	18

(Source: Own elaboration)

As shown in Table 1, the conditions with the highest number of studies identified were Malaria, Diarrhoeal Disease, Malnutrition, Meningitis and Adverse perinatal and neonatal outcomes. COVID-19 has been separated from other respiratory diseases, as it is a complex multi-system disease with epidemiological and pathological effects that extend beyond respiratory disease (Baskett et al., 2022).

The map shown inFigure 8 - Number of studies per country included in literature review

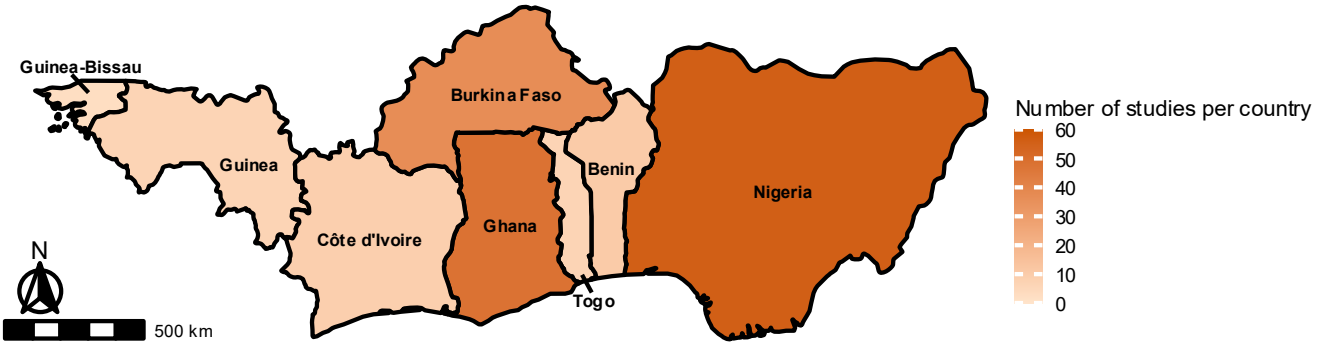

below shows the geographical distribution of studies reviewed. It highlights a dearth of literature on climate change and health focussed on Togo itself, as well as countries within the region. By extension,

there is a lack of support to the evidence-based insights on the potential impact of climate change on health in Togo.

Figure 8 - Number of studies per country included in literature review

(Source: Own elaboration)

As Figure 8 shows, the majority of the evidence came from Nigeria, Ghana and Burkina Faso, respectively. Only nine studies included disaggregated data from Togo specifically, compared to 58 studies from Nigeria.

4.3.2 Prioritisation - Multi Criteria Decision Analysis (MCDA)

Following compilation of the results from the literature review, a bivariate decision analysis (a simple Multi-Criteria Decision Analysis) was used to determine priority diseases for the Climate Rationale, adapting the methodology used for the preliminary Climate Rationale stage.

The MCDA was conducted to identify climate-sensitive health outcomes most relevant to Togo—i.e., those with high health impact, strong local relevance, and substantial available evidence on climate–health linkages. These were represented by: 1) evidence volume, measured as the number of publications linking climate change to the outcome in West Africa from our climate-health literature review; and 2) disease burden in Togo, using Global Burden of Disease estimates of DALYs (Level 3) (Institute for Health Metrics and Evaluation, 2023).

Each criterion was standardized by 1) min–max normalization, and 2) computing a (weighted) composite score, which was then ranked to obtain the final ordering. Robustness of the ranking was assessed with sensitivity analyses that varied the weights and by substituting DALYs for Deaths, also from IHME GBD data. Table 2 summarises the results.

Table 2 - MCDA for selection of priority climate-sensitive health outcomes for Togo. Columns show standardised ranks based on the min-max method (original ranking of 1 = highest). The total is the sum

Cause (GBD Level 3 category)	Studies	DALYs	Studies scaled	DALYs scaled	Priority Score	Ranking
Malaria	50	3694.74	1.000	0.730	0.865	1
Neonatal disorders	12	5050.84	0.208	1.000	0.604	2

Diarrhoeal diseases	21	3761.07	0.396	0.743	0.569	3
Meningitis	13	709.17	0.229	0.135	0.182	4
Malnutrition	13	332.38	0.229	0.060	0.145	5
Mental health conditions	3	727.85	0.021	0.139	0.080	6
COVID-19	7	275.26	0.104	0.049	0.076	7
Other respiratory diseases	8	61.32	0.125	0.006	0.065	8
Measles	4	181.65	0.042	0.030	0.036	9
Schistosomiasis	4	89.38	0.042	0.011	0.027	10
Other cardiovascular and circulatory diseases	2	244.04	0.000	0.042	0.021	11
Dengue	3	31.74	0.021	0.000	0.010	12

(Source: Own elaboration)

Following the prioritisation process, the health outcomes selected as priorities for modelling were:

- Malaria
- Diarrhoeal disease
- Preterm birth

Malaria

Malaria transmission is strongly influenced by environmental conditions, which affect mosquito vector (*Anopheles* spp.) ecology, parasite development and human vulnerabilities over short (days to weeks), medium (seasonal) and long term (interannual and decadal) time horizons (Megersa & Luo, 2025; van der Deure et al., 2025). For example, temperature influences mosquito development rates, adult survival, and biting behaviours, as well as the malaria parasite's extrinsic incubation period. Rainfall and surface water define the availability and seasonality of habitats in which mosquitoes lay eggs and larvae develop (van der Deure et al., 2025). Humidity further affects adult survival and biting behaviour (Komba, 2024). Climate change therefore has potential to alter environmental suitability for malaria transmission, which may influence geographic distribution, length of the transmission season, intensity of transmission and long-term temporal trends in prevalence and burden (van der Deure et al., 2025). In addition, extreme events such as flooding can create temporary mosquito breeding sites and impact infrastructure, intervention campaigns and health care services, exacerbating malaria impacts (Megersa & Luo, 2025).

Previous studies on malaria in Togo indicate the disease is endemic across the country, with year-round transmission, seasonal peaks tied to rainfall, and high heterogeneity across regions. In 2023, 2,367,706 confirmed cases and 1281 deaths were recorded on a population of ~8 million people (World Health Organization, 2024). Children <5 accounted for 31.6% of cases. Prevalence ranged from 2.6% in the commune of Lome up to 43.0% in the northern Savanes region (Kombate et al., 2022). A target has been set to eliminate malaria in Togo by 2030 under the Programme National de Lutte contre le Paludisme (PNLP; also called the National Malaria Control Program), with four coordinated plans carried out to date to achieve this. Intervention effort has thus been high, including chemical larval control since 1975, and intermittent preventive treatment (IPT) and seasonal chemoprevention for pregnant women and children under 5 since 2005. Management of vector resistance to insecticides was introduced in 2006. Since 2008 vector control methods including long lasting insecticide treated bed nets (LLINs) have been used, and biolarvicide has been used at household level since 2010. Such interventions have had an impact on malaria prevalence and mortality patterns (Bakai et al., 2020).

In a study analysing monthly data compiled from medical records and Community Health Worker (CHW) reports at multiple levels of the healthcare system (community, district, regional, and central), total malaria cases increased nearly fourfold over the period from 2008 to 2017, while the population increased by a factor of 1.3 (Bakai et al., 2020). This equates to an increase from 50 to 160 cases per 1000 people, and a mean annual increase nationally of 13.1%. Increases were observed in all regions and subgroups, with smaller increases in the Commune of Lome (8.1%) and a larger increase in the Centrale region (16.7%). Increases were greater in children <5 (13.1%) and people >5 (14.4%) than

pregnant women (10.4%). The only decrease was in pregnant women in the Lome Commune (-3.2%). By contrast, malaria deaths decreased nationally in all regions and subgroups. The Central and Plateaux regions saw the smallest decreases. Pregnant women showed larger decreases (-15.7%) than children <5 (-6.6%) or people >5 (-5.6%). Only pregnant women in the Kara region showed an increase in deaths (12.1%). Evidence from this dataset highlights a seasonal pattern in malaria prevalence with a peak in cases over July, August, September, corresponding to the rainy season.

Thomas et al recently used the same dataset for the period 2013-2017 to develop malaria prediction models by health district and target group using a range of meteorological (precipitation, humidity, temperature, wind speed) and environmental predictors (Normalized Difference Vegetation Index - NDVI) to forecast malaria cases nationally (Thomas et al., 2024). Models were trained on data from 2013-2016 and then used to predict the number of cases in 2017 as a test of predictive performance. They used four different models of varying characteristics. The authors concluded that, although during the model training period the models had reasonable explanatory power (ranging from ~40-80% deviance explained), generally the models exhibited poor performance in predicting the number of cases in the subsequent year. The authors thereby warn against using such data / models for forecasting at present, particularly for informing control strategies and decision making, but point to some avenues for potential improvement including use of finer spatial scale climatic predictors (<0.5 deg), finer temporal scale outcome data (weekly malaria case data – see below), and inclusion of other covariates (e.g., proximity to water, land cover, housing characteristics, socioeconomic variables, intervention data).

The most recent malaria indicator survey (MIS) was conducted in 2017-2018, with 171 cluster locations selected across the country (The DHS Program, 2017). Analysis of these data indicated that malaria incidence is spatially clustered in Togo and associated with climatic and environmental factors including positive associations with mean temperature, precipitation, aridity and proximity to water bodies (Kombate et al., 2024). Trends in malaria incidence through time were also evaluated by linking routine surveillance data (see below; provided by District Health Information System 2 (DHIS2)) to the MIS cluster locations. Contrary to the trends reported above, this analysis showed a general decrease in incidence through time across 4 time points (2000, 2005, 2010 and 2015) in most regions, except in the northern Kara and Savanes regions, which showed incidence peaking in 2010 before decreasing in 2015.

Finer temporal scale malaria outcome data do also exist in Togo, but spatial coverage is limited. Since 2017, the PNLP in collaboration with the Global Fund to Fight AIDS, Tuberculosis and Malaria, implemented a malaria sentinel surveillance program, consisting of real-time data collection and analysis to support decision-making. Data comes from 16 health facilities (“sentinel sites”), 4 hospitals and 12 peripheral care units across 2 health regions (Savanes, Plateaux). Weekly data on malaria morbidity and mortality are reported for children < 5, people ≥ 5, and pregnant women. Preliminary analysis of this dataset from 2017-2019 confirmed the pattern of increasing cases and deaths during the rainy season, and concentration of deaths among children <5 (Thomas, 2020).

Of studies that make projections of malaria incidence/ prevalence under climate change, results of malaria in Togo are equivocal. Fall et al., (2023) used a mechanistic vector-transmission model (VECTRI) forced by CMIP6 climate model projections for two SSPs (SSP2/4.5 and SSP5/8.5) to estimate change in the entomological inoculation rate (EIR), a disease transmission indicator based on vector abundance and inferred biting rate, across West Africa (Fall et al., 2023). The key climatic parameters used in the model are temperature and precipitation. Results over Togo suggest relatively minor changes in risk over this period, with high-risk areas in the north of the country remaining high risk in future with an average EIR in the 60-75 ib/p/m range (inferred from maps, Togo specific results not presented). Areas in the far northeastern corner and southern coast region are projected to have slight declines in risk. The study suggests minor extensions (~0-2 months) of the malaria season, particularly in northern regions that are already highly seasonal (Fall et al., 2023).

Diarrhoeal Disease

Diarrhoea incidence is impacted by several environmental factors, which can influence both the survival, dispersal and replication of causative pathogens (viral, bacterial or parasitic), as well as the pathways through which people are exposed to these pathogens. There is a large body of evidence linking climate

hazards to diarrhoea worldwide, including drought, flooding, heavy rainfall and temperature (Carlton et al., 2016; Flückiger & Ludwig, 2022; Levy et al., 2016), with most of this evidence on temperature and rainfall (Levy et al., 2016).

There are several complex pathways through which temperature can increase incidence of diarrhoea. For example, higher temperatures can increase both reproductive rates and survival probability of some causal bacteria. However, this effect appears to differ between different pathogens, with epidemiological evidence showing that temperature may have differing effects for bacterial, protozoal and viral diarrhoea (Carlton et al., 2016; Miller et al., 2025). Environmental factors also affect exposure pathways for diarrhoea, as pathogens are frequently spread through contaminated food or water, as well as from person-to-person due to poor sanitation practices (World Health Organization, 2025a). There is some evidence of droughts increasing diarrhoea incidence; for example, by decreasing water availability, and therefore increasing the population with inadequate water, sanitation and hygiene (WASH) conditions (Levy et al., 2016).

Evidence suggests rainfall and flooding also impact diarrhoea incidence, largely through their effect on exposure pathways (Levy et al., 2016). This effect may be mediated by season, with some studies finding rainfall is associated with increased risk following dry periods but decreased risk following wet periods. This could be because in the short-term heavy rainfall and flooding can increase transport of pathogens, mobilizing pathogens into surface water and contaminating groundwater; while in the long term they may have a dilution effect, with heavy rainfall diluting pathogen concentration (Levy et al., 2016).

A recent systematic review and meta-analysis examining the relationship between climate hazards and childhood diarrhoea world-wide found a small but significant positive association between diarrhoea risk and both increased temperature (1.04; 95% CI [1.03, 1.05]) and increased rainfall (1.14; 95% CI [1.03, 1.27]). This effect was exacerbated by poor WASH facilities (Geremew et al., 2024). More locally to Togo, a recent study using data from ten West African countries found increased odds of diarrhoea associated with higher temperature, and a non-linear relationship with precipitation (Dunn & Johnson, 2018).

In Togo diarrhoeal disease is widespread, representing the fifth highest cause of death as of 2021 (World Health Organization, 2025b). While little research exists focussing on diarrhoea in Togo specifically, our literature review identified several pieces of country specific research examining the relationship between climate hazards and diarrhoea in neighbouring countries. These papers showed a range of different and complex relationships between climate factors (including temperature, precipitation, drought and season) and diarrhoea. The most common climate hazards that were found to have a relationship with diarrhoeal disease were precipitation and temperature, although the nature of these relationships were not consistent across studies. For example, a recent study carried out in Ghana used meteorological data and information for Ghana Health Services to model incidence of diarrhoea (Asare, 2022). This paper found a relationship between diarrhoea and temperature; however, the strength and direction of associations with temperature differed across the four different ecological zones in Ghana. They also found a weak biannual seasonality with major and minor peaks in June and October, respectively, coinciding with the rainy seasons (Asare, 2022).

Another paper modelling patterns of climate related diseases in children found only a weak relationship between precipitation and diarrhoea (Adeboyejo, 2020). A recent study examining the seasonality of cholera in sub-Saharan Africa found no seasonal relationship in Togo or Ghana but did find evidence of seasonal relationship in Benin and Burkina Faso (Perez-Saez et al., 2022).

A recent systematic review examined the potential future climate change-attributable diarrhoea burden globally (Miller et al., 2025). This study found that the majority of identified research predicted an increase in diarrhoeal diseases in the near (2020–2040), mid (2040–2060) and long term (2060+) future due to climate change. They also found that high baseline burden of diarrhoeal disease, as it is in Togo, was associated with larger increases in burden (Miller et al., 2025).

Together, this evidence highlights that while the specific pathways linking climate hazards to diarrhoeal disease vary across settings and pathogens, the overall evidence suggests there is a relationship between climate change related hazards and diarrhoeal disease, which may have meaningful

implications for Togo. Here, we aimed to quantify how climate variability and projected climate change may influence under-5 diarrhoeal incidence in Togo.

Preterm birth

Rising temperatures and extreme heat events are now widely recognised as threats to maternal and newborn health. Exposure to high temperatures during pregnancy has a range of physiological effects, including a reduction in placental blood flow (Wang et al., 2020) and an inflammatory response that may trigger early labour (Chersich et al.). Preterm birth (PTB) (delivery < 37 completed weeks' gestation) is the leading cause of neonatal and under-5 child mortality worldwide (Lakhoo et al., 2025). Complications of preterm birth (PTB) are the sixth leading cause of mortality in Togo, with 33.7 deaths per 100,000 population in 2021 (World Health Organization, 2025b). The rate of PTB in Togo was estimated to be 13.3% of all live births in 2010 (Blencowe et al., 2012). More recent (2020) estimates did not include Togo; however, PTB rates for nearby countries in West Africa, including Benin and Nigeria, showed no change over time (Ohuma et al., 2023).

There is strong evidence that short-term exposure to high ambient temperatures increases the risk of PTB (Chersich et al., 2022) (Lakhoo et al., 2025). A recent systematic review of heat exposure impacts on maternal, foetal, and neonatal health identified 84 studies on PTB with high levels of agreement (very high confidence). Meta-analysis revealed a 4% (95% CI 3-6%) increased odds of PTB per 1°C increase in temperature 0-4 weeks before delivery and a 26% (8-47%) increased odds during a heatwave versus non-heatwave period (typically defined as 2 or more days above the 90th percentile of local temperatures) (Lakhoo et al., 2025). The vast majority of studies have been conducted in high-income countries, but there is some evidence to suggest that the heat-PTB impact is stronger in lower-middle-income countries (OR: 1.61, 95% CI: 1.39-1.86) (Lakhoo et al., 2025).

Few studies have been conducted in sub-Saharan Africa. Limitations in data quality and accessibility (both PTB and environmental data) likely explains the relative paucity of climate-PTB research in sub-Saharan Africa. McElroy et al (2022) documented a strong tendency towards an increased risk of PTB with daily maximum temperatures >20°C (approximating a 5% increased odds per 1°C increase, 0-7 day lag) using Demographic Health Survey (DHS) data from 14 LMICs, including Benin and Nigeria (McElroy et al., 2021). The association with maximum temperature was not statistically significant; however, this study was limited by a small number of PTB cases and potential outcome misclassification (PTB measure based on self-reported length of pregnancy in months). Diurnal temperature range showed a stronger association with PTB (14°C vs 16°C: OR=1.76, 95% CI=1.23-2.54).

Our review found nine studies on the effects of heat on neonatal outcomes; however, only two specifically investigated preterm birth (Ahmed et al., 2024; Reddam et al., 2025). In Kaduna State, Nigeria, correlation analysis of monthly birth records from Barau Dikko Specialist Teaching Hospital (2015–2023) indicated that cold daytime temperatures (Tmax <10th percentile) were positively associated with preterm births (r = 0.491), whereas warm night-time temperatures (Tmin >90th percentile) were negatively associated (r = -0.301) (Ahmed et al., 2024). However, this study did not account for seasonal or long-term trends. A Ghana-based study in Kintampo North & South used daily maximum shaded wet bulb globe temperature and heat index to assess this association among participants of GRAPHS, a cluster randomized cookstove intervention trial (Reddam et al., 2025). They found that a 1° increase in average wet bulb globe temperature (humid-heat) in the 2nd trimester was associated with 1.53 (95% CI: 1.00-2.35) higher odds of preterm birth.

Although most studies focus on the short-term effects of heat exposure in the week or month preceding delivery, accumulating evidence suggests that high temperatures in early and mid-pregnancy may also be important. Several studies report larger effect sizes when heat events occur more than four-weeks before birth, with a recent meta-analysis finding 1.37-fold higher odds of PTB (95% CI: 1.08-1.74) at higher temperatures during these longer-lag periods (Lakhoo et al., 2025).

Additional climate-sensitive health outcomes

Although the results from the literature review and MCDA identified malaria, diarrhoeal disease and preterm birth as the three priority climate-sensitive health outcomes, the literature review highlighted several other areas where evidence exists linking climate change to health outcomes that are relevant to Togo due to their presence in other countries in the region with similar climatic characteristics.

Meningitis and malnutrition had thirteen studies each quantifying their relationship to climate change and came fourth and fifth in the MCDA with significant burdens of disease in the country. There were also eight studies linking general mortality to climate hazards that will be affected by climate change, specifically precipitation, temperature, flooding, drought, seasonality and humidity. This shows the underlying importance of climate-sensitive health outcomes as drivers of mortality in the West Africa region beyond malaria, diarrheal disease and preterm birth. The remainder of this report nevertheless focusses on these three priority outcomes.

4.4 Data

This report required extensive climate, health and demographic data for Togo. This has been obtained from a wide variety of sources. The main data sources and the variables used from these sources is summarised below and in the data table in Appendix 1.

4.4.1 Scenario analysis

When modelling future risks from climate hazards, there is no single prediction of how climate change will unfold. Instead, scenario-based approaches are commonly used to explore several potential futures according to plausible combinations of different assumptions about how societies may develop and co-develop, the implications these assumptions have on the release of anthropogenic greenhouse gas emissions into the atmosphere, and the consequent impacts on global climate.

The Shared Socioeconomic Pathways (SSPs) is the scenario analysis framework presented in AR6 (Pörtner & Löschke, 2022). The SSPs are a set of five ‘narratives’ that consider future human development by contrasting different plausible conditions that drive socio-economic development into the future. The five standard scenarios are: sustainable development (SSP1), middle-of-the-road development (SSP2), regional rivalry (SSP3), inequality (SSP4) and fossil-fuelled development (SSP5) (**Error! Reference source not found.**) (Pörtner & Löschke, 2022).

Figure 9 - The SSP framework used in AR6

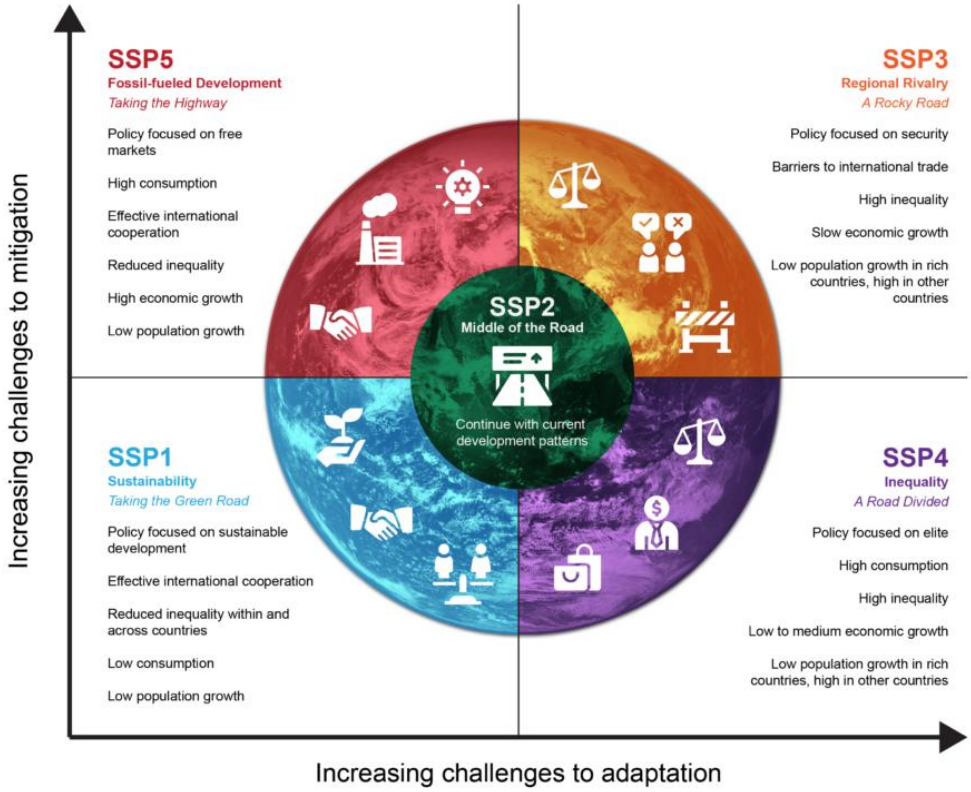

(Climate Data Canada, 2025)

Importantly, the SSPs couple these trajectories with expectations about the extent to which each may contribute to rising anthropogenic greenhouse gas emissions into the future, and the extent to which these emissions impact the climate (emissions forcings). In previous IPCC assessments, emissions forcings trajectories have been represented by Representative Concentration Pathways (RCPs). Emissions production and the extent to which societies mitigate them to limit climate change are also highly uncertain, giving rise to multiple plausible combinations of SSPs and RCPs (**Error! Reference source not found.**).

Figure 10 - SSP and RCP (emissions forcing) combinations in AR6. Tier 1 combinations are the most commonly explored (dark blue). In this Climate Rationale, we focus on SSP2-4.5 and SSP5-8.5

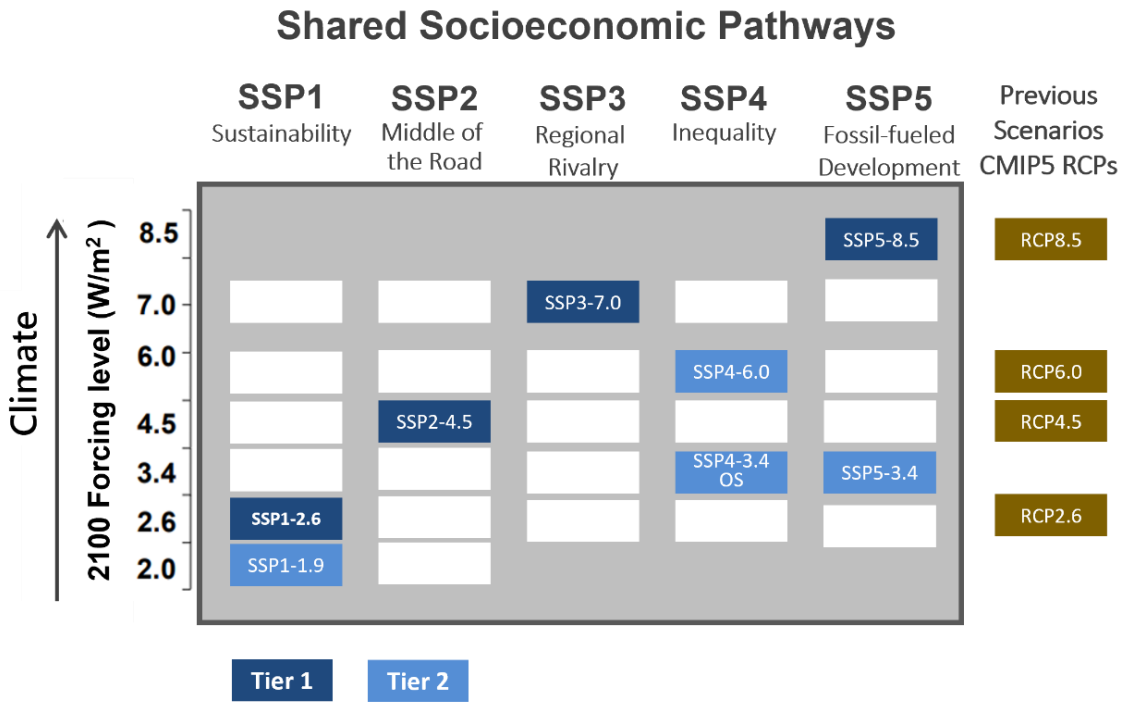

(Source:(TCCiP, 2025)

4.4.2 Geometries and base grid

A base grid of 0.1° (approx. 11x11km at the equator) was established to consistently present and organise information used in this study. We used a 0.25° buffer around a shapefile for Togo to set a bounding box for cropping and presenting all data that were derived from larger scales (e.g., global climate models). Shapefiles from the Global Administrative Areas Database (GADM v4.1) (GADM, 2022) were used for deriving administrative boundaries at various levels (canton, prefecture, region) and for aggregation, summary statistics and presentation as required. GADM compiles boundaries from official national sources and other public maps, and is freely available for academic, non-commercial use. All data were initially compiled/prepared for the whole country of Togo where possible and summarised accordingly. For analyses focussing on the priority health outcomes / regions, data were later cropped to the three northernmost regions (Centrale, Kara, Savanes) (**Error! Reference source not found.**).

Figure 11 - A) Togo showing 0.1 deg base grid; B) Zoom to priority regions

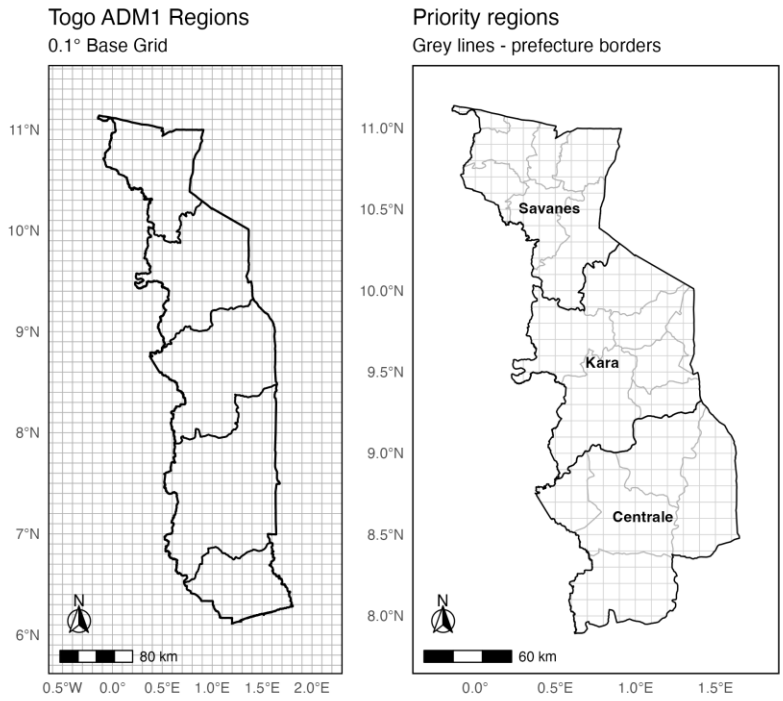

(Maps: own elaboration; shapefile source: GADM, 2022).

4.4.3 Climate data sources and processing

Historical observed climate data

We used the Multi-Source Weather dataset (MSWX) (Beck et al., 2022) when presenting data on historical observed trends and for use in models (training). MSWX is a global, observation-based meteorological dataset that is part of the MSWEP/MSWX family of 'blended' climate products (https://www.gloh2o.org/mswx/). MSWX provides near–real-time daily meteorological fields (1980 – a few months before present) at 0.1° (~11 km at equator) spatial resolution. It combines *in-situ* weather station observations (sourced from global weather station databases and various national networks), satellite remote sensing, and reanalysis datasets.

We extracted and processed the full time series available for all variables in the MSWX dataset (Jan 1981 - Aug 2025). Variable and methodological details on variable selection and processing is provided in section 8.4.3.1 below.

Other historical observed datasets exist, and we initially selected a subset of these to evaluate their suitability for use in this report, including:

- The European Centre for Medium-Range Weather Forecasts (ECMWF) Reanalysis v5 – Land dataset (ERA5-Land), a 0.1° reanalysis climate product consistent with ERA5 (~0.25°), providing higher spatial detail over land (Muñoz Sabater, 2019),
- The Multi-Source Weighted-Ensemble Precipitation dataset (MSWEP), a bias-corrected 0.1° dataset considered one of the best performing precipitation datasets for West Africa (Beck et al., 2019),
- The Climate Hazards Group InfraRed Precipitation with Station dataset (CHIRPS), a hybrid rainfall dataset for trend analysis and drought monitoring at 0.05° (The Climate Hazards Group, 2018).

For comparisons, all historical observed data were initially aggregated to a daily timestep from their native (e.g., hourly / 3-hourly) resolution. We systematically compared datasets for the area covering Togo by overlaying daily time series and performing correlation analyses. For individual variables (e.g., mean temperature, precipitation), all were highly correlated between products (correlation coefficient ~0.9) but not entirely congruent when overlaid as time series. Rather than mix data products (e.g., rainfall from CHIRPS, temperature from MSWX), we selected the MSWX dataset for all subsequent analyses, as this is already an internally consistent, bias-corrected and harmonised dataset providing all the target variables.

We summarised the historical observed data for the period 1980-2024 for our core variables of interest. For presentation, each variable's time series is presented with an overall linear trendline to illustrate general trend over the whole period, as well as trendlines for a reference baseline period (1981-2000) and the remainder of the available time series (2001-2024). Trends were assessed using Mann-Kendall (MK) tests and Sen slope estimates (Helsel, 2020). Where statistics are cited for a time slice or a difference between time slices, we use average values over each period. If citing a rate of change, we use the slope of a trendline and, where necessary multiply by a suitable reporting period (e.g., x10 to give change per decade on a yearly time series). As an incomplete year, 2025 was omitted from all statistics cited. An example (for mean temperature) is shown in **Error! Reference source not found.**. For consistency, the same reference baseline period is used for the projections (see 8.4.6.2).

Figure 12 - Example time series for historical observed climate data, illustrating how summary statistics of trends / change were derived. Grey line is the time series for a climate variable. Solid orange line is the trend over the whole period. Dashed line is trend over the reference baseline period. Dotted line is the trend over the recent period. Black lines are means of each time slice.

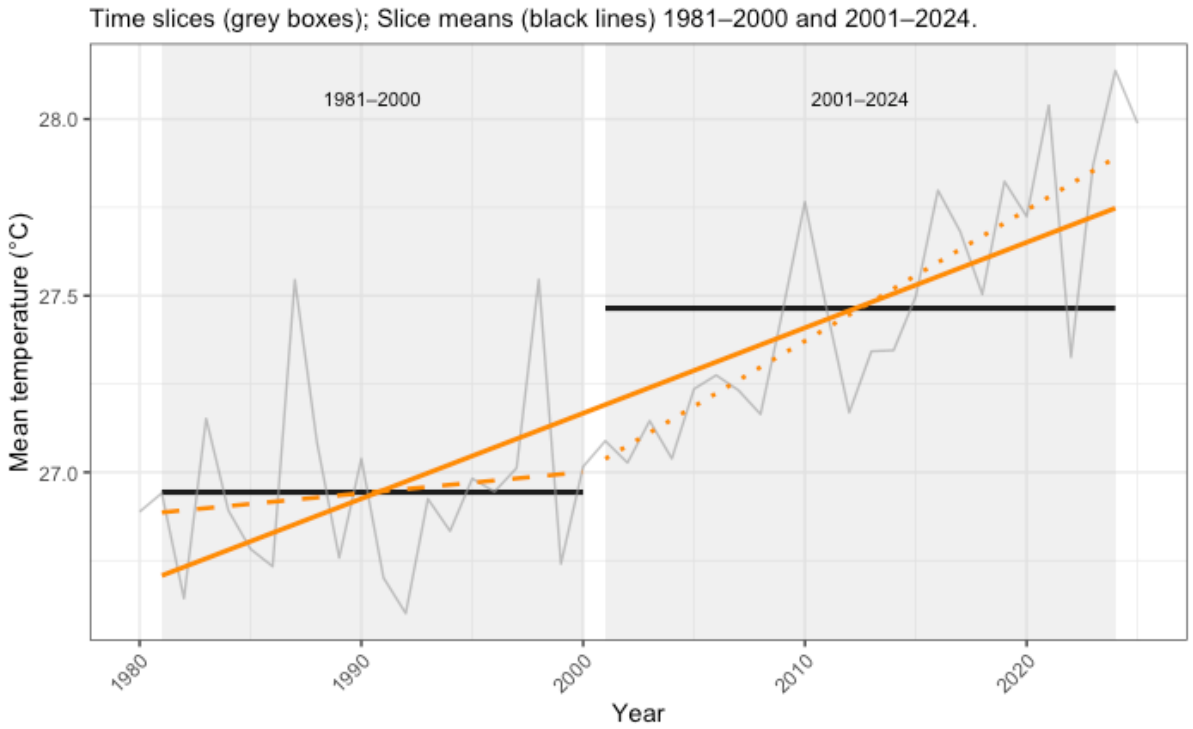

(Source: Own elaboration)

Future climate projections

For projections, we used the NASA NEX-GDDP-CMIP6 suite of models (Thrasher et al., 2022), a daily 0.25 degree (~28km at equator) downscaled, and bias-corrected dataset suited to regional climate analysis. Of more than 30 general circulation models (GCMs) available in this dataset, we selected 5 (GFDL-ESM4, IPSL-CM6A-LR, MPI-ESM1-2-HR, MRI-ESM2-0, UKESM1-0-LL) to represent a range of sensitivities to anthropogenic emissions and corresponding climate change predictions. Data in the NASA NEX dataset come in two temporal blocks. 'Historical experiments' (1950-2014) are those for

which GCMs are forced with observed / estimated greenhouse gas emissions (GHGs), aerosols and other contributions to climate processes (e.g., land-use). These are validated against historical climate observations. Future projections are represented by the 'scenario experiments' (2015-2100), for which GCMs are forced by estimates of greenhouse gas emissions from the various sectors according to different socio-demographic and emissions trajectories embedded in the shared socioeconomic pathways (SSPs) framework. GCMs have differing sensitivities to the effects of these forcings, providing a range of predictions about future climate responses under each SSP (Kyu et al., 2025).

For the projections block, we used two of the four "Tier 1" greenhouse gas emissions scenarios for our analyses: SSP2-4.5 (middle of the road) and SSP5-8.5 (fossil-fuelled development). Variables extracted matched those from the MSWX historical dataset (as below 8.4.3.1). For summaries, we again use averages to capture variation for 20-year time slices covering the period of interest (1981-2060) and trend tests to assess change for the projection block within the study focal period (2015-2060). The process of generating and summarising climate projections (including model results) is illustrated in

Figure 13 - Example time series for climate / model projections. Illustrates time slices (grey boxes) used for summary statistics (boxplots). Faint grey lines are individual GCMs. Solid lines are ensemble means for each scenario

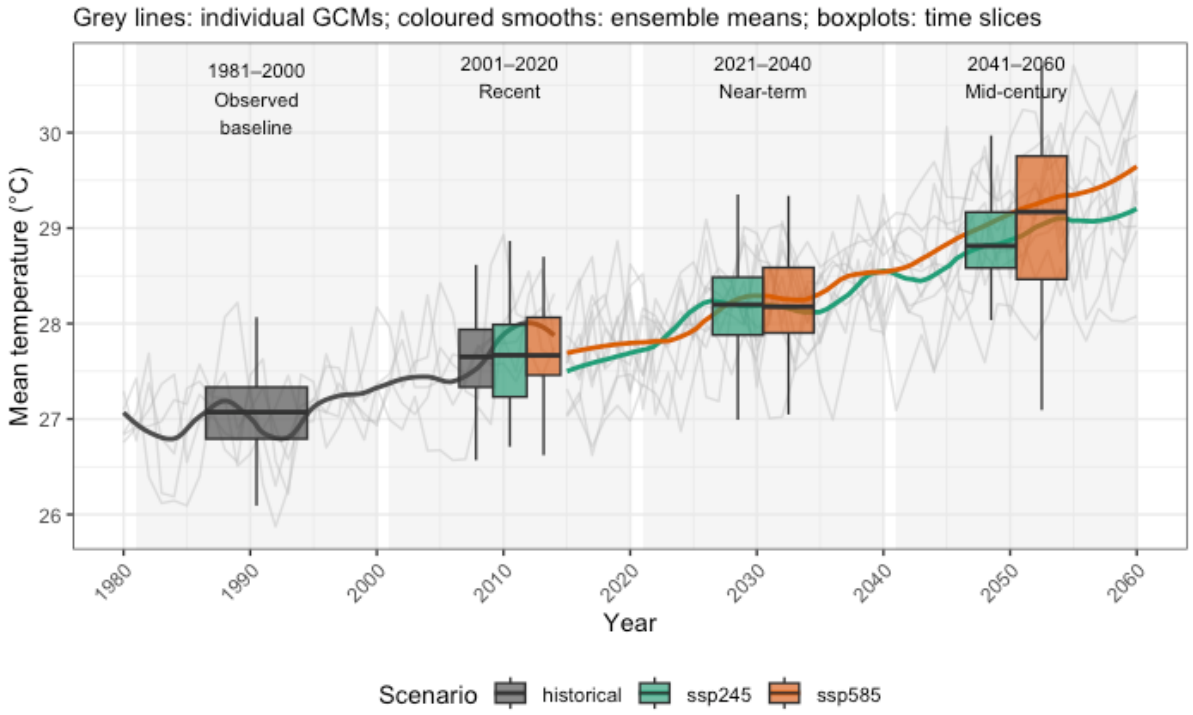

(Source: Own elaboration).

Climate Metrics Calculation

From the daily climate variables extracted from MSWX (historical) and NASA NEX-GDDP-CMIP6 (projections), we derived a suite of climate metrics relevant to health impacts. All calculations were performed at the grid cell level (0.1° for MSWX; 0.25° for NEX-GDDP) before aggregating to prefecture level for subsequent analysis. The baseline period for calculating thresholds and defining extreme events was 1981-2000 for both MSWX historical data and NEX-GDDP data.

Core climate variables

Monthly mean values were calculated for temperature (mean, maximum, minimum), precipitation,

relative humidity, and daily temperature range (Tmax - Tmin). These provide the foundational measures used in trend analysis and as inputs to epidemiological models.

Extreme temperature events

Hot days were defined using percentile-based thresholds calculated from daily maximum temperature (Tmax) during the three hottest months of the year within the baseline period for each prefecture. Thresholds were calculated at the 90th, 95th, and 99th percentiles. A hot day occurred when daily Tmax exceeded the relevant threshold. Hot days were summed monthly to provide counts of days exceeding each percentile threshold.

Heatwaves were identified using a two-stage algorithm. First, consecutive hot day sequences were identified (≥2 consecutive days exceeding the relevant Tmax percentile threshold). Second, heatwave events were flagged at the start of each consecutive sequence. Heatwave metrics included: (1) binary indicator of any heatwave occurrence within a month (yes/no), (2) count of heatwave events initiated in each month, and (3) total number of heatwave days within each month. These were calculated separately for the 90th, 95th, and 99th percentile thresholds.

Extreme precipitation events

Extreme precipitation days were defined analogously to hot days, using the three wettest months within the baseline period to establish prefecture-specific percentile thresholds (90th, 95th, 99th) for daily precipitation. Days exceeding each threshold were summed monthly.

Compound dry-hot days (CDHD)

Compound dry-hot days represent periods of concurrent heat stress and water scarcity, calculated using calendar-day-specific thresholds for maximum temperature. For each calendar day (1-366), Tmax thresholds were calculated at the 90th, 95th, and 99th percentiles across all years in the baseline period. A CDHD occurred when: (1) daily Tmax exceeded the calendar-day-specific threshold, AND (2) the preceding 10-day cumulative precipitation was less than 5mm. CDHD events were summed monthly for each percentile level.

Aggregation and outputs

All daily-level metrics were aggregated to monthly summaries at the prefecture level using spatial averaging (weighted by grid cell area where appropriate). For MSWX data, we generated complete monthly time series from 1980-2025 for all 39 Togolese prefectures, and for NEX-GDDP projections, we generated monthly time series from 1950-2100 under historical, SSP2-4.5, and SSP5-8.5 scenarios for each of the five selected GCMs (GFDL-ESM4, IPSL-CM6A-LR, MPI-ESM1-2-HR, MRI-ESM2-0, UKESM1-0-LL). Monthly datasets included all core climate variables and derived extreme event metrics, providing comprehensive inputs for subsequent epidemiological modelling and risk assessment.

4.4.4 Socioeconomic and health data sources and processing

National Institute of Statistics and Economic and Demographic Studies (INSEED) Census 2022

Household geographic coordinates (longitude and latitude) were used to assign each record to the corresponding prefecture or canton due to slight mismatches in area names and codes between datasets. Population estimates were then calculated at the prefecture/canton level, both overall and for specific demographic subgroups (e.g., children under five years of age, women of reproductive age), using the weighting factors provided in the dataset. At the same administrative level, proportions of selected vulnerability indicators (e.g., access to air conditioning, use of improved drinking water sources) were computed at the household level (INSEED, 2022).

District Health Information system (DHIS2)

Data extraction from the DHIS2 platform (DHIS2, 2025) was conducted at the prefecture level and at a monthly resolution, covering the period from January 2018 to August 2025. Following download,

variables were aggregated and compiled to enable analysis at consistent spatial scales. Prefectures were classified into each of the five regions. Data was available for 39 prefectures. The lowest available event count value was 1 rather than 0. The presumption of NA being 0 was decided individually per outcome.

Malaria Indicator Survey (MIS)

Data extraction from the 2017 MIS began by merging the individual (PR), household (HR) and children's (KR) recodes using unique cluster, household, and child identifiers (The DHS Program, 2017). Individuals were restricted to children under 5 years and while key malaria biomarker variables and other specified socioeconomic and environmental covariates were included, all other redundant variables were removed. The linked dataset was then merged with DHS cluster GPS coordinates and cleaned further by converting variables into categorical formats, collapsing sparse categories, and computing derived covariates such as wealth, education, and housing quality. Variables were then aggregated to the cluster level, of which there were 141, covering 39 prefectures.

Published data sources

Access to healthcare facilities was estimated using a published dataset compiled by the Malaria Atlas Project, estimating travel time in minutes to the nearest facility using motorised vehicles (Weiss et al., 2020). Data, originally available at a 1km spatial resolution, was averaged across prefectures. The calculation was made as a function of distance, land cover and topography, among other factors.

Access to improved housing material was also derived from a published Bayesian analysis based on results of various public health surveys including the Demographic and Health surveys (DHS) and Multiple Indicator Cluster surveys (MICS). Although available at a 0.05 decimal degree resolution, values were again averaged over prefectures. The coverage of improved walls, floors and roofs was averaged to produce a composite improved housing index. Detailed calculation methodologies for both indicators are available in respective publications (Colston, 2024; Weiss et al., 2020).

4.5 Risk Models

Our analysis workflow for risk modelling was separated into two stages. Stage 1 comprised assembly of data according to each of the hazard, exposure and vulnerability components outlined above, followed by overlays to provide a preliminary risk assessment. Results of the Stage 1 analysis were used to prioritise regions and inform epidemiological model development (e.g. vulnerability factor selection), which was conducted in Stage 2. Each stage is described separately in more detail in the sections below.

For both stages, we followed the above-described IPCC definitions of hazard, exposure and vulnerability. These differ considerably from similar terminology conventionally used in the public health/epidemiological literature. These differences are summarized in
Table 3 below to avoid confusion.

Table 3. Comparison of terminology used in climate change risk assessment (e.g., IPCC) vs public health / epidemiology.

Term	IPCC AR6 meaning	Epidemiology / public health meaning	Notes for this Climate Rationale
Hazard	Climate/physical driver with potential to cause harm (e.g., heatwave, extreme rainfall, climate-driven vector suitability)	Often the agent or dose (e.g., heat index, pathogen or toxicological concentration)	In modelling, dose/contact is usually handled inside the hazard or disease model.

Exposure	People/assets co-located with the hazard in space/time	Measured contact with an agent (dose, duration, timing)	Exposure = who/where/when (population/person-days). Do not re-count dose as “exposure.”
Vulnerability	Propensity to be harmed; composed of Sensitivity and Adaptive capacity	Effect modifiers	
Risk	Potential for adverse consequences as a function of H × E × V	Probability or rate of an outcome (incidence, risk ratio, hazard rate)	We label map products as “risk index (HxExV)”; or specific modelled parameters (incidence/cases/burden).

(Source: Own elaboration)

4.5.1 Climate hazards

Climate hazard information was typically calculated directly from climate data products. These were tailored by health outcome for preliminary presentation purposes, before being incorporated into models and subsequently updated or refined as required. Hazard metrics are intended to isolate the climate-specific factor(s) that are proximate to a health impact, and as such could be purely physical (e.g., extreme temperature) or biophysical (e.g., suitability for disease transmission).

4.5.2 Exposure groups (population at risk, PAR)

The focal population group considered as our ‘Exposure’, was those for which climatic hazards posed the greatest risks. These populations at risk were considered as children under 5 years for malaria and diarrhoeal diseases, and pregnant mothers and foetuses for preterm birth.

Evidence supports these groups being among the most vulnerable to the impacts of climate change and climate-sensitive health outcomes. In Sub-Saharan Africa children, especially under 5’s, are disproportionately impacted by infectious diseases including malaria and diarrhoeal diseases, which are among the leading causes of death in this age group (Kyu et al., 2025; World Health Organization, 2025d). Pregnant women and infants are especially vulnerable to the health harms resulting from climate change including preterm birth, small for gestational age, hypertensive disorders, and other adverse birth and maternal outcomes (Lakhoo et al., 2025).

4.5.3 Vulnerability factors

Vulnerability to health risks can be disaggregated into two broad categories – sensitivity and adaptive capacity following AR6 terminology (Pörtner & Löschke, 2022). Sensitivity (also known as susceptibility) factors are those that lead an individual to be more likely to be negatively affected by a condition. These can refer to the social, environmental and biological determinants of health that might predispose or increase a person’s risk of a negative health outcome. Adaptive capacity refers to an individual’s ability to prepare for hazard and respond to the consequences of ill health. This can refer to a person’s access to health care including prevention measures and treatment.

Vulnerability factors included here are factors that predispose an individual to infection with malaria, diarrhoea, or preterm birth and the selection was tailored to each health outcome based on the global and regional literature. Some determinants such as wealth, education or age are shared across all three conditions, influencing both underlying susceptibility and the capacity to seek prevention or care. Others are condition-specific, such as WASH exposures for diarrhoeal disease or mosquito-net use for malaria. Distinguishing these shared and specific factors helps clarify how populations may experience overlapping or unique vulnerabilities.

Sensitivity/susceptibility

We identified several sensitivity pathways conferring vulnerability to the three selected health outcomes:

Demographic characteristics: Age, sex and ethnicity influence biological susceptibility across the three outcomes. For malaria, young children and older adults are at greater risk because of immature or

waning immunity (Ranjha et al., 2023). For diarrhoeal diseases, younger children have a higher likelihood of infection due to underdeveloped immune systems (Worede et al., 2025) For heat-related outcomes, maternal age contributes to the risk of preterm birth, with both younger and older mothers showing increased vulnerability (Behrman RE, 2007). These demographic factors therefore shape the baseline level of sensitivity across all conditions.

Socio-economic status: Socio-economic conditions such as poverty and low educational attainment influence vulnerability across malaria, diarrhoeal disease and heat-related outcomes. Poverty limits access to resources, safe environments and preventive measures, while education shapes awareness of disease risks and health-promoting behaviours. For example, maternal education and household poverty are consistently associated with diarrhoea prevalence in children under five (Worede et al., 2025). Similar socio-economic gradients are observed in malaria risk, as lower-income households often experience greater exposure to mosquitoes and have fewer protective options (Gaston & Ramroop, 2020). For heat-related preterm birth, poverty can exacerbate exposure to high temperatures due to poorer housing quality and limited ability to mitigate heat stress (Brimicombe et al., 2024; Chersich et al., 2022).

Health status: Underlying health conditions modify susceptibility to all three outcomes, often by compromising immune function. In malaria, pregnant women are more likely to experience severe disease due to immunological changes (Schantz-Dunn, 2009). In diarrhoeal disease, chronic illness and malnutrition elevate risk and severity (Kyu et al., 2025). For heat-related preterm birth, maternal comorbidities such as hypertension or gestational diabetes may increase sensitivity to thermal stress. Health status thus interacts with environmental and social factors to shape individual vulnerability (Li-Maloney et al., 2025)

Environmental and household conditions: These represent a major pathway through which exposure occurs, but the relevant factors differ by health outcome. For diarrhoeal disease, WASH-related determinants such as unimproved water sources, inadequate waste management, and lack of sanitation, substantially increase susceptibility, while overcrowding facilitates the spread of enteric pathogens (Worede et al., 2025). For malaria, housing structure affects mosquito entry; poor ventilation, broken screens or open eaves heighten exposure to vectors and therefore susceptibility to infection (Snyman et al., 2015). For heat-related preterm birth, high household temperatures, poor ventilation, and low-quality construction materials can intensify heat exposure and physiological stress on pregnant women (Behrman RE, 2007). Although these environmental pathways differ across diseases, they all demonstrate how living conditions shape sensitivity.

Adaptive capacity

Access to care: Timely and appropriate healthcare reduces vulnerability to adverse health outcomes by enabling diagnosis, treatment and routine preventive care. Limited access, whether due to distance to facilities, shortages of trained personnel, or financial barriers, heightens vulnerability across all three outcomes (Levesque et al., 2013).

Service readiness: Similarly to access to care, service readiness can affect the outcome of many health conditions. Service readiness including; availability of medicines, equipment, diagnostics and trained staff, determines whether individuals receive effective care once they reach a facility. Well-equipped services can reduce vulnerability to malaria through rapid diagnostic testing and appropriate treatment, manage dehydration and infections associated with diarrhoea, and provide supportive care for pregnant women exposed to extreme heat (Kimario et al., 2024; Ssempiira et al., 2018).

Protective interventions: Protective factors will reduce an individual's vulnerability to disease. There are many potential interventions, which differ based on health conditions. For malaria, long-lasting insecticidal nets (LLINs) and other vector-control measures decrease exposure to mosquito bites and are strongly associated with reduced incidence (Ranjha et al., 2023). For diarrhoeal disease, vaccination, improved water treatment and sanitation facilities, and breastfeeding, which strengthens immunity, provide important protection. For heat-related preterm birth, adaptive measures such as indoor cooling strategies, increasing urban green space and improving clinician-patient education can reduce maternal heat exposure (Li-Maloney et al., 2025).

Static, prefecture-level data for the majority of these factors were derived from INSEED census (2022), DHIS2 (2018-2025) or the MIS (DHS) (2017-2018) datasets. In some cases, we also accessed published datasets available via the peer reviewed literature (e.g., travel time, improved housing).

4.5.4 Stage 1: Preliminary risk assessment and regional prioritisation

Preliminary climate risk mapping followed the IPCC risk assessment framework, where overall risk is conceptualised, as described in detail above, as:

Risk = Hazard × Exposure × Vulnerability

Assessments were conducted at the prefecture level to match the highest common spatial resolution available across indicators. Variables available at higher resolution were aggregated to prefectures. Regional level summaries are provided to facilitate evaluation of priority regions. This stage also facilitated the assembly of important Stage 2 model components, concerned with the future projection of health risks. Therefore, this initial risk assessment stage was conducted only at the recent temporal scale.

Hazards

Malaria
Climate suitability for malaria transmission was represented by an indicator representing length of the transmission season (LTS), defined as the number of months per year satisfying concurrent temperature, precipitation and relative humidity conditions. For LTS, climate variable ranges and thresholds followed the Lancet Countdown malaria indicator (LCMI), which defines suitable transmission conditions as the coincidence of monthly precipitation ≥80 mm, mean temperature 18–32 °C, and relative humidity ≥60% (Colón-González et al., 2021). The combined values are considered indicative of the lower limit for *P. falciparum* transmission in sub-Saharan Africa. With this indicator, areas with increasing LTS are considered to be of generally increasing suitability from a climatic perspective for malaria transmission, and those with decreasing LTS, generally decreasing suitability.

Diarrhoea
Two diarrhoea-relevant hazard pathways were considered to capture distinct biophysical mechanisms. A 'wet contamination' pathway was used to represent flooding/heavy-rain processes that mobilise pathogens and compromise water quality (Cann et al., 2013; Carlton et al., 2014). The primary hazard indicator is the frequency of days with 1-day rainfall/precipitation exceeding the 90th percentile (relative to local historical baseline). A 'hot–dry' pathway was used to represent scarcity/concentration mechanisms where heat and lack of rainfall jointly elevate risk (Yu et al., 2025; Yusa et al., 2015). Hot and dry conditions are hypothesised to increase diarrhoea risk because water scarcity concentrates pathogens in limited water sources, increasing exposure risk; while high temperatures accelerate bacterial growth in food and water, amplifying contamination and exposure. The primary hazard indicator is days when the maximum daily temperature exceeds the 90th percentile (relative to local historical baseline) and the trailing 10-day precipitation sums to less than 5 mm.

Preterm birth
A range of indices have been used to assess the impacts of heat on maternal-child health outcomes, including dry-bulb air surface temperature, heat index, apparent temperature, wet bulb globe temperature and universal thermal climate index (Brimicombe et al., 2024), which incorporate factors such as humidity, radiation and wind. However, there is currently no consensus on the most appropriate heat metric to use in the epidemiological assessment of heat-related PTB risk. Unpublished comparisons of heat metrics in the maternal and perinatal health field suggest that dry-bulb air temperatures provide the most precise effect estimates. Further, most published studies utilise mean or maximum air temperatures, which enables systematic assessment of health impacts attributable to an additional 1°C increase in temperature or to heatwave events (Del Carretto et al., 2025). Despite definitions of heatwaves varying by number of days and exceedance thresholds, we selected an

indicator suitable for identification of extended heat shock events (≥2 consecutive days) at a monthly temporal scale. This heatwave definition aligns with previous literature in this field (Chersich et al., 2022; Lakhoo et al., 2025).

Overall, one hazard indicator was selected for malaria (LTS), two for diarrhoeal disease (extreme precipitation days; compound hot and dry days), and one for preterm birth (number of heatwaves). These metrics were calculated and averaged separately across the most recent 20-year period of available observed climate data (2001 – 2024) and the historical reference period (1981- 2000). The difference in means between these two periods was used as a 'change indicator' to capture areas experiencing the most significant climatic changes and therefore necessitating a greater rate of adaptation. Such an indicator has previously been used in hazard maps for Togo (PROVIDE, 2025) Details for the calculation of individual hazard indices are given in Section 4.4.3: Climate Metrics Calculation).

Exposure

Exposure population was derived as the proportion of the target group within the total population by prefecture, to highlight areas with relatively higher concentrations of populations at risk. For Stage 1 prioritisation, exposure was expressed in relative terms rather than absolute population counts, to support comparative risk screening across prefectures. For malaria and diarrhoeal disease, we calculated the proportion of children under 5 years of age relative to the total population (Kouakou, 2024) from the 2022 INSEED census data. For preterm birth, we calculated the proportion of live births relative to the population of women of reproductive age from 2024 DHIS2 data.

Vulnerability

Vulnerability factors for each outcome were selected following an evidence review and initial risk factor modelling. Initially, an inclusive set of candidate variables was identified and then prioritised on the basis of 1) diverse causal pathway representation (Appendix 1, Table 8), 2) suitable data availability, 3) presence of sufficient variability in the distribution of values (approximate normality preferred) and, 4) minimisation of collinearity (pairwise Pearson correlation analysis $r<0.8$). Indicators were classified as either 'sensitivity' or 'adaptive capacity' indicators based on their dominant role in the causal pathway, recognising that some variables (e.g. education, service coverage) influence risk through multiple mechanisms.

Five vulnerability indicators were subsequently selected per health outcome. For malaria, these included low household wealth, low caregiver education, poor housing quality, low insecticide treated bed net (ITN) ownership and low healthcare access (defined by travel time). For diarrhoeal diseases, selected factors included household overcrowding of children under 5 years, lack of exclusive breastfeeding, unimproved water and sanitation facilities and low healthcare access (defined by travel time). Finally, preterm birth vulnerability factors included low household wealth, no formal maternal education, low maternal age (defined by adolescent motherhood), lack of A/C facilities and lack of timely healthcare access (first trimester antenatal care visits were used as a proxy for timely access throughout pregnancy). Vulnerability factors selected in Stage 1 were subsequently tested in Stage 2 models.

Risk mapping

All selected variables were standardised using the min-max method (scaled 0-1). Composite hazard and vulnerability scores were derived as the arithmetic mean of the contributing variables. Sensitivity analyses comprised assignment of random weights to the vulnerability factors to assess the robustness of the results to different weighting structures. In operational terms, standardised hazard, exposure and vulnerability indices were multiplied and re-standardised to give an overall composite risk score per prefecture, consistent with a screening-level application of the IPCC risk framework. The raw score was then reclassified into three risk levels (High, Medium, Low) using the Jenks method, which groups data into a pre-specified number of classes by minimizing the variance within each class while maximizing the variance between classes. Hazard, exposure and vulnerability indices were averaged across regions, re-standardised and combined into a composite index using the same steps as for prefecture-level scores.

Figure 14 to Figure 16 summarise the key hazards, exposures and vulnerabilities used in the Stage 1 risk assessment for each health outcome. Table 4 details the metrics, definitions and data sources used.

The impact chains presented below take the before mentioned hazard, vulnerability and exposure factors, and visually represent how these factors can potentially increase the risk of incidence of the three health outcomes. These impact chains are representations for the risk maps and factors that were considered in the modelling, and so only contain the factors that have been accounted for in these sections. The impact chains also highlight the roles of adaptive capacity and sensitivity/susceptibility within the wider category of vulnerability.

Figure 14 - Impact chain – risk of malaria

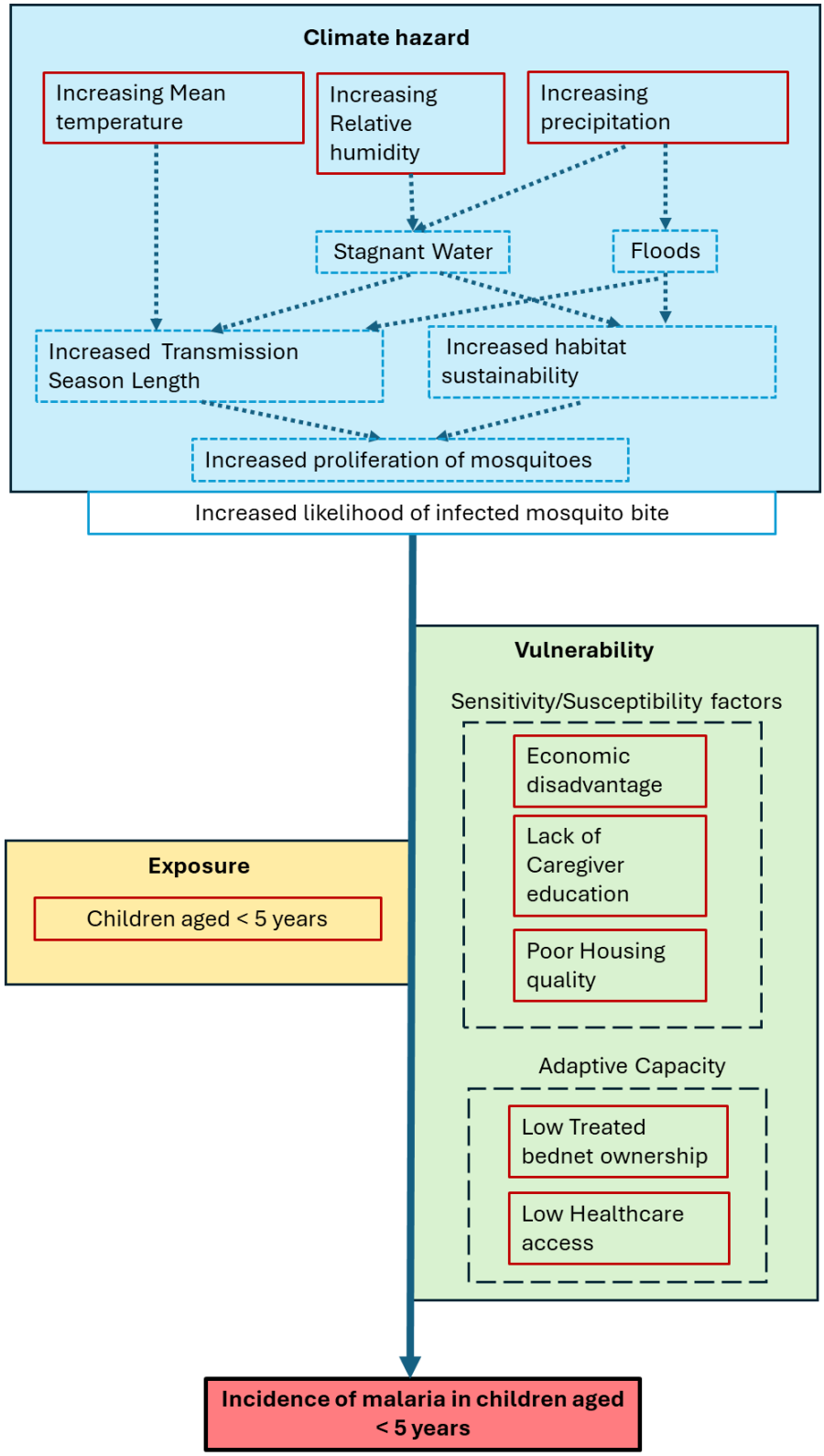

(Source: Own elaboration)

Figure 15 - Impact chain – risk of diarrhoeal disease

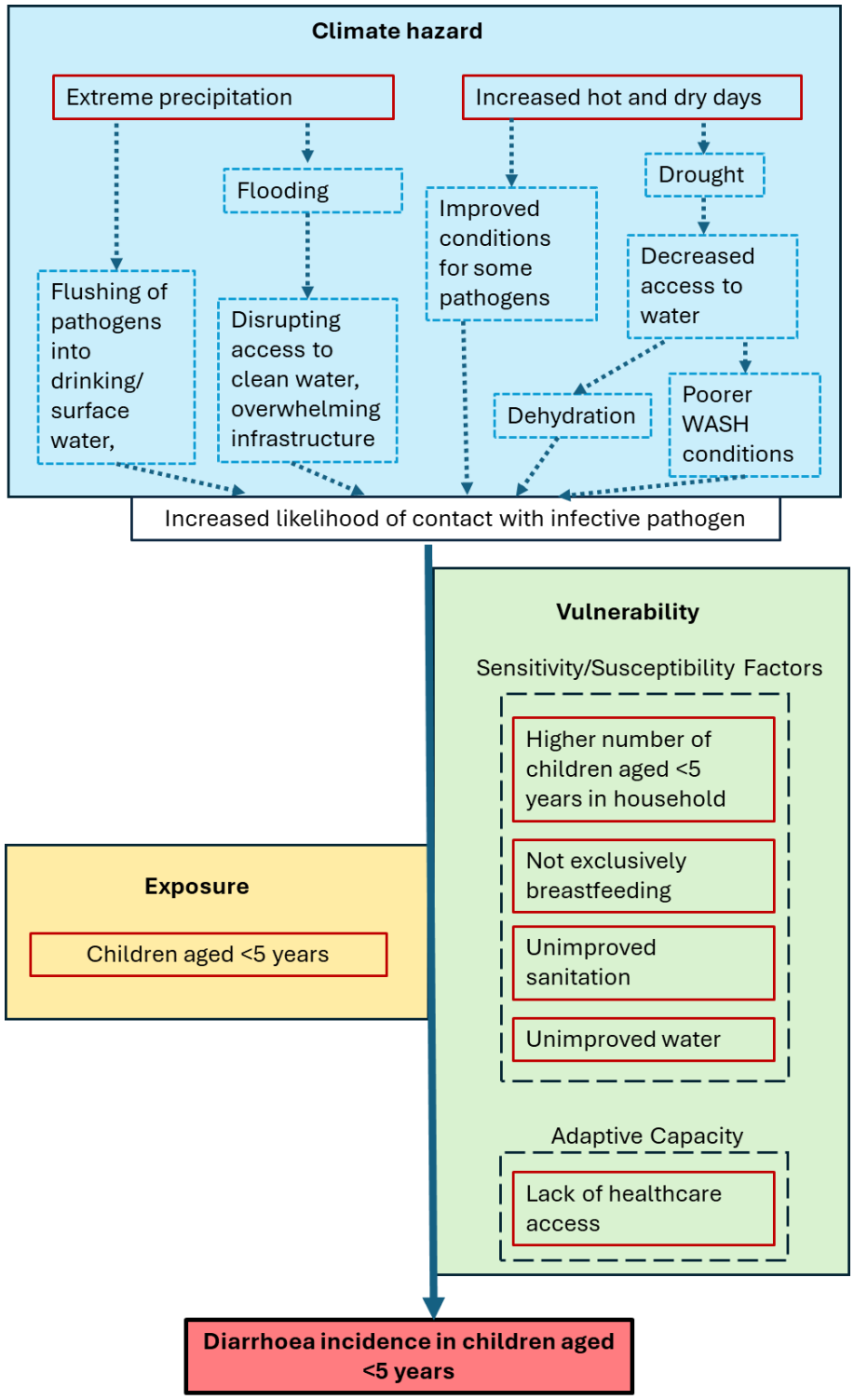

(Source: Own elaboration)

Figure 16 - Impact chain – risk of preterm birth

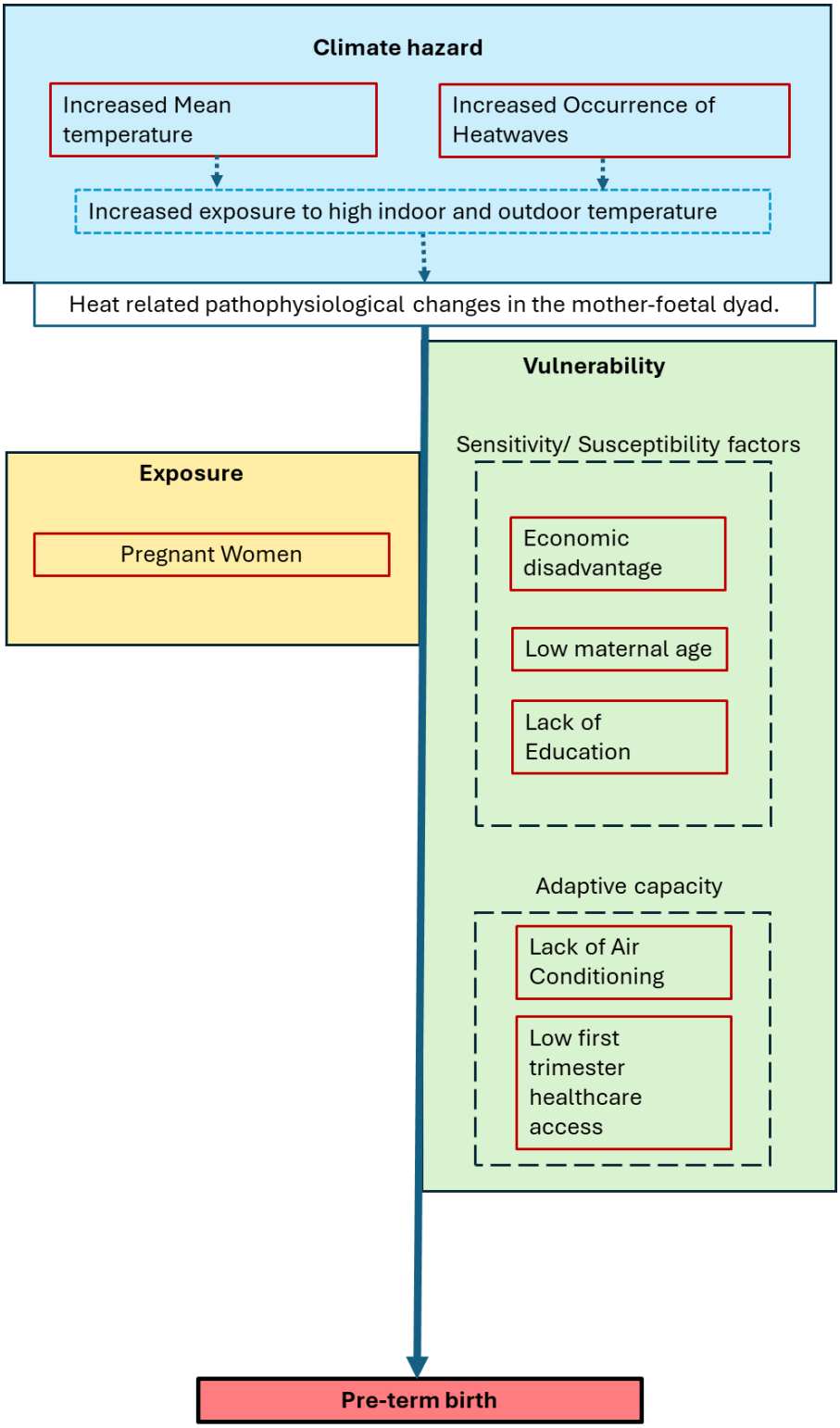

(Source: Own elaboration)

The table below summarises the concepts included in the impact chains, and the data sources for each of these indicators.

Table 4 - Summary of components in stage 1 composite risk scores

Health outcome	Component	Variable name	Additional details	Indicator	Source
Malaria	Hazard	Length of the Malaria transmission season (LTS)	Coincidence of mean monthly temperature 18-32°C; mean monthly precipitation ≥ 80 mm; Mean monthly relative humidity ≥ 60% - averaged across recent (2001-2024) and historical reference (1981-2000) periods. The difference was taken between these means.	Difference in mean number of months per year suitable for malaria transmission between recent and historical reference periods	MSWX 2005-2024
	Exposure	Children under 5 years	Relative to the total population	% children under 5	INSEED census, 2022
	Vulnerability	Wealth/socio-economic status	Derived as a score between 0-5, whereby higher scores denote greater wealth.	Wealth score	MIS, 2017
		Caregiver education	Derived as a score between 0-3, with 0 being no education, 1 primary education, 2 secondary education and 3 tertiary education. Averaged across prefectures.	Education score	MIS, 2017
		Insecticide-treated mosquito bed net utilisation		% coverage of mosquito bed net usage	MIS, 2017
		Housing quality	The prefecture level coverage of improved floor, wall and roof material was averaged to obtain a composite score.	% coverage of households with access to improved housing	(Colston, 2024)
		Healthcare access	The time (in mins) using motorised transportation to access nearest healthcare facility was averaged over the prefecture level.	Motorised time (in mins) to healthcare	Malaria Atlas Project, 2020
Diarrhoea	Hazard	Extreme precipitation days	Days with rainfall above the 90th percentile of the historical baseline - averaged across recent (2001-2024) and historical reference (1981-2000) periods. The	Difference in mean number of days per year of extreme precipitation between recent	MSWX 2005-2024

			difference was taken between these means. The difference was taken between these means.	and historical reference periods	
		Compound hot and dry days (CHDH)	Days when Tmax > 90th percentile of the historical baseline and the trailing 10-day precipitation sum < 5 mm - averaged across recent (2001-2024) and historical reference (1981-2000) periods. The difference was taken between these means.	Difference in mean number of CHDH events per year between recent and historical reference periods	MSWX 2005-2024
	Exposure	Children under 5 years	Relative to the total population.	% children under 5	INSEED census, 2022
	Vulnerability	Exclusive breastfeeding		% of mothers practising exclusive breastfeeding	DHIS2, 2024
		Improved drinking water facilities	Includes access to improved piped and improved other facilities.	% coverage of households with access to improved drinking water facilities	INSEED census, 2022
		Improved toilet facilities	Includes access to improved sewer/septic and improved other facilities.	% coverage of households with access to improved toilet facilities	INSEED census, 2022
		Household crowding of children under 5 years		Mean household number of children under 5 years	INSEED census, 2022
		Healthcare access	The time (in mins) using motorised transportation to access nearest healthcare facility was averaged over the prefecture level.	Motorised time (in mins) to healthcare	Malaria Atlas Project, 2020
Preterm Birth	Hazard	Heatwaves	Heatwave event defined as ≥2 consecutive hot days (Tmax above the 95th percentile of the historical baseline) - averaged across recent (2001-2024) and historical reference (1981-2000) periods. The difference	Difference in mean number of heatwaves per year between recent and historical reference periods	MSWX 2005-2024

			was taken between these means.		
	Exposure	Live births	In women of reproductive age population (15-49)	% of live births per woman	DHIS2, 2024
	Vulnerability	Wealth/socio-economic status	Derived as a score between 0-5, whereby higher scores denote greater wealth.	Wealth score	MIS, 2017
		Caregiver education		% of mothers who never attended school	INSEED census, 2022
		Maternal age	High or low maternal age were selected. However, high maternal age was not available in the data.	% of adolescent mothers (≤19 years)	INSEED census, 2022
		Air conditioning (A/C) usage		% of households with A/Cs	INSEED census, 2022
		Healthcare access	Access to timely healthcare in the first trimester is taken as a proxy for access throughout the pregnancy.	% of births with access to antenatal care in the first trimester	DHIS2, 2024

(Source: Own elaboration)

4.5.5 Stage 2: Epidemiological Modelling

Malaria

Malaria data

We noted some inconsistency of results in previous studies from existing malaria models for Togo (trends and associations with select socio-economic and climate variables). This could conceivably arise due to a large range of factors. Of the malaria datasets available for Togo, the monthly prefecture scale data available in the DHIS2 dataset was considered to be a good balance between data consistency over the time periods available, of a sufficient temporal resolution relevant to malaria epidemiology and for isolating climate signals suited to climate projections, and of sufficient spatial coverage (national). As such, for this analysis, monthly, prefecture-level under-5 malaria confirmed case counts for Togo were obtained from the DHIS2 for all prefectures and the full period available (January 2018 – August 2025). Corresponding under-5 population estimates for each prefecture were also obtained from DHIS2 for the same years and used to calculate and model incidence (cases per child <5 years).

Climate and environmental data

For Stage 2 modelling, we did not use the composite indicator (LTS) used in Stage 1 and instead allowed the model to determine the best fitting climate response associations given the data. For model training, we used the high-resolution daily (MSWX) data aggregated to months and prefectures, as described in 8.4.3.1. Climate variables selected for malaria modelling included: mean, minimum and maximum temperature (°C), temperature range (Tmax-Tmin) (°C), precipitation (mm/day), relative humidity (%) in addition to selected temperature and precipitation extremes. In addition, we obtained monthly time series data for the normalised difference vegetation index (NDVI) for Togo for the same period, again aggregating to monthly prefecture levels from the native 1km resolution dataset (Didan, 2021). All climatic and environmental variables were standardised (z-scores) prior to use in modelling.

Static covariates

Data on selected vulnerability factors identified in Stage 1 (section 8.5.4) were used as static socio-economic covariates for the malaria modelling. In addition, due to the inability to project NDVI into the future, we created a static NDVI variable by averaging across the monthly NDVI dataset to capture broad inter-prefectural differences. The final static covariate set included: mean travel time to a health facility, mean household wealth score, mean education score, mean housing quality index, and the proportion having slept under a treated bednet. None of the covariates were available as spatially explicit time-varying metrics and so were held constant for both the model training (2018-2024), and the projections (1950-2100).

Modelling climate-malaria associations

We modelled monthly counts of confirmed malaria cases in children under 5 at prefecture level using a spatio-temporal generalized additive model (GAM) framework with a negative-binomial family and log link. This approach is well suited to over-dispersed count data and allows flexible, non-linear relationships between the outcome and climate terms. A population offset (log(population <5)) was included so the model estimates incidence rather than raw counts. To capture temporal structure we used a smooth function of time for long-term trends, and a cyclic spline for month to model seasonality. We also included a random intercept for prefecture to allow for spatial heterogeneity and prefecture-specific temporal deviations. Climate terms, including both concurrent and lag-1 values, entered the model as smooths so we could flexibly estimate non-linear, potentially delayed effects without imposing *a priori* functional forms. Static (or slowly varying) covariates were included as linear terms. Incident rate ratios (IRR) were used to evaluate the strength and direction of term effects on the outcome.

Incorporating climate

We evaluated multiple specifications of the model by varying climate term combinations in a systematic variable selection step. This involved conducting sensitivity analyses around a core set of climate predictor variables grouped into blocks of similar variables (e.g., temperature block had mean, minimum and maximum temperature). To help minimise model complexity and concurvity, the starting model contained 1 variable per block, with all blocks included (temperature, temperature range, precipitation, relative humidity, extreme precipitation, extreme heat). From this, we selected a candidate set containing all models within AIC=10 of the best model. Next, we added the 1-month lag terms for all climate variables remaining in the candidate set and conducted a second search to identify the best models combining both contemporaneous and lagged terms. From this, a final subset of the most explanatory climate variables was obtained by model averaging, again over all models within AIC=10 of the 'best' model. The single best model following this procedure was then selected for further analysis, with sensitivity analyses later used to check the effect of including any highly ranked variables that were nevertheless not selected.

Future projections

Following model checking and validation (see below), the final GAM was predicted onto the full historical (1950–2014) and projected (2015–2100) NASA NEX CMIP6 climate data for each of the five GCMs and each of the two SSPs, giving 10 model runs in total spanning a 150-year time series. All static covariates were held constant at their values used in model training. Projections were visually inspected as raw time series of incidence (cases per 1000 population of children <5). Projections were summarised using the above time-slices and mapped at prefecture level for spatially explicit interpretation, reporting percentage change of incidence relative to the baseline period and reporting uncertainty (combining parametric and inter-model uncertainty). From the uncertainty metrics, we further calculated the probability of malaria incidence increasing from the most recent period (2001-2020) to the next two time slices (2021-2040; 2041-2060).

Validation

Usual model checks were performed to assess goodness of fit and explanatory performance, including residual diagnostics, checks for overdispersion and concurvity, and comparison of alternative specifications using AIC and deviance explained. Sensitivity analyses were used to confirm the robustness of key results.

We examined alternative offset specifications (using annual under-5 population versus mean population) and tested first-order autoregressive structures to account for temporal autocorrelation, as well as alternative spatial smooths using thin-plate splines. We then computed prefecture-level mean residuals and assessed spatial dependence using Moran's I. Finally, we performed temporal hold-out validation, fitting the model to data from 2018–2021 and evaluating short-term predictive performance on held-out data from 2021–2025. For projections, we assessed specifications with and without the long term and seasonal splines to allow additional variation to be attributed to the climate variables, We examined the risk of extrapolation by fitting a separate model in which each climate covariate in the projection dataset was clamped to its 5–95% range observed in the training data, and comparing these "clamped" projections to the original, unclamped predictions.

Diarrhoeal disease

Diarrhoeal disease data

For diarrhoeal disease, we followed the same general spatio-temporal modelling framework as for malaria, but applied to a different outcome and vulnerability profile. Monthly prefecture-level counts of reported diarrhoea cases were obtained from the national DHIS2 system for all prefectures and the full period available in the study window. Corresponding population estimates for the relevant age group were obtained from DHIS2 for the same years and used to calculate and model incidence (cases per person per month).

Climate and environmental data

Climate and environmental data for diarrhoea modelling were prepared using the same workflows as for malaria (high-resolution MSWX data aggregated to monthly prefecture-level time series). In addition to the core variables, we focused on diarrhoea-relevant hazard constructs identified in the literature review, specifically the wet contamination and hot–dry pathways described in the previous section (8.5.4). These hazard indices were derived from daily MSWX temperature, precipitation and humidity, aggregated to prefecture and standardised (z-scores) prior to inclusion in the models.

Static covariates

Static socio-economic and vulnerability covariates for diarrhoeal disease were derived from the Stage 1 vulnerability assessment, with an emphasis on WASH- and crowding-related factors rather than vector-control indicators. The selected covariates included: exclusive breastfeeding coverage, improved toilet (sanitation) coverage, improved water source coverage, travel time to motorised health care / transport and mean number of under-5 children per household. As with malaria, these covariates were only available as spatially explicit but time-invariant (or slowly varying) metrics, and were held constant over both the model training period and the projection horizon.

Modelling climate–diarrhoea associations

We modelled monthly diarrhoea incidence at the prefecture–month level using the same spatio-temporal generalised additive model (GAM) framework as for malaria: a negative-binomial family with log link and a population offset so that the model estimates incidence rather than raw counts. Temporal structure was represented with a smooth function of time to capture long-term trends and a cyclic spline for month to model seasonality, with a prefecture random intercept and prefecture-specific temporal smooths to account for spatial heterogeneity and local temporal deviations. Climate variables (including the wet-contamination and hot–dry indices, and concurrent and lag-1 values) entered the model as smooth functions of their z-scored values, allowing non-linear and potentially delayed effects without imposing *a priori* functional forms. The static vulnerability covariates were included as linear terms. Incident rate ratios (IRR) per 1-SD increase in each hazard index were used to quantify the strength and direction of associations with diarrhoea incidence.

Future projections and validation

Future projections and model validation for diarrhoeal disease followed the same general procedure as for malaria. After model checking and validation (including residual diagnostics, checks for overdispersion and concurvity, comparison of alternative hazard specifications using AIC and deviance

explained, and sensitivity analyses), the final GAM was projected onto historical and future climate scenarios using the diarrhoea hazard indices derived from NEX-GDDP-CMIP6 climate data, holding static covariates fixed at their training-period values. Projections were summarised for the predefined time slices and mapped at prefecture level as percentage changes in diarrhoea incidence relative to a baseline period, with uncertainty combining parametric and inter-model sources. Validation steps, including checks for spatial dependence of residuals (Moran's I), alternative offset specifications, alternative long-term and seasonal time specifications, temporal hold-out validation, and clamping of climate covariates to the observed 5–95% training range to assess extrapolation risk, were implemented analogously to the malaria workflow.

Heat impacts on preterm birth

Preterm birth data

Monthly, prefecture-level (n=39) counts of premature births (priority outcome) and live births (denominator) were obtained from the DHIS2, spanning January 2018 – December 2024. No zero counts were recorded in the raw data. Rare missing (NA) values were replaced with zeros after verifying that the number of live births in those months and prefectures was very small. This approach reflects the low baseline numbers of PTBs (minimum observed = 1) and the plausibility of true zero-case months in sparsely populated prefectures.

Climate and environmental data

For model training, we used the high-resolution daily MSWX data aggregated to months and prefectures, as described in 4.4.3. Three hazard families were considered. First, monthly mean Tmax (°C) as a continuous metric. Second, hot-day frequency: for each threshold (P90, P95, P99), the monthly hot-day count was the number of days with daily Tmax above that threshold. Third, heatwave events: for each threshold, a heatwave was defined as at least two consecutive days with Tmax above that threshold. Monthly summaries for heatwave hazard were (i) a binary indicator of any heatwave and (ii) the number (count) of heatwave events. During model training, all heat effect estimates were adjusted for monthly mean relative humidity (rh) as a time-varying confounder.

Static covariates

Prefecture-level, time-invariant vulnerability factors were derived from the Stage 1 vulnerability assessment. These included the percentage of mothers who never attended school, air conditioning (A/C) coverage, mean household wealth, coverage of first trimester antenatal care (ANC) attendance, and percentage of adolescent mothers. Our model training approach differed from that described above for malaria and diarrhoeal disease. In line with the most recent advances in epidemiological modelling of climate and non-communicable diseases, we applied a two-stage training approach involving a separate time-series regression model for each prefecture and meta-analysis of exposure-lag-response functions. Prefecture-level static covariates were therefore adjusted for, by design, and potential moderating effects were assessed through stratification at national level.

Modelling heat-preterm birth associations

We modelled monthly counts of live PTBs within each prefecture using a quasi-Poisson generalised linear model with log link to account for overdispersion inherent in count data. A population offset (log(live births)) was included to estimate rates rather than raw counts. This is particularly important for birth outcomes as the population at risk (live births) shows strong seasonal variation in many contexts. A Distributed Lag Non-linear Model (DLNM) with 0–8 month lags was used to capture potential delayed and cumulative effects of heat throughout pregnancy. Heat may act through early-gestation pathways (e.g., placentation, placental perfusion, inflammation) as well as late-gestation mechanisms related to thermoregulatory or uterine stress. Because the timing of vulnerability is uncertain and likely multifaceted, the 0-8-month window approximates the full gestation period and allows both immediate and delayed effects to be estimated.

Modelling the heat-PTB association within each prefecture separately allowed for spatial heterogeneity. Prefecture-specific log rate ratios and standard errors were then pooled using random-effects meta-

analysis to produce national estimates. Prefectures with more than 10 NA/0 months were excluded. Best linear unbiased predictions (BLUPs) were derived to stabilise estimates in prefectures with few PTB cases; shrinking imprecise estimates toward the national meta-analytic mean while preserving genuine spatial variation.

To avoid collinearity, each hazard metric was analysed in a separate model. Preliminary analyses were conducted to select the most appropriate heat metric on which to base the future projections. When aggregating continuous daily temperature metrics (e.g. Tmax) to monthly temporal resolution, short-term extreme events are "averaged out", hindering detection and assignment of temperature extremes. Ultimately, a binary heatwave metric (at least one heatwave of ≥2 consecutive days with Tmax >P95) was selected to adequately capture acute heat-shocks, maximise model stability, and to align with published global estimates (Chersich et al., 2022; Lakhoo et al., 2025).

The single best-fitting model was selected through minimisation of AIC and residual diagnostic testing. The final model estimated the association between monthly heatwave exposure during pregnancy and PTB. The hazard was defined using a binary heatwave indicator (any heatwave vs no heatwave in a given month). The exposure-response was modelled using a linear term (consistent with the binary heatwave metric), while the lag-response over gestation (0-8 months) was captured using a natural cubic spline with two internal knots. Models adjusted for seasonality (calendar month). Long-term trends (calendar year), and mean relative humidity over pregnancy (spline, 2 df). Results are presented as lag-specific incidence rate ratios (IRRs) for each gestational month (0-8-month lags), and as a cumulative IRR summarising the overall effect of heat hazards throughout pregnancy, with 95% confidence intervals.

Prefecture-level, static vulnerability factors, were tested for effect modification using meta-regression. Pooled cumulative IRR estimates were based on stratification of prefectures; classification was based on whether the vulnerability factor for the prefecture was below or above the median. Vulnerability factors not appearing to significantly alter the heatwave-PTB relationship were omitted from the future projections.

Future projections

Future projections used the 150-year monthly heatwave time series (1950-2100) derived from CMIP6 historical (1950-2014) and future (2015-2100) climate model outputs. For each prefecture, month, and scenario, heatwave indicators were lagged 0-8 months to align exposure in each gestational month with the corresponding month of birth. These lagged exposures were then combined with the prefecture-specific lag-response functions from the DHIS2-based DLNM to estimate monthly heatwave effects.

Monthly prefecture live births were generated by first bias-correcting SSP-specific 1-km WRA projections to the 2022 INSEED census and raking them annually to follow UN WPP 2022 trajectories while preserving spatial variation. These corrected WRA surfaces were combined with census-derived under-1/WRA fertility multipliers to disaggregate UN WPP national births for 1950-2021, and were extended using SSP-specific WRA–TFR projections for 2022-2100. Because DHIS2 (2018-2024) showed strong and persistent seasonality in deliveries, prefecture-specific monthly birth proportions were applied to each annual prefecture-year-scenario total, ensuring realistic temporal patterns in future births. For Lomé Commune (absent in DHIS2), Golfe's seasonal pattern was used.

Baseline expected PTBs were obtained by multiplying these projected monthly live births by the raked prefecture-specific PTB proportion, scaled so that the national PTB rate equalled 13%. For each prefecture-month and climate model, cumulative heatwave effects were computed by summing lag-specific log-rate ratios (0-8 months). These were converted into an attributable fraction (AF = (IRR–1)/IRR), an attributable number of PTBs (AN = AF × baseline PTBs), and an attributable incidence (per 1,000 live births). Monthly AF, AN, and incidence were then aggregated to annual prefecture and regional totals. Uncertainty was propagated by drawing 100 Monte-Carlo samples of each lag-specific BLUP coefficient from its estimated distribution and recomputing the full projection pipeline across all CMIP6 climate models. Final 95% uncertainty intervals therefore reflect combined epidemiological and climate-model variability.

Validation

Validation for the prefecture-level time-series models assessed whether model residuals met assumptions of independence, lack of undue autocorrelation, and appropriate functional form for the exposure-lag relationship. We also checked whether model fit was sensitive to alternative specifications, including simpler lag-response curves, excluding months with 0/NA PTB counts, and removing adjustment for relative humidity. For the meta-analysis, we evaluated whether distributional assumptions were reasonable and whether pooled estimates were unduly influenced by any single prefecture.

For the projection pipeline, we tested robustness to key assumptions by reducing the heat effect (RR* = RR^0.75), holding births constant over time, and substituting prefecture- and lag-specific RRs with a published global estimate for heatwaves in the month of birth (OR=1.26, 95% CI: 1.08-1.47) (Lakhoo et al., 2025) These checks ensured that projected heatwave-attributable PTB burdens were not driven by specific modelling choices.

5. Results

5.1 Climate change in Togo

5.1.1 Observed changes/trends

Compared to a 1981-2000 historical baseline, recent (2001-2024) average temperatures have universally increased while changes in rainfall patterns have been more variable (Figure 17). Highland central and southern regions have experienced overall declines in rainfall and relative humidity while the northernmost areas have seen a slight increase (Figure 17). These changes are analysed in more depth by region below.

Figure 17 - Climate information for Togo. Top row) Historical man annual temperature (°C); Second row) Historical mean precipitation (mm/day); Third row) relative humidity (%)).

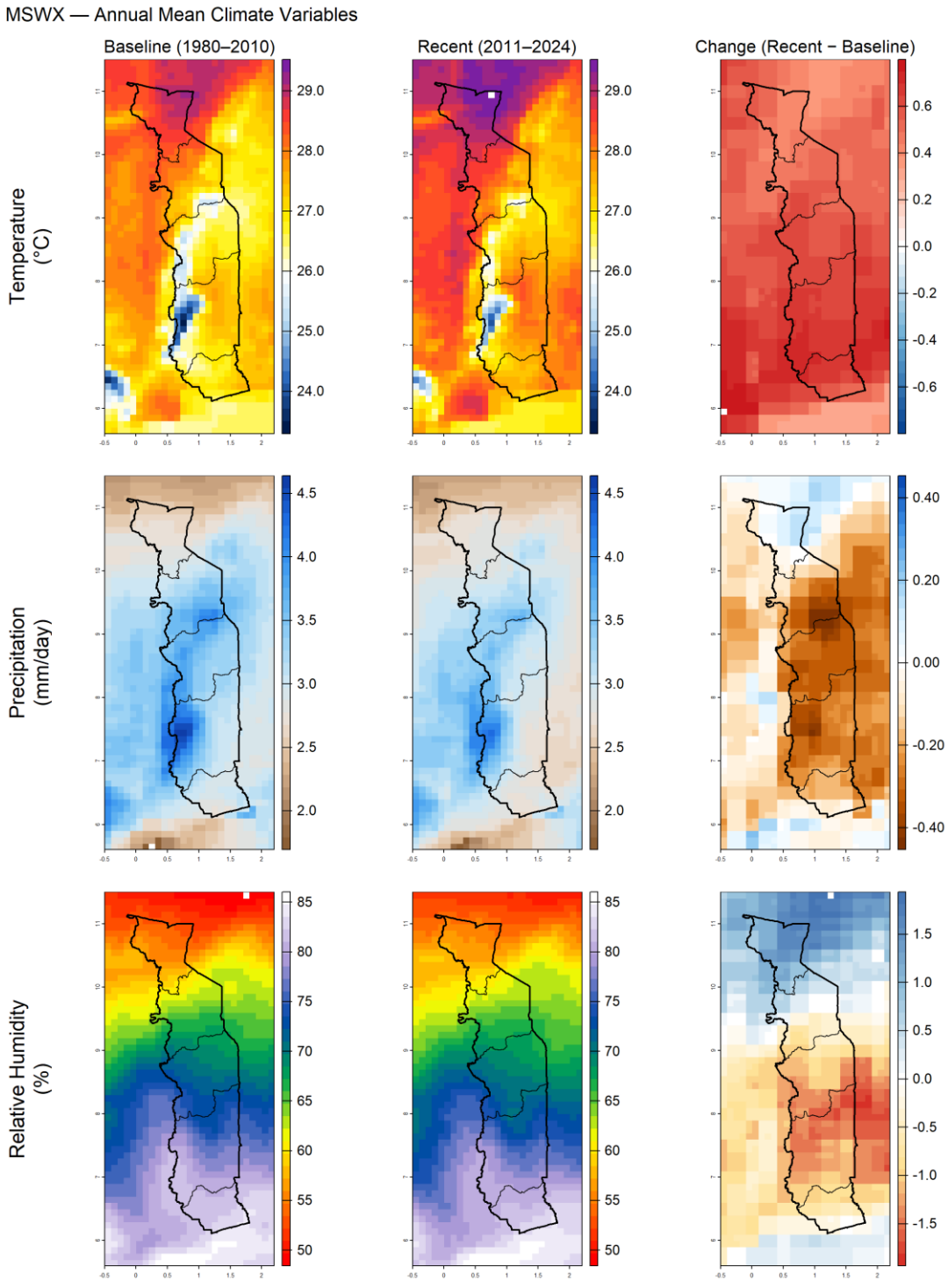

(Source: MSWX)

Climate trend analysis at the regional level over the reference periods 1981–2000, 2001–2024 (see Appendix 2) and the full period 1981–2024 (see also Table 5 at end of section) reveals clear and accelerating signals of climate change. For temperature variables (maximum, minimum and mean temperature), trends during 1981–2000 are generally weak and non-significant across regions. By contrast, from 2001–2024, maximum, mean and minimum temperature increased significantly in all regions (all Mann–Kendall $p<0.05$) (Figure 17) (Appendix 2), with minimum temperatures rising more rapidly (mean increase across regions +0.46°C) than maximum temperatures (mean +0.40°C), particularly in the northern regions.

Mean precipitation has declined significantly (all $p<0.05$) in all regions except Savanes over the full time series (1981-2024) (Figure 18) (Table 5), but trends were not individually significant within the comparison periods (1981-2000 or 2001-2024) for any region.

Mean relative humidity was stable in the 1981-2000 period but declined in the three southern regions in the subsequent period (Appendix 2). Over the full time series, Plateaux showed a significant decline, while Savanes showed a significant increase, the only region to do so (Table 5)

Figure 18 - Trends in average temperature (°C), precipitation (mm/day) and relative humidity (%) in Togo by region.

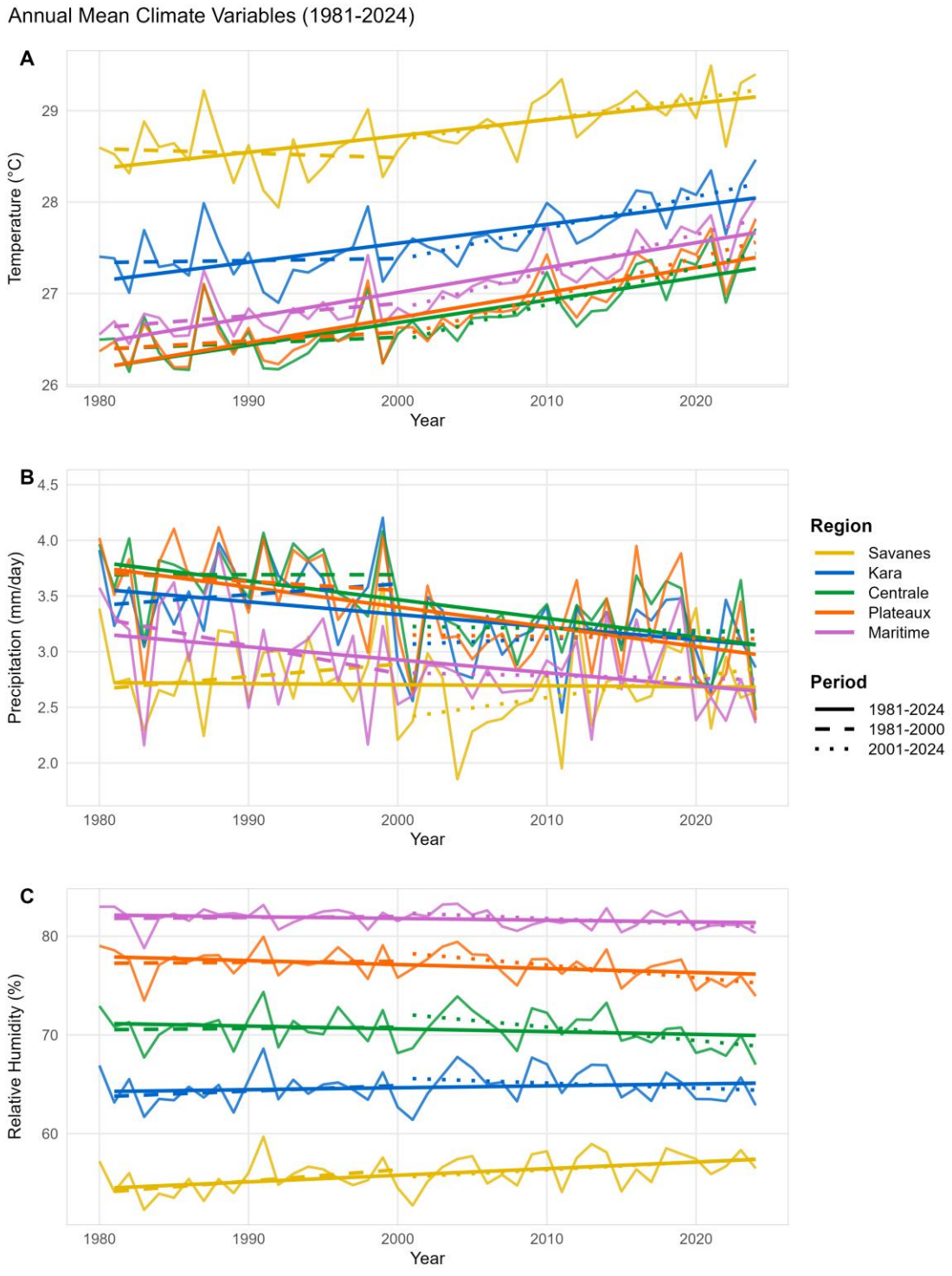

(Source: Own elaboration)

Extreme event indicators – temperature, rainfall

For extreme heat days (p95), only the three southern regions showed significant increases over the full time series (Table 5). However, when comparison periods were analysed separately, no regions showed an increase in the 1981-2000 period, but all regions showed significant increases in the recent period (2001-2024) (all $p<0.05$) (Appendix 2).

For extreme precipitation days above the 95th percentile, no significant trends were observed in any time period (Table 5).

Overall, these results indicate an increasingly hot and, in parts of the country, drier climate, particularly in northern regions, characterised by rising temperatures, more frequent heat extremes and declining rainfall.

Figure 19 - Trends in extreme heat and precipitation days per month in Togo by region.

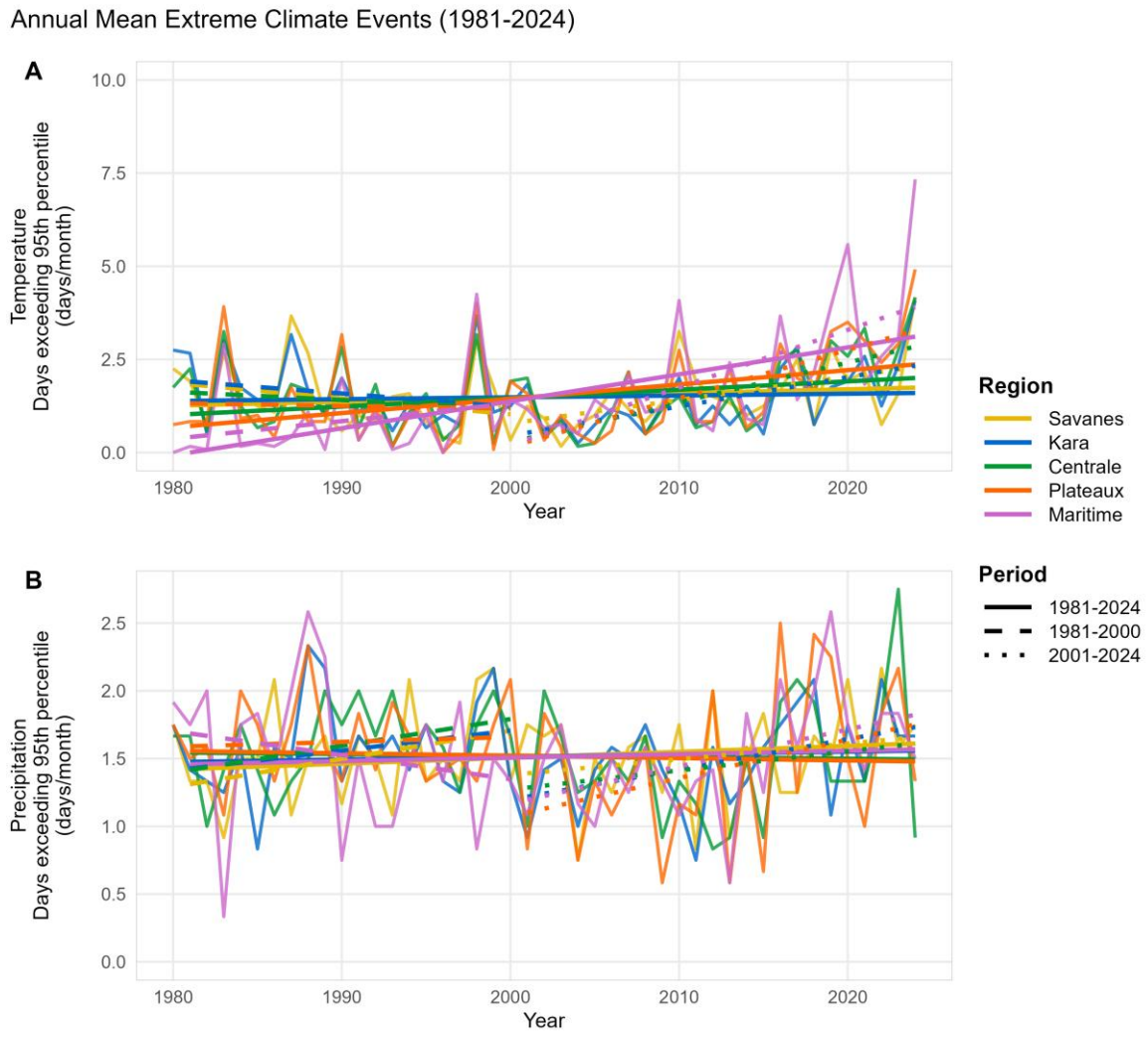

(Source: Own elaboration)

Monthly trends

Analysis of average monthly trends reveal the increasing temperature signal is present fairly evenly throughout the year, but heightened during the hottest parts of the year (March-April) (Figure 20). For precipitation, the overall declines observed in the annual time series are evident in the monthly averages and are concentrated within the early wet season period (Feb-July) across prefectures.

Increases in extreme heat events are concentrated in the hottest period of the year (Feb-March), with the biggest increases observed in Maritime and Savanes regions. Although no overall change in the number of extreme precipitation events was observed in the annual time series, decreases in extreme rainfall events are observed in the early wet season and increases are observed in the peak of the wet season particularly for Savanes and Kara (August) and Maritime (September) (Figure 21).

Taken together, the results suggest that in parallel with long term climate shifts, Togo is experiencing seasonal shifts in rainfall distribution, dry periods, and magnitudes of extremes in the hottest and wettest parts of the year. Such changes have implications for health, with many climate health exposures exhibiting strong seasonal patterns due to changes in human behaviours (e.g., farming practices, time spent outdoors) and pathogen and vector ecologies (e.g., mosquito breeding, pathogen proliferation). Such seasonal changes will require targeted adaptation and climate resilience measures, even where long term declines in risk may be observed (see Chapter 5.4).

Figure 20 - Seasonal trends in mean temperature and precipitation in Togo by region

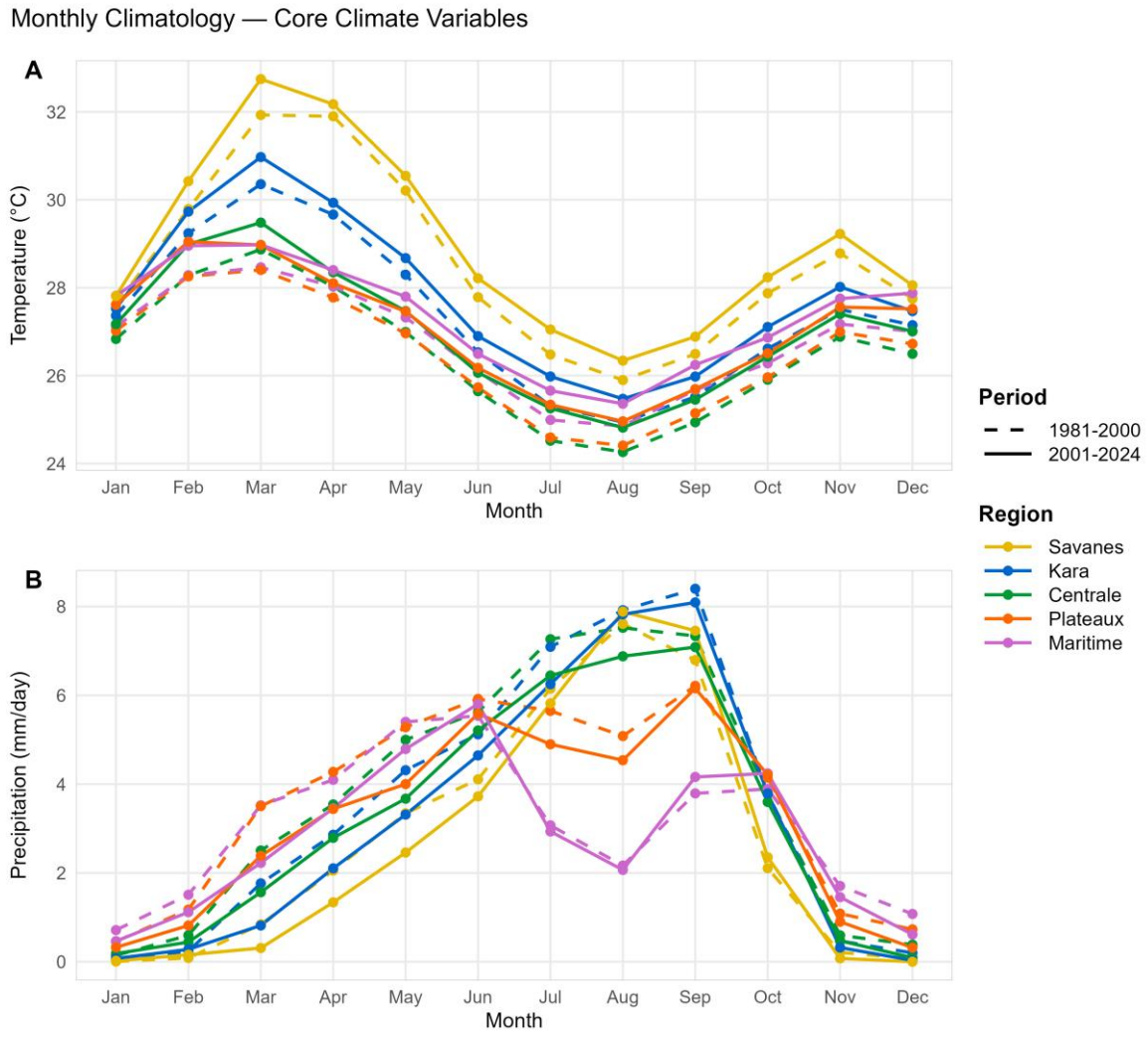

(Source: Own elaboration)

Figure 21 - Seasonal trends in extreme temperature and precipitation days per month in Togo by region

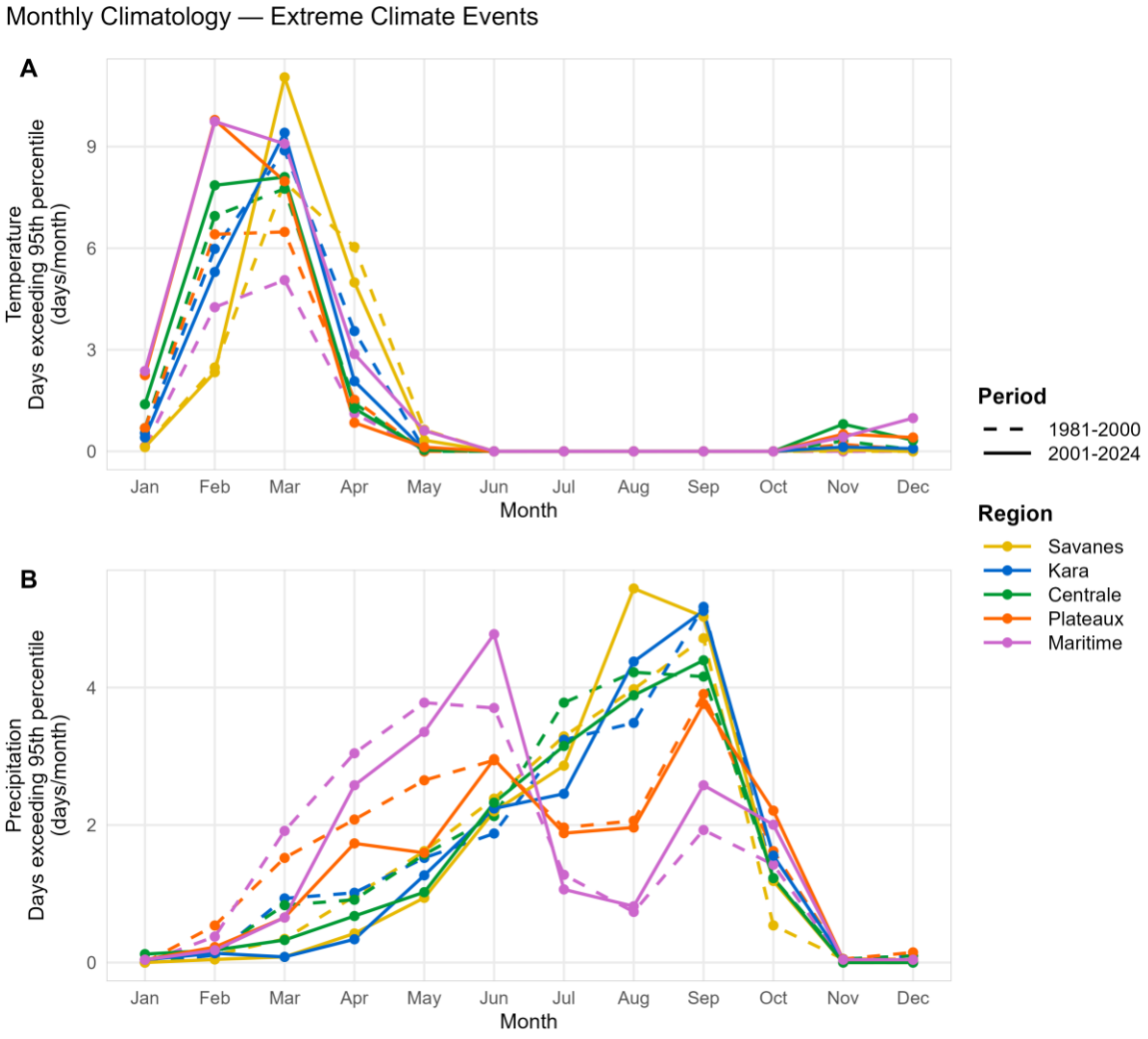

(Source: Own elaboration)

Table 5– Non-parametric Mann-Kendall trend test results on key variables from the historical climate dataset (source: MSWX). A p-value <0.05 indicates a significant monotonic trend (shown in green). Slope sign indicates the directionality of change (-ve is decreasing trend (shown in blue); +ve is increasing trend (shown in red)). Change per decade (if significant) is shown in original units.

Variable	Region	tau	p value	Sen slope	Change per decade
Maximum temperature (°C)	Savanes	0.249	0.017	0.012	+0.122
	Kara	0.347	0.001	0.014	+0.135
	Centre	0.459	0	0.022	+0.219
	Plateaux	0.552	0	0.026	+0.262
	Maritime	0.619	0	0.027	+0.270
Mean temperature (°C)	Savanes	0.499	0	0.02	+0.199

	Kara	0.571	0	0.022	+0.217
	Centre	0.63	0	0.025	+0.254
	Plateaux	0.674	0	0.029	+0.290
	Maritime	0.677	0	0.026	+0.263
Minimum temperature (°C)	Savanes	0.579	0	0.028	+0.280
	Kara	0.619	0	0.024	+0.243
	Centre	0.628	0	0.025	+0.247
	Plateaux	0.666	0	0.028	+0.280
	Maritime	0.693	0	0.029	+0.289
Precipitation (mm/day)	Savanes	-0.038	0.723	-0.001	no sig. change
	Kara	-0.285	0.007	-0.011	-0.114
	Centre	-0.387	0	-0.017	-0.175
	Plateaux	-0.351	0.001	-0.022	-0.217
	Maritime	-0.252	0.017	-0.013	-0.130
Relative Humidity (%)	Savanes	0.349	0.001	0.069	+0.691
	Kara	0.085	0.424	0.019	no sig. change
	Centre	-0.135	0.199	-0.03	no sig. change
	Plateaux	-0.258	0.014	-0.048	-0.479
	Maritime	-0.18	0.087	-0.018	no sig. change
Extreme heat days (p95)	Savanes	0.146	0.166	0.014	no sig. change
(count per month)	Kara	0.036	0.739	0.002	no sig. change
	Centre	0.228	0.03	0.027	+0.274
	Plateaux	0.338	0.001	0.051	+0.507
	Maritime	0.552	0	0.077	+0.770
Extreme precipitation days (p95)	Savanes	0.093	0.379	0.003	no sig. change
(count per month)	Kara	0.017	0.879	0	no sig. change
	Centre	-0.146	0.166	-0.005	no sig. change
	Plateaux	-0.129	0.221	-0.005	no sig. change
	Maritime	-0.184	0.08	-0.013	no sig. change

(source: own elaboration)

5.1.2 Projected future climate change

Across all regions and both SSPs, the projections show a very robust warming signal consistent with a continuation of the historical trends. Maximum, mean and especially minimum temperatures increase significantly everywhere ($p < 0.001$), with typical rates of about 0.35–0.45°C per decade under SSP2-4.5 and up to 0.5–0.57°C per decade for minimum temperature under SSP5-8.5 in Centrale, Kara and Savanes regions (Figure 22).

Figure 22 - Projected changes in temperature variables by region, SSP and time slice

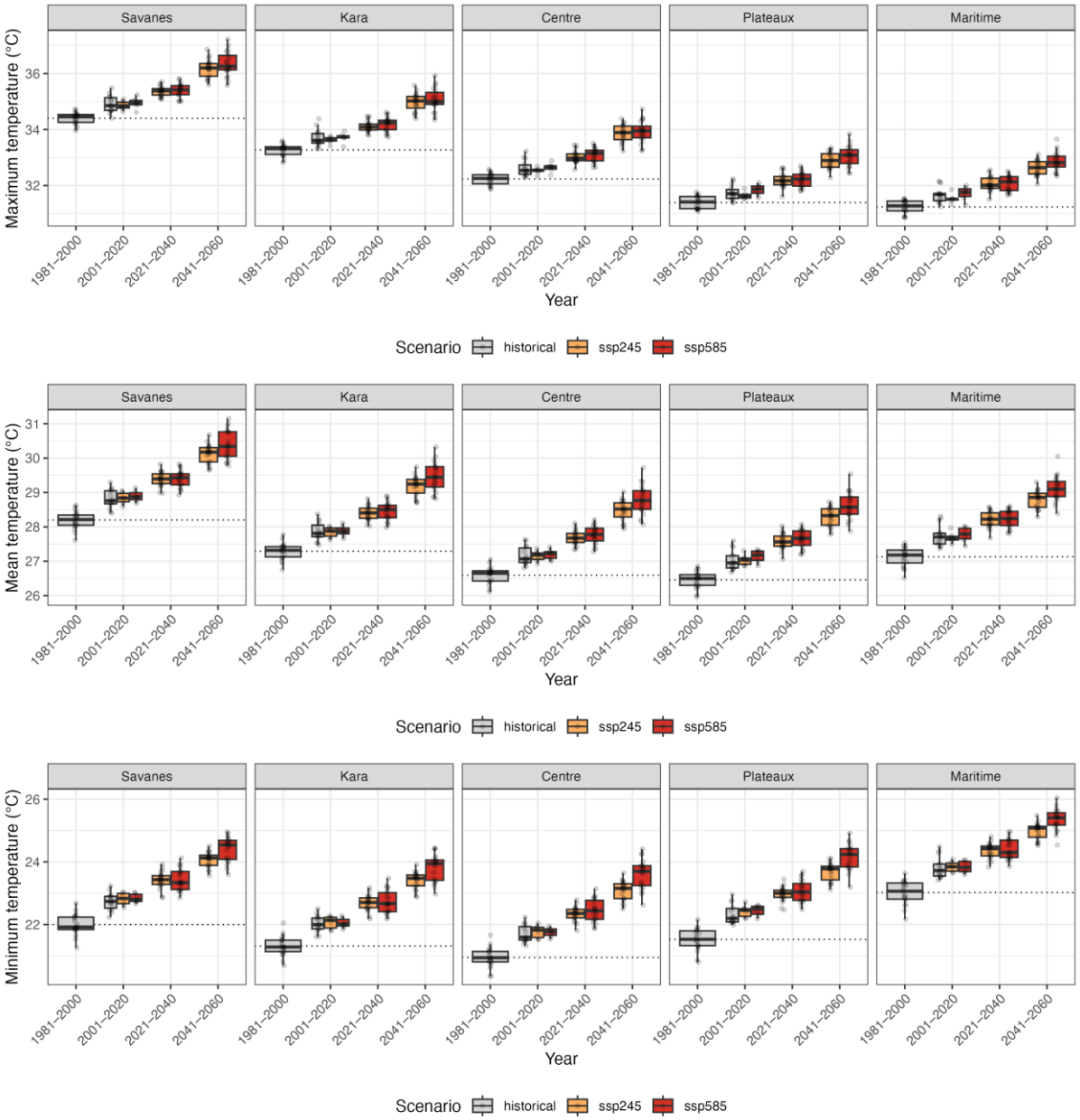

(Source: Own elaboration)

Mean precipitation generally declines under SSP2-4.5 in all regions except Savanes, with significant drops of around 0.05–0.08 mm/day per decade, and similar but slightly more mixed declines under SSP5-8.5 (strongest in Centre, Plateaux and Maritime) (Figure 23). These results are consistent across national studies (Koffi Djaman, 2017), regional studies (Tano et al., 2023) and CMIP6 projection based studies that predict decreasing precipitation trends under both mid- and high-emission scenarios across

West Africa with some regional variations (Ilori & Adeyewa, 2025; Sow et al., 2025; Taguela et al., 2025).

Relative humidity tends to increase slightly in the near term but overall decreases are observed across most regions by mid-century under both SSPs (Figure 23).

Figure 23 - Projected changes in precipitation and relative humidity by region, SSP and time slice.

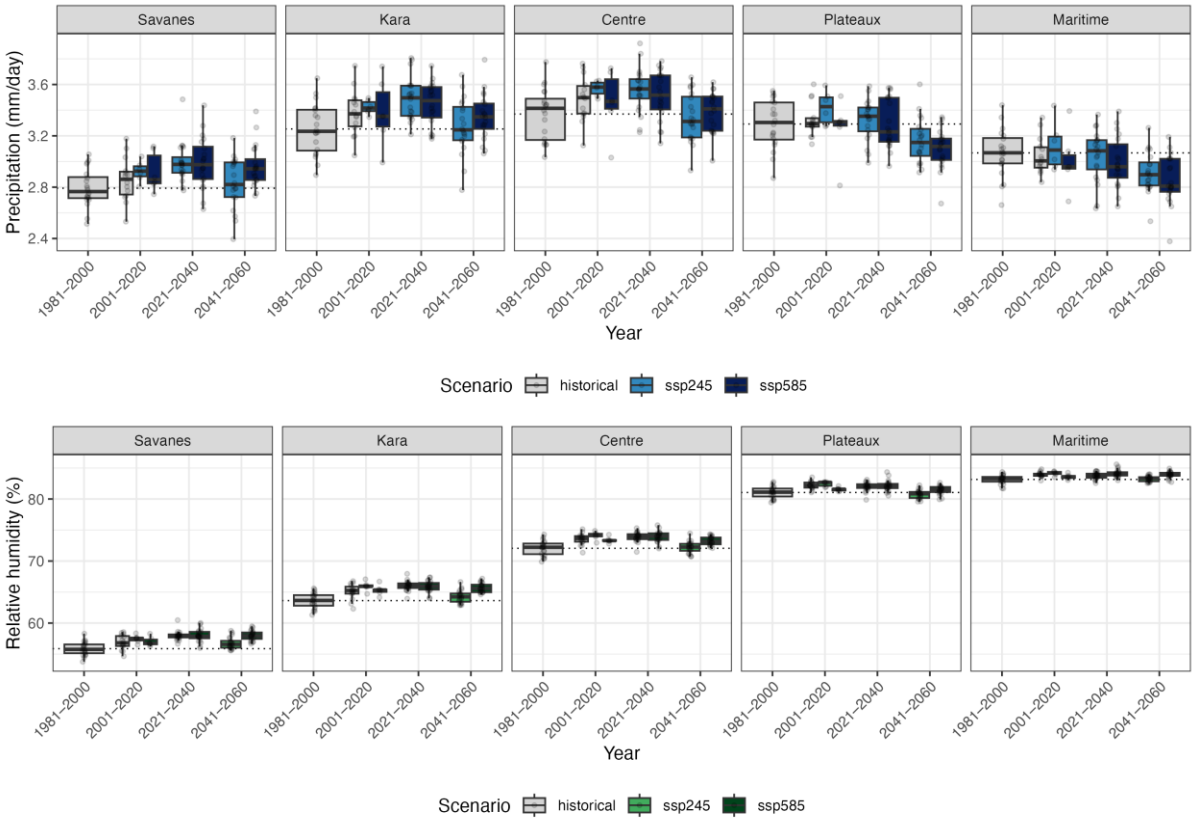

(Source: Own elaboration)

Heat-related extremes intensify consistently. Hot days above the 95th percentile are projected to increase significantly in all regions and under both scenarios, typically by 0.3–0.6 extra hot days per month per decade, with the largest increases under SSP5-8.5 in Savanes and Kara.

Extreme rainfall days above the 95th percentile show modest but significant increases mainly under SSP5-8.5 in Savanes and Kara (≈0.04–0.05 extra days per month per decade), while trends elsewhere are weak or non-significant (Figure 24). Overall, the data points to a future climate that is warmer everywhere, generally drier (especially in the interior) and more prone to hot extremes, with some regional strengthening of intense rainfall under the higher-emissions pathway (Appendix 3).

Figure 24 - Projected changes in extreme heat and rainfall days by region, SSP and time slice. Extreme heat and rainfall days are defined as days on which the corresponding variable (Tmax; 1-day precipitation) exceeds the 95th percentile of its distribution in the historical baseline period (1981-2000).

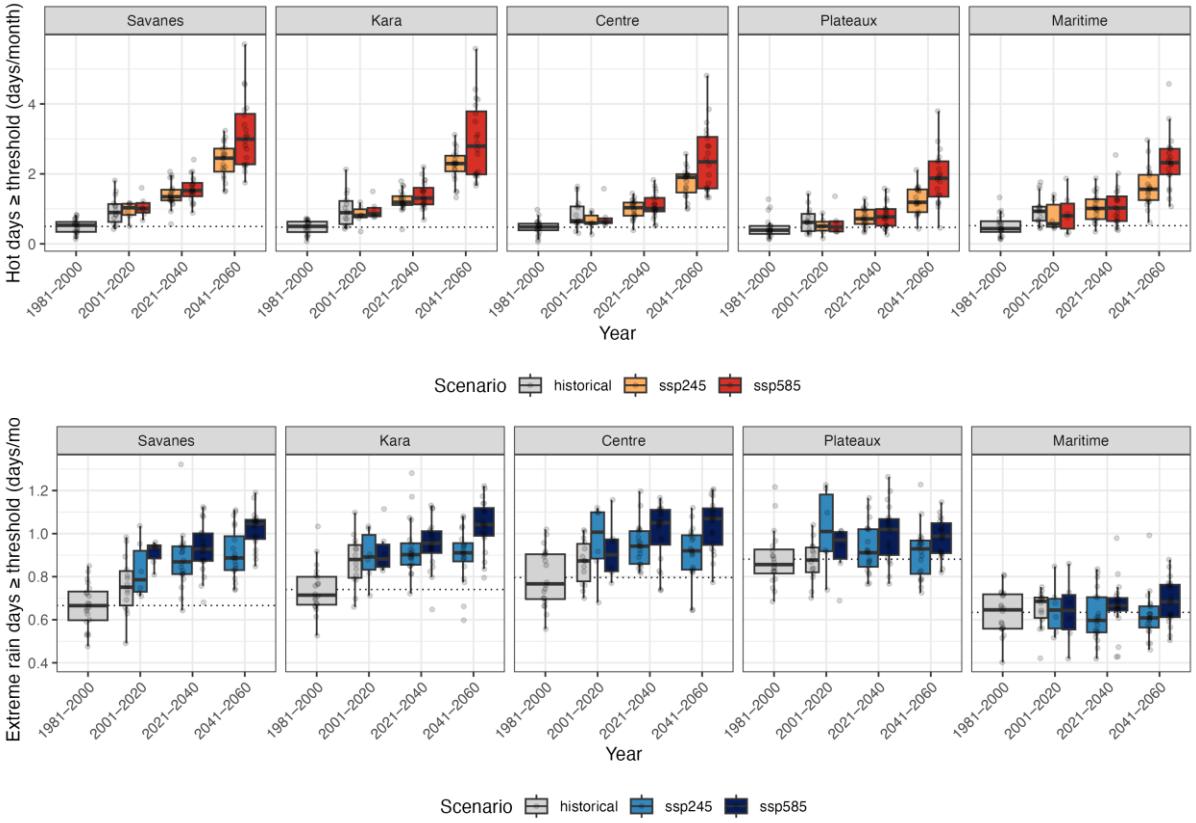

(Source: Own elaboration)

Future climate change trend tests are included in the appendices (Appendix 3).

5.2 Stage 1: Preliminary risk assessment and regional prioritisation

For the risk maps, relevant hazards, exposure groups and vulnerability factors were included based on evidence from the literature, as described in the Methods section. The mechanisms associated with potential increase in risk of incidence of the conditions are presented in the Impact Chains in chapter 8.5.4. This section describes the hazard, exposure and vulnerability for each health outcome, and shows the final overall risk scores. This is then used to identify priority regions, with the highest risk, for Stage 2 of the analysis to focus on.

Hazard trend tests are included in the Appendices (Appendix 4).

5.2.1 Malaria

Hazard

For malaria, the suitability hazard (length of transmission season, LTS) increased in the period from 1981-2000 and 2000-2021. However, declines in suitability are projected in future over time in every region, and these downward trends are statistically significant (Mann–Kendall $p < 0.05$) for most regions under SSP2-4.5 (all except Maritime) and for Centre, Plateaux and Maritime under SSP5-8.5. Under SSP2-4.5, Savanes, Kara, Centre and Plateaux lose about 0.4–0.5 suitable weeks per decade, while under SSP5-8.5 Plateaux and Maritime show larger, significant losses of ~1 week of suitability per decade, suggesting a gradual shortening of optimal transmission conditions, particularly in the south (Appendix 4).

Figure 25 - Hazard maps for malaria across Togolese prefectures and regions - change in the number of months suitable for malaria transmission per year (LTS – length of transmission season). This was calculated as the difference between the recent period (2001-2024) and the historical reference period (1981-2000).

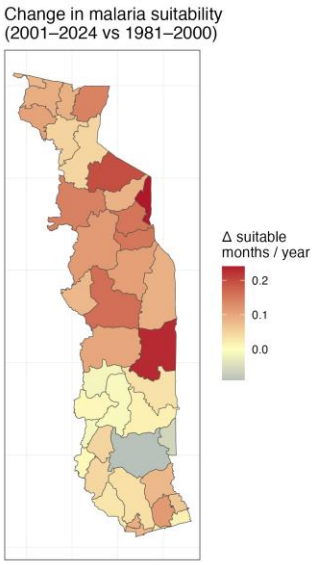

(Source: Own elaboration).

Figure 26 - Hazard projections for malaria by region - change in the number of months suitable for malaria transmission per year (LTS – length of transmission season). This was calculated as the difference between the comparison periods (2001-2020, 2021-2040, 2041-2060), and the historical reference period (1981-2000).

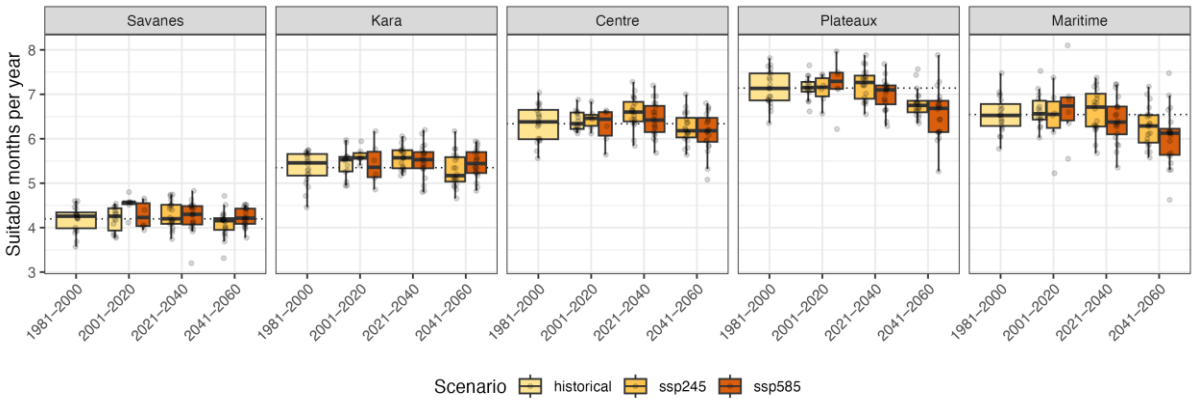

(Source: Own Elaboration)

Exposure (Population at risk)

The distribution of the current proportion of the population under 5 years old is displayed below (Figure 27). The proportion of children under 5 ranges from 10.4% to 19.7% across the prefectures and is generally higher in the North of Togo compared to the South.

Figure 27 - Exposure map illustrating the percentage of children under 5 years across Togolese prefectures. INSEED census-based estimates, 2022. Darker blue shades denote greater proportions of at-risk exposure population.

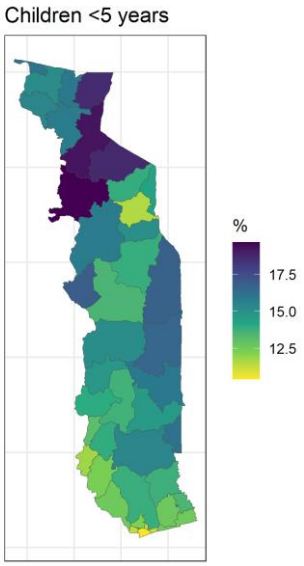

(Source: Own elaboration)

Vulnerability

Figure 28 highlights a clear spatial pattern to all three socioeconomic vulnerability factors for malaria including household wealth, mothers' education level and housing condition. Northern prefectures exhibit substantially higher vulnerability compared to southern prefectures, suggesting a structural and spatially persistent pattern of disadvantage. Unlike socioeconomic indicators, insecticide-treated net (ITN) coverage and travel time to health care do not display strong geographic clustering across the country. Travel time to care is lowest in the southernmost prefectures surrounding Lomé, reflecting better health service availability in and around the capital, but outside this zone the pattern is more variable and not strongly regionalised.

Figure 28 - Vulnerability factors for malaria across Togolese prefectures. Left to right, indicators include mean household wealth (MIS, 2017), mean caregiver education level (MIS, 2017), coverage of treated bednet ownership (MIS, 2017), coverage of improved housing (Colston, 2024) and mean motorised travel time to healthcare (Weiss et al., 2020). Darker purple shades denote greater vulnerability in all indicator maps.

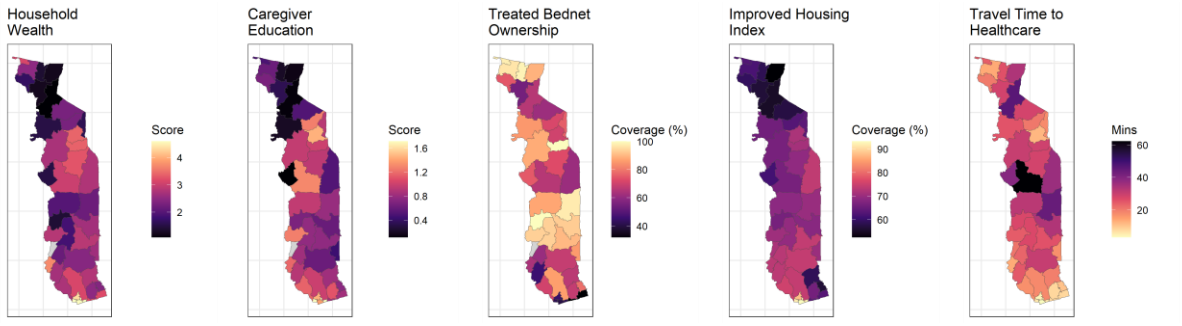

(Source: Own elaboration)

Risk

Hazard, exposure, and vulnerability indices were combined to estimate the multiplicative risk of malaria across Togolese prefectures. Figure 29 shows the resulting relative risk, the corresponding low–medium–high classification, and the aggregated regional picture.

Both exposure and vulnerability are more heavily concentrated in the North, and the hazard itself increases in frequency in northern and, to a lesser extent, southern prefectures. Together, these patterns produce a distinct North–South gradient, with Northern regions consistently exhibiting higher overall risk. Prefectures classified as high-risk typically display both high exposure and high vulnerability, again predominantly in the North. In contrast, Plateaux and Maritime regions show the lowest overall malaria risk.

Figure 29 - Risk assessment for malaria in children under 5. Top row) Prefecture-level component indices (rescaled 0-1); Second row) Categorisation into low, medium, high based on the Jenks method; Bottom row) Aggregation of component indices to region level. Hazard data reflect the change between recent (2001-2024) and historical (1981-2000) conditions; exposure data are from 2022; vulnerability data span 2017–2024.

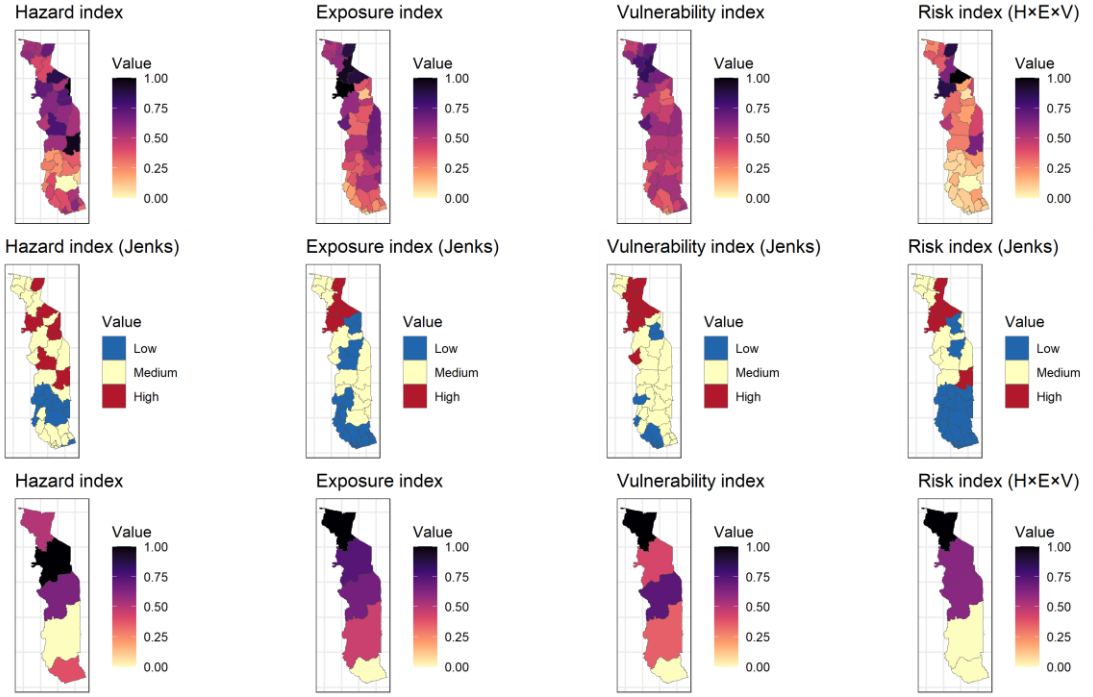

(Source: Own elaboration)

5.2.2 Diarrhoeal disease

Hazards

For diarrhoeal disease, extreme rainfall days (p95) show small changes that are only occasionally significant: Savanes and Kara under SSP5-8.5 exhibit modest but statistically significant increases of roughly 0.04–0.05 extra extreme-rain days per month per decade, whereas most other region–scenario combinations are non-significant. By contrast, compound dry-hot days ≥P95 increase strongly and significantly ($p<0.05$) in almost all regions and scenarios. In the northern regions (Centre, Kara, Savanes) these rise by about 0.25–0.45 days per month per decade, with somewhat smaller but still significant trends in Plateaux and Maritime (Maritime SSP2-4.5 being the main borderline/non-significant case). This points to a robust intensification of the hot-dry diarrhoeal hazard, especially in the north (Appendix 4).

Figure 30 - Hazard maps for diarrhoeal diseases across Togolese prefectures and regions. A) Change in the number of extreme precipitation days per year and B) Change in the number of dry-hot

days per year. These indicators were calculated as the difference between the recent period (2001-2024) and the historical reference period (1981-2000).

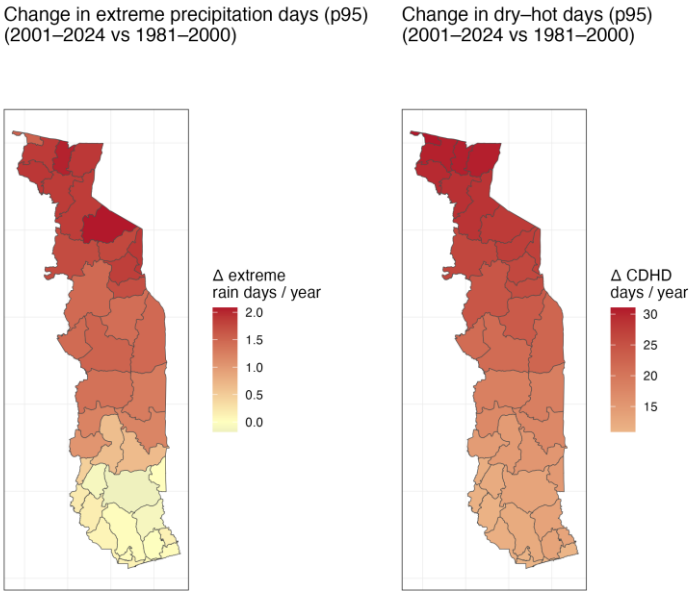

(Source: Own elaboration)

Figure 31 - Hazard projections for diarrhoeal diseases by region. Top row)) Number of extreme precipitation days per month (p95), Bottom row) Compound dry-hot days per year (p95). These were calculated as the difference between the comparison periods (2001-2020, 2021-2040, 2041-2060), and the historical reference period (1981-2000).

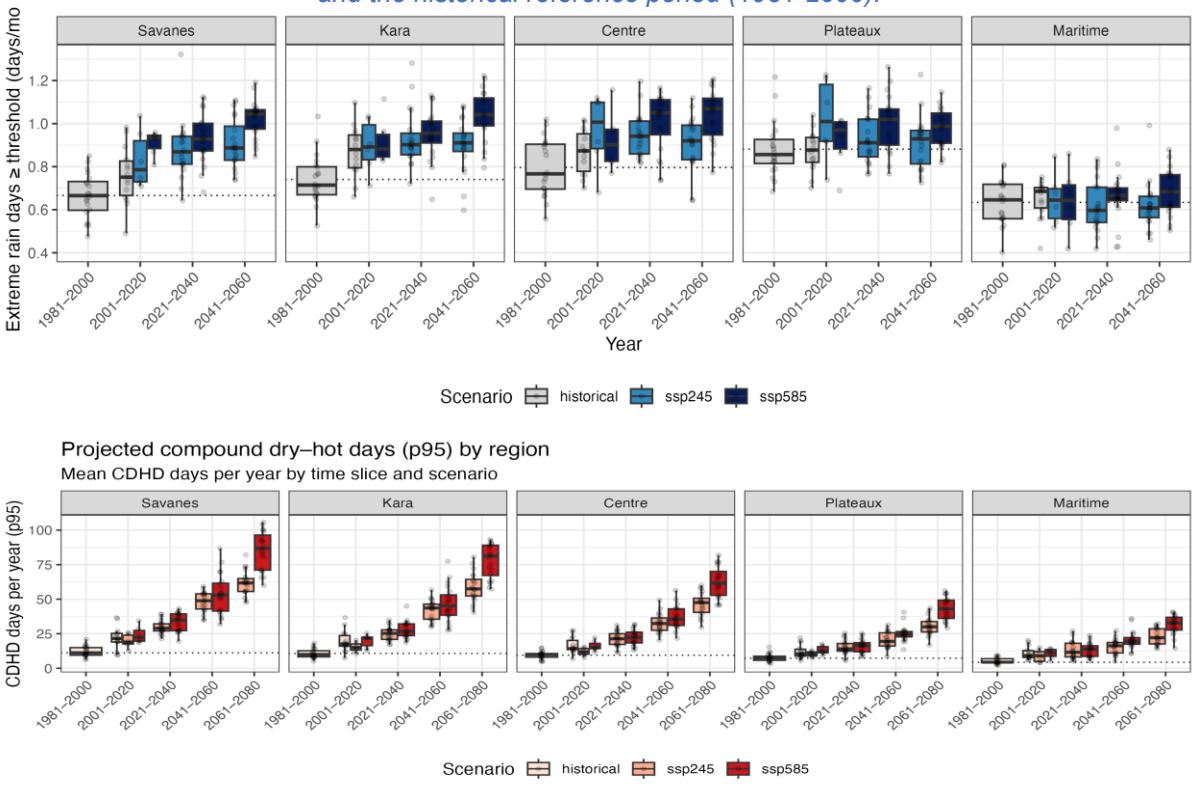

(Source: Own elaboration)

Exposure
The distribution of the current proportion of the population under 5 years old is the same for diarrhoeal disease as for malaria (see Section 5.2.1).

Vulnerability
Figure 32 illustrates the spatial distribution of diarrhoeal diseases vulnerability factors across Togo and highlights key regional differences. The proportion of children that are exclusively breastfed is generally high across Togo with no strong geographical pattern, suggesting relatively uniform practices, with a couple of prefectures falling behind. Mean household number of children under 5 years is relatively higher at the northern regions indicating these regions would have greater vulnerability due to household crowding of children under 5 years. Access to improved water is lowest in the Savanes and Plateaux regions, indicating these regions have heightened vulnerability related to water quality and availability. This vulnerability is compounded by relatively low levels of improved sanitation across Togo, with the exception the prefectures Lomé, Golfe and Agoé-Nyvié that surround the capital. This trend highlights a pronounced urban–rural divide. Travel times are shortest in the prefectures surrounding Lomé, reflecting the concentration of health services in the capital. Outside this urban area, travel times are longer but do not exhibit strong regional clustering, pointing to an inconsistent distribution of healthcare access.

Figure 32 - Vulnerability factors for diarrhoeal disease across Togolese prefectures. Left to right, indicators include mean household number of children under 5 years (INSEED, 2022), mean motorised travel time to healthcare (Weiss et al., 2020), coverage of improved drinking water facilities (INSEED, 2022), coverage of improved sanitation facilities (INSEED, 2022), and coverage of mothers practising exclusive breastfeeding (DHIS2, 2024). Darker purple shades denote greater vulnerability. in all indicator maps.

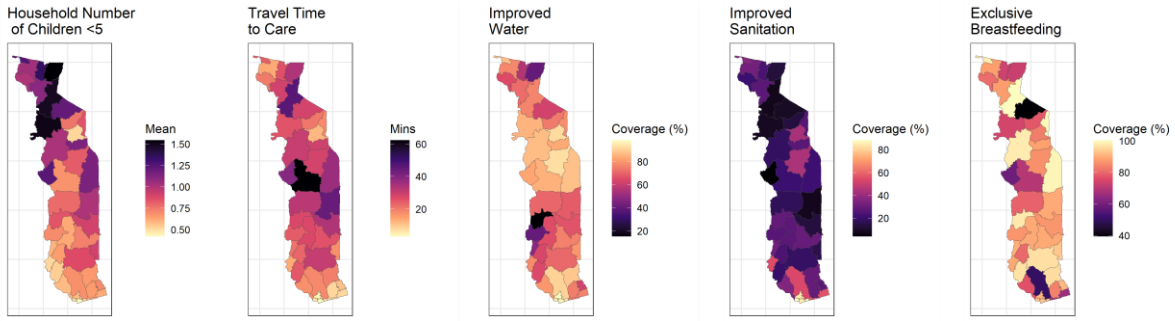

(Source: Own elaboration)

Risk
The diarrhoeal disease risk index and its distribution across Togolese prefectures is illustrated in Figure 33.

A composite hazard index was utilised, combining extreme rainfall days and compound dry-hot days. Once combined, the hazard showed an intensified signal in the North of Togo. Exposure prevalence was higher in the North whilst vulnerability is more evenly distributed across the territory. All high-risk prefectures are located in the North, and, although most low-risk prefectures are located in the South, a couple were apparent in Kara and Centrale regions.

Figure 33 - Risk assessment for diarrhoeal diseases in children under 5. Top row) Prefecture-level component indices (rescaled 0-1); Second row) Categorisation into low, medium, high based on the Jenks method; Bottom row) Aggregation of component indices to region level. Hazard data reflect the

change between recent (2001-2024) and historical (1981-2000) conditions; exposure data are from 2022; vulnerability data span 2020–2024.

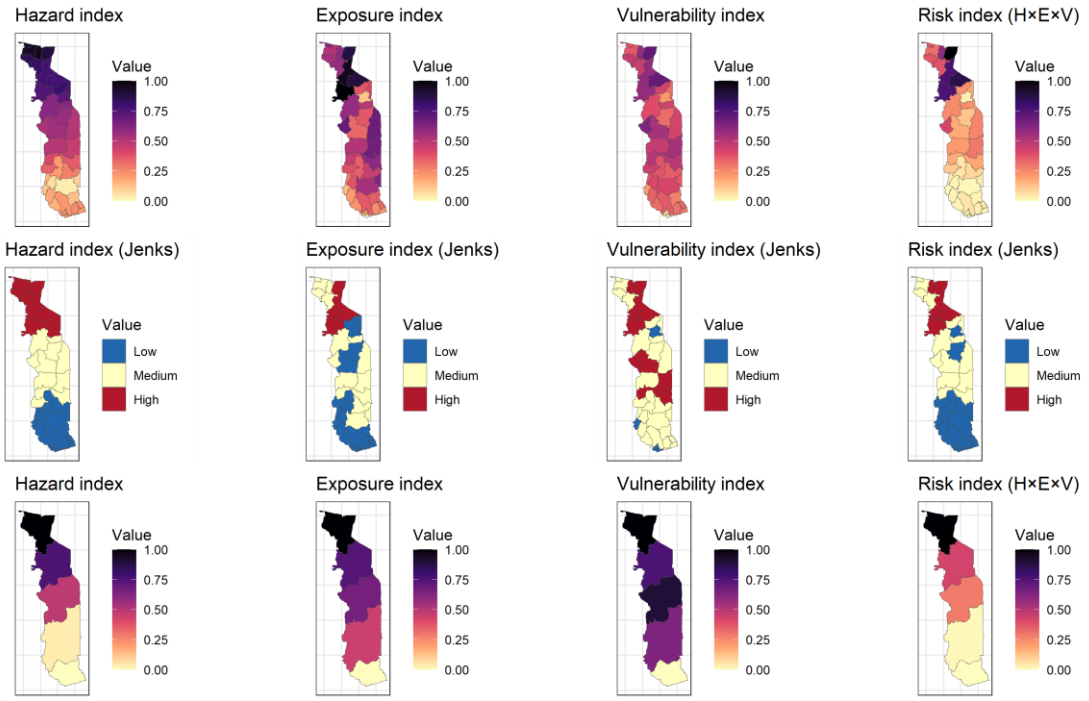

(Source: Own elaboration)

5.2.3 Preterm birth

Hazard

For preterm birth, the hazard heatwave events (p95) show consistently strong and statistically significant increases across all regions and both scenarios ($p<0.001$). Under SSP2-4.5, heatwave events rise by roughly 0.1–0.2 events per month per decade, and under SSP5-8.5 by ~0.18–0.29 events per month per decade, with the largest increases in Savanes and Kara. Overall, Mann–Kendall tests confirm robust monotonic warming and heat-hazard intensification (Appendix 4).

Figure 34 - Hazard map for preterm birth across Togolese prefectures and regions. - change in the number of heatwaves per year. This was calculated as the difference between the recent period (2001-2024) and the historical reference period (1981-2000).

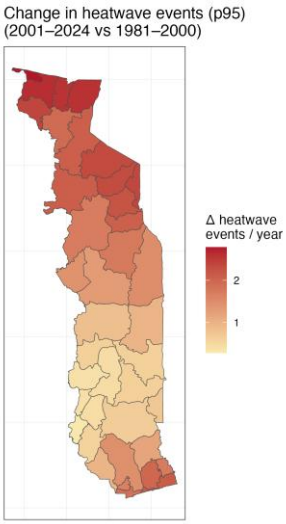

(Source: Own Elaboration)

Figure 35 - Hazard projections for preterm births by region - change in the number of heatwaves per year. This was calculated as the difference between the comparison periods (2001-2020, 2021-2040, 2041-2060), and the historical reference period (1981-2000).

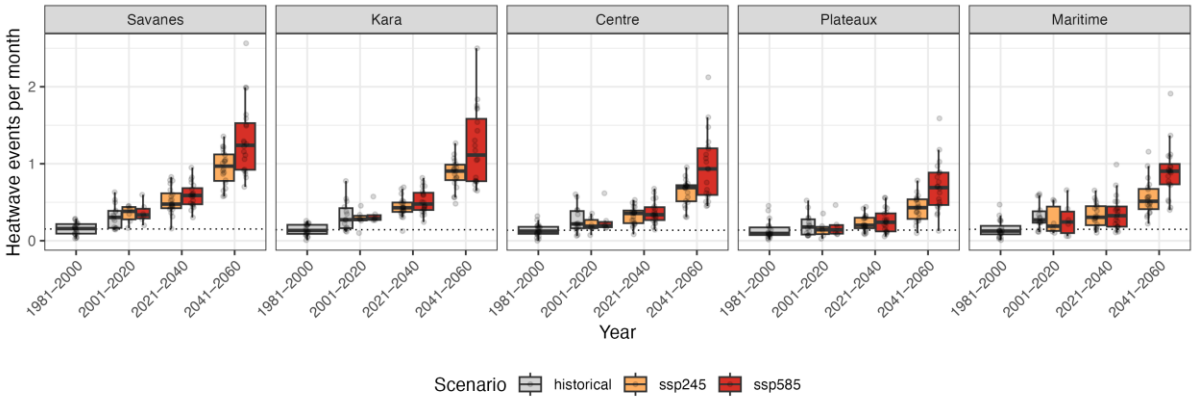

(Source: Own elaboration)

Exposure

The distribution of the current proportion of live births is presented in Figure 36. Birth rate among women of reproductive age varied between 22.5% and 33.5% and was relatively evenly distributed across the territory.

Figure 36 - Exposure map for the percentage of live births by women of reproductive age across Togolese prefectures. DHIS2-based estimates, 2024. Darker blue shades denote greater proportions of at-risk exposure population. in all both maps

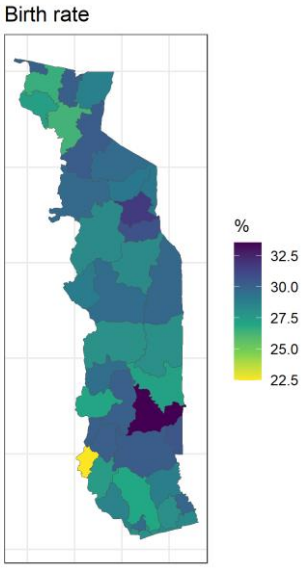

(Source: Own elaboration)

Vulnerability

Figure 37 illustrates the spatial distribution of preterm birth vulnerability factors across Togo and highlights key regional differences. Socioeconomic vulnerabilities including wealth and school attendance show a strong north–south gradient, with the northern prefectures consistently exhibiting poorer socioeconomic outcomes than the central and southern regions. Across all vulnerabilities, except for first trimester ANC, the capital Lomé and surrounding prefectures experience better outcomes compared to the rest of Togo. This underscores a clear urban-rural divide and the socioeconomic benefits of urbanisation. First-trimester ANC coverage, however, demonstrates a

distinct spatial pattern: access is substantially lower in the southern Maritime and Plateaux regions compared with Centrale, Kara, and the southern prefectures of Savanes. This suggests region-specific barriers to early antenatal care that diverge from broader socioeconomic patterns. The proportion of adolescent mothers remains elevated across most prefectures, with no strong geographical clustering beyond the capital region. This widespread distribution highlights adolescent pregnancy as a national priority issue rather than a region-specific concern. Lastly, air-conditioning coverage outside of the capital is very low, reflecting the widespread lack of material resources and socioeconomic constraints in Togo.

Figure 37 - Vulnerability factors for preterm birth across Togolese prefectures. Left to right, indicators include mean household wealth (MIS, 2017), coverage of air conditioning (INSEED, 2022), coverage of first trimester antenatal care attendance (DHIS2, 2024), percentage of adolescent motherhood (INSEED, 2022), and percentage of mothers without formal education (INSEED, 2022). Darker purple shades denote greater vulnerability in all indicator maps.

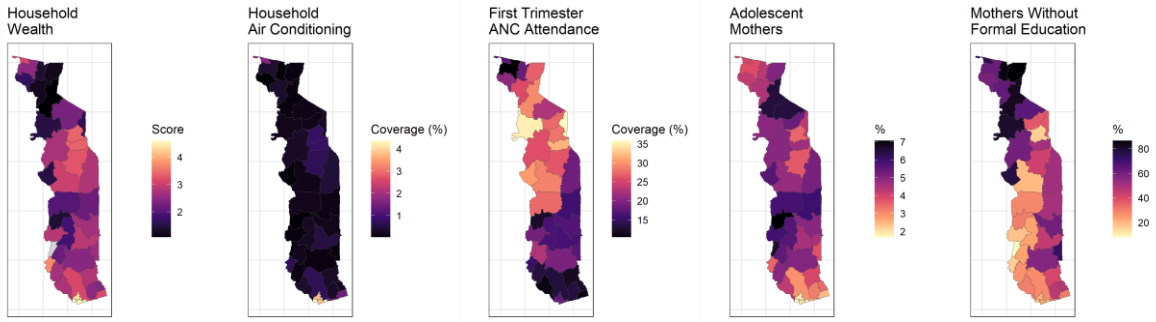

(Source: Own elaboration)

Risk

Hazard, exposure, and vulnerability indices were combined to estimate the multiplicative risk of preterm birth burden across Togolese prefectures.

Figure 38 shows the resulting relative risk at the prefectural and regional levels.

Hazard frequency increased throughout the far north and south of the region whilst exposure groups are most prevalent in the Plateaux region. The composite vulnerability index highlights high vulnerability across the territory with areas of low vulnerability only surrounding Lome. Although high exposure and vulnerability co-occur in Plateaux, the low change in heatwave hazards means that this region is classified primarily as low risk. Coincidence of the three components at high levels occurs only in the northernmost regions of Savanes and Kara.

Figure 38 - Risk assessment for preterm birth in children under 5. Top row) Prefecture-level component indices (rescaled 0-1); Second row) Categorisation into low, medium, high based on the Jenks method; Bottom row) Aggregation of component indices to region level. Hazard data reflect the change between recent (2001-2024) and historical (1981-2000) conditions; exposure data are from 2024; vulnerability data span 2017–2024.

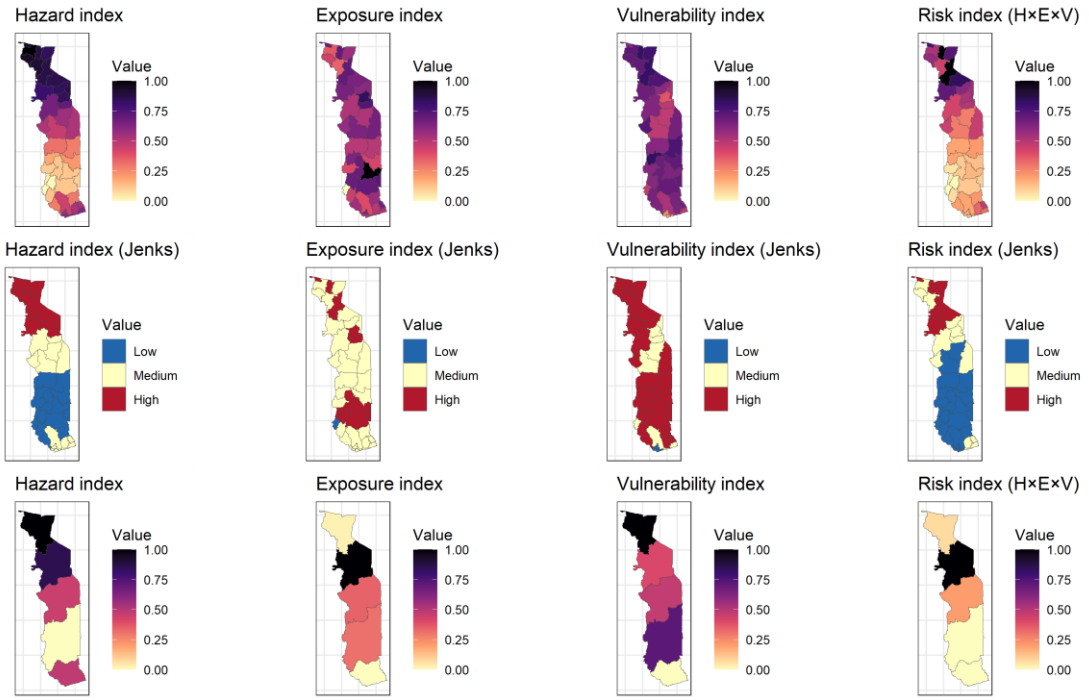

(Source. Own elaboration)

5.2.4 Discussion

Figure 29, Figure 33 and

Figure 38 illustrate a clear north-south gradient of risk, with the northern regions exhibiting higher levels of current risk, for all health outcomes. High-risk prefectures for all three health outcomes were consistently located in the northern three regions (Table 6). All of the low-risk prefectures for malaria and diarrhoea were located in the southern regions, whilst a large majority were located in the south for preterm birth.

Table 6 - Total number of prefectures in each risk category by region and health outcomes

	Malaria			Diarrhoea			Preterm birth		
	Low	Medium	High	Low	Medium	High	Low	Medium	High
Savanes	0	5	2	0	4	3	0	3	4
Kara	2	3	2	1	4	2	0	5	2
Centrale	1	4	0	1	4	0	3	2	0
Plateaux	11	0	1	9	3	0	12	0	0
Maritime	9	0	0	9	0	0	6	3	0
Total	23	12	5	20	15	5	21	13	6

(Source: Own elaboration)

In summary, the Stage 1 risk assessment clearly identifies the areas with the highest risk, based on the hazard, exposure and vulnerability mapping, as the northern three regions of Centrale, Kara and Savanes. A sensitivity analyses was performed, assigning vulnerability weights, and this did not change this conclusion (see Appendix 1 *Figure 56 to Figure 58*). These three regions were therefore prioritised, and the focus of Stage 2,epidemiological modelling. Accordingly, the model results displayed will only include these three regions.

5.3 Stage 2: Epidemiological Modelling

5.3.1 Malaria

Model training

A total of 3,172,922 confirmed cases of malaria were included in the DHIS2 dataset spanning from January 2018 - August 2025. For years with complete data, mean incidence nationally was 33.1 cases per 1000 children under 5 per year in this dataset, and there was no indication of a clear increasing or decreasing trend over the study period at the country level. Incidence varied by prefecture. The three priority regions had the highest mean incidences nationally (Figure 3939).

Figure 39 - Mean incidence rate (+/- 1 SD) of malaria per 1000 children under 5 per region averaged across the years 2018-2024. The dashed line is the national mean incidence rate over the same period.

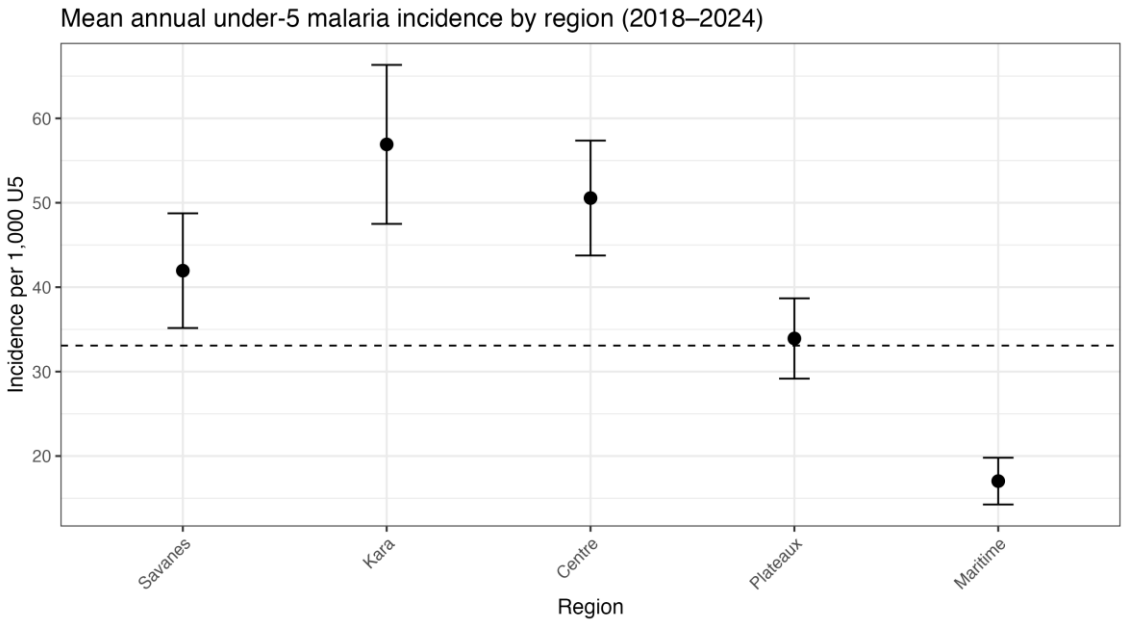

(Source: Own elaboration)

The final malaria model explained 76.5% of the variation in malaria incidence patterns over the training period and was able to replicate the strong seasonality observed in the data. In the temporal hold-out validation using 2018–2021 for model fitting and 2021–2025 for out-of-sample evaluation, the mean correlation between predicted and observed under-5 malaria cases nationally was 0.74, with a median error (RMSE) of approximately 18.7 cases and a median prediction bias of around +1.7 cases per 1000 children under 5 (U5) population (Figure 40). Across prefectures, median temporal correlation in the hold-out period was lower at 0.70 (median RMSE 12.1 and median bias +2.3 cases per 1,000 U5), indicating reasonably good predictive skill capturing overall trends.

Figure 40 - Temporal model validation showing observed vs predicted national malaria incidence (cases per 1,000 children under 5). The final GAM was refitted using only the first half of the time series (2018–2021) (dotted vertical line) and used to predict the hold-out period (2022–2025). In the hold-out years, the correlation between observed and predicted incidence was 0.74 at the national level, and the median prefecture-level correlation was 0.70.

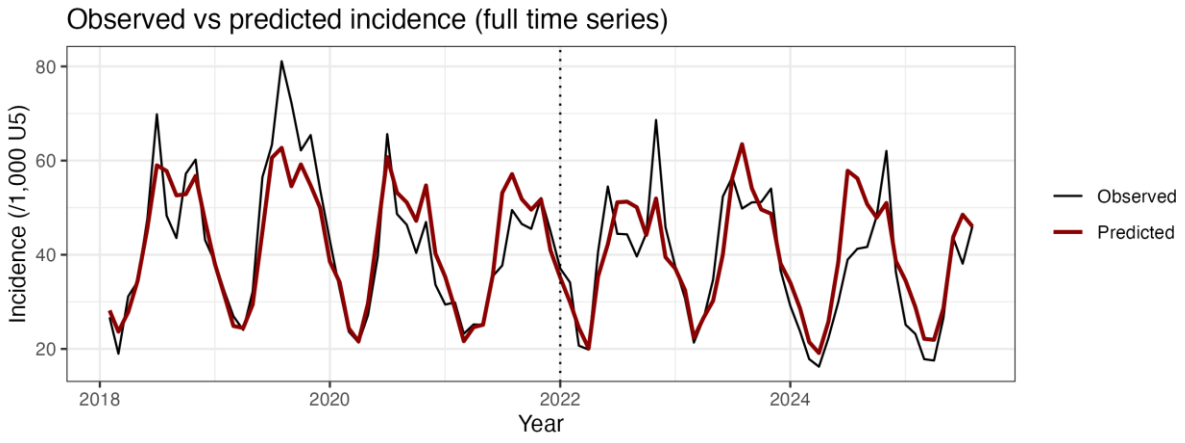

(Source: Own elaboration)

Climate effects

The fitted model showed clear and biologically plausible relationships between climate and under-5 malaria incidence. Overall, the model suggests that malaria risk is most strongly driven by lagged heat, humidity and diurnal temperature range, with a limiting effect of high mean temperature (Figure 41). A 1-SD increase in the number of very hot days (p95) is associated with higher incidence, especially at 1-month lag (IRR = 1.10, 95% CI 1.05–1.16), and lagged relative humidity shows a large positive effect (IRR = 1.41, 1.24–1.60), as does lagged temperature range (IRR = 1.19, 1.07–1.33). In contrast, once these variables are included, total precipitation and extreme rainfall days have small, uncertain effects (e.g. mean precipitation IRR = 1.02, 0.98–1.07; extreme precipitation days (p95) IRR = 1.00, 0.97–1.03). Crucially, mean temperature itself shows a negative association, both in the current month (IRR = 0.88, 0.83–0.94) and especially at 1-month lag (IRR = 0.61, 0.58–0.65), consistent with many locations already being close to or above the thermal optimum for transmission (Figure 41).

Figure 41 - Partial climate effects from the GAM. Estimated percentage change in under-5 malaria incidence versus the top four most influential climate variables (raw units), holding other covariates at typical values. Solid lines show effects in the same month and dashed lines 1-month lagged effects; shaded bands are 95% CIs. Rugs indicate the distribution of observed climate values, with dotted vertical lines marking the minimum and maximum observed range in training data; curves are truncated to this range ±10% to limit extrapolation.

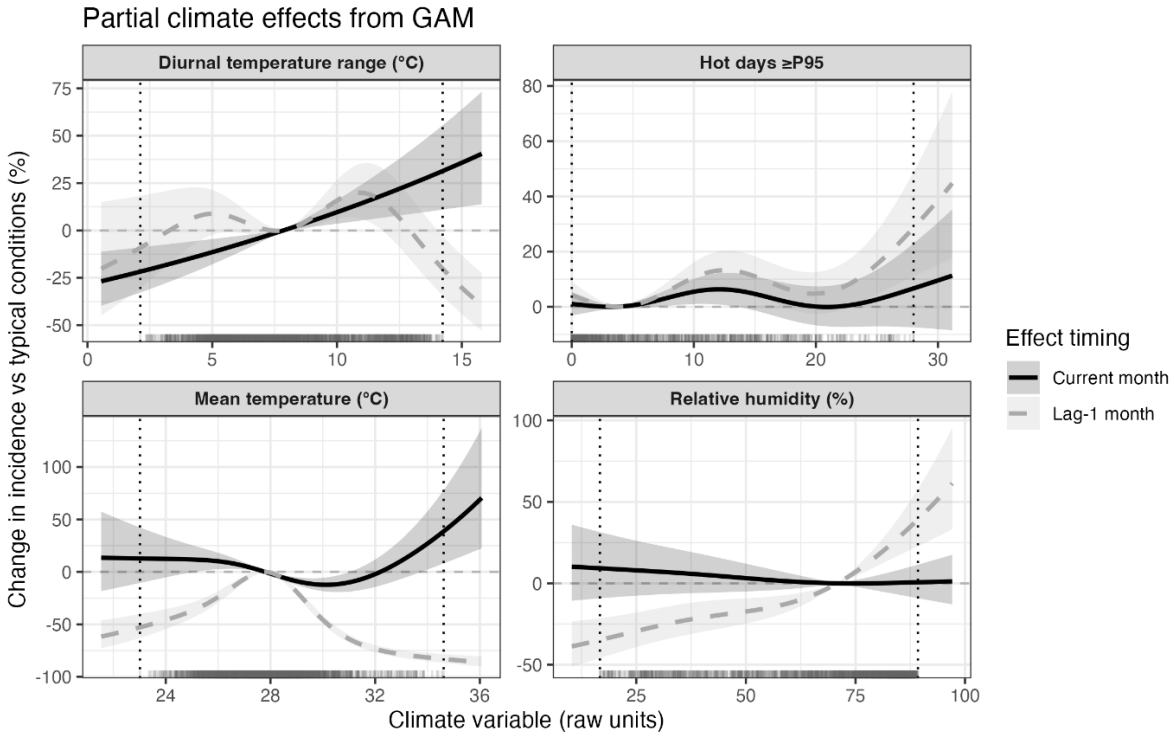

(Source: Own elaboration)

Vulnerability factors

In contrast to the clear climate effects, most static vulnerability covariates showed relatively weak and statistically uncertain associations with malaria incidence at prefecture level. The largest point estimate was for motorised travel time, where a one–standard deviation increase in time to the nearest health facility (≈ +12 minutes) was associated with about a 15% higher incidence (IRR 1.15, 95% CI 1.00–1.32), suggesting that poorer physical access to care may amplify risk, although the confidence interval just overlaps the null. Wealth and housing quality showed protective tendencies, with a 1-SD increase in mean wealth score and housing index corresponding to roughly 13–15% lower incidence (wealth IRR 0.87, 95% CI 0.71–1.08; housing IRR 0.85, 95% CI 0.70–1.03). Mean education score and the proportion of children sleeping under treated bednets had small positive coefficients of about 6% higher incidence per SD (education IRR 1.06, 95% CI 0.88–1.27; treated bednet coverage IRR 1.06, 95% CI 0.93–1.20), a non-significant pattern that likely reflects residual confounding or reporting artefacts (e.g. greater targeting of nets and better detection in historically high-burden areas). Overall, these results

suggest that in this dataset access to health services stands out as the clearest structural vulnerability, while other socioeconomic indicators probably interact with health-system performance and surveillance in more complex, less precisely estimated ways.

Future projections

Projections had relatively wide confidence intervals when full uncertainty (parametric plus inter-model variability) was accounted for, but overall, a moderate 5-10% declining trend in the ensemble mean per time slice emerged in projected malaria incidence across the three priority regions (Figure 42). This was projected to continue in the near-term (2021-2040) and by mid-century for both SSPs. Despite these projected declines, some areas in the elevated areas of Centrale region are projected to see slight (up to 5%) increases in the near-term in both SSPs but this trend does not continue to mid-century in either SSP, suggesting that long term warming may ultimately limit malaria even in highlands. Given the uncertainty, a non-trivial potential for future increases in incidence in the near-term and by mid-century due to climate change remains across the northern region of the country (Figure 42, Figure 43, Figure 44).

Figure 42 - Projected changes in malaria incidence in children under 5 years in the priority regions. Points are ensemble mean values relative to the 2001-2020 period mean (dashed line). Error bars are 95% Cis.

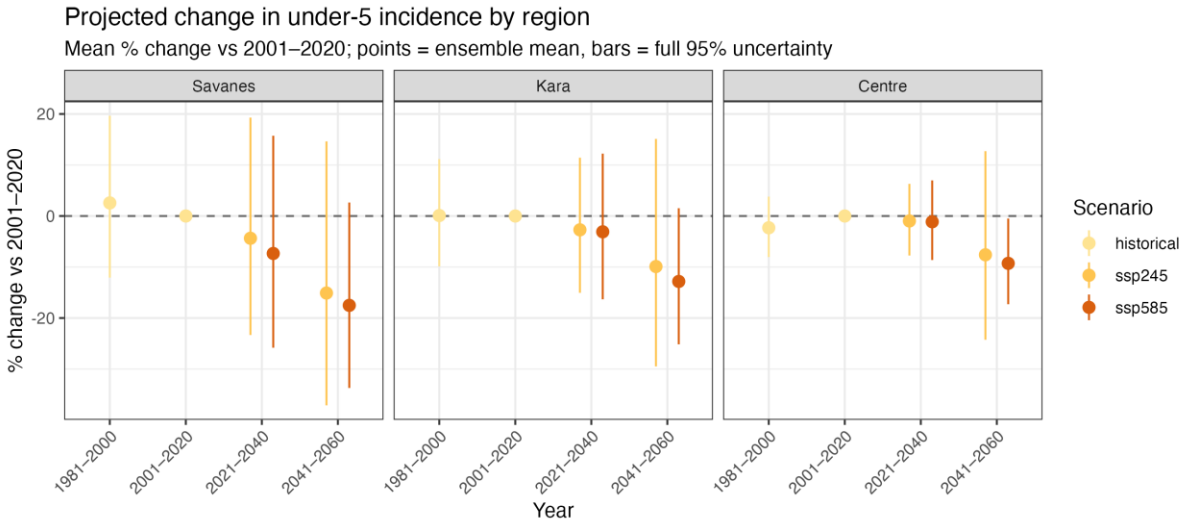

(Source: Own elaboration).

Figure 43 - Projected spatio-temporal changes in malaria incidence in children under 5 years in the priority regions by prefecture.

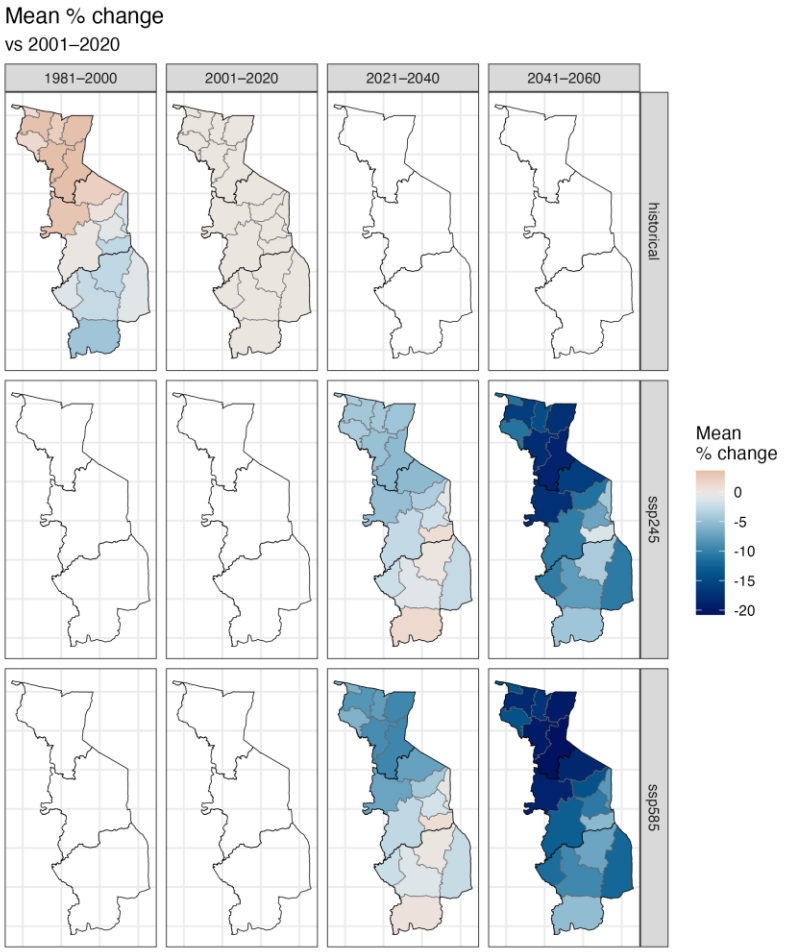

(Source: Own elaboration)

In all three northern regions, the model reproduced the strong baseline seasonality of malaria, with low incidence in February-March and a marked peak in the late rainy and early dry season (around August–September). Under future climate scenarios, this basic seasonal pattern is preserved, but the timing and relative magnitude of risk shift. Across the ensemble, early- and mid-year months (roughly April–June) are projected to remain fairly consistent with current conditions in the near term but by mid-century under both SSPs suppression in the early part of the malaria season is projected to be followed by higher peak incidence around August-September, particularly under SSP5. Taken together, climate changes are projected to already be concentrating malaria incidence in children under 5 into higher elevation areas where this trend may continue in the near-term, while decreases in incidence are projected elsewhere and changing seasonal patterns may have impacts on off-season (reduction) and peak season (increase) incidence.

Figure 44 - Projected seasonal changes in malaria incidence in children under 5 years in the priority regions by prefecture.

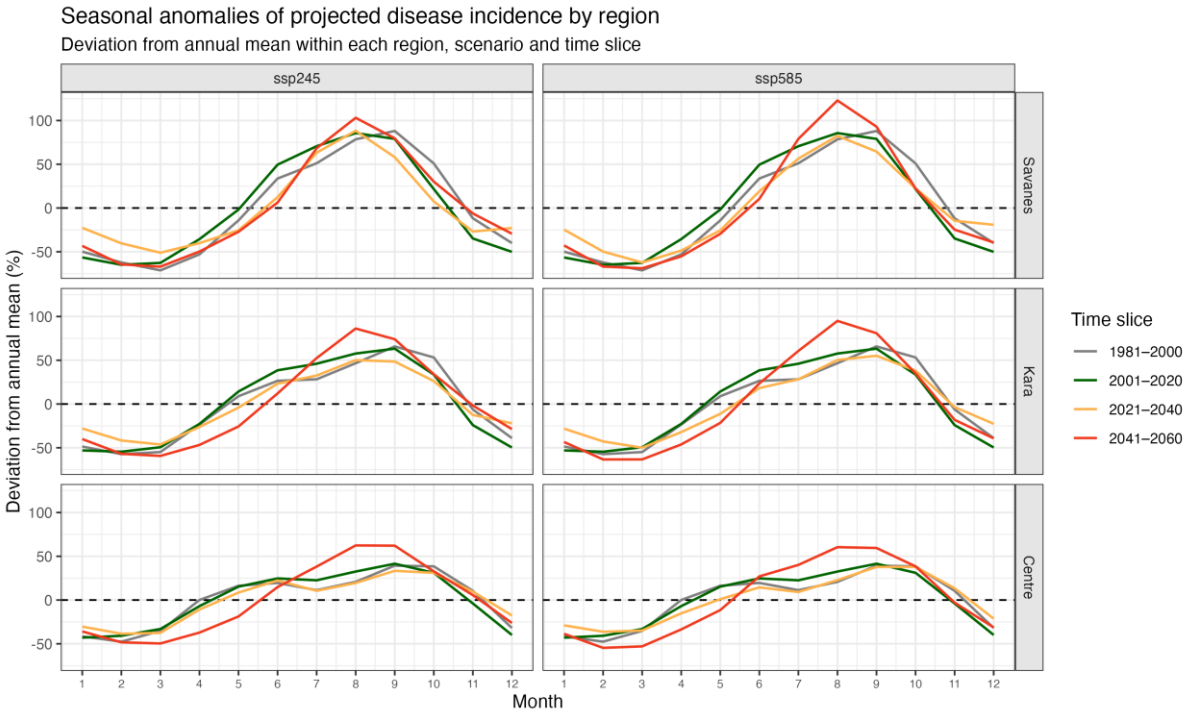

(Source: Own elaboration)

Validation and limitations

Overall, the spline basis dimensions chosen for the final malaria model were appropriate. Checks on k-indices for climate smooths (a parameter that helps control the complexity of the relationship without overfitting) did not support changes to the original values used (k=5) for any term.

Residual temporal autocorrelation plots for malaria showed a consistent pattern across prefectures, with moderately positive lag-1 autocorrelation (around 0.4–0.8) that decays over subsequent lags and little evidence of strong oscillatory or long-range structure. This indicates that some short-term dependence in malaria transmission and/or reporting remains unexplained, but that major seasonal and interannual patterns are well captured. Adding an explicit AR(1) structure did not improve model fit or materially change the estimated climate effects, so we retained the simpler GAM; any remaining autocorrelation may slightly understate uncertainty for month-to-month predictions but is unlikely to alter the direction or magnitude of projected climate–malaria relationships.

Residual spatial autocorrelation was also detected, implying unmeasured spatially structured malaria determinants (for example vector habitat, health-system reach or ecological gradients). Mean deviance residuals showed significant positive spatial structure, and adding an additional thin-plate spline over prefecture centroid coordinates reduced this only marginally and did not improve overall information criteria. Climate effect surfaces and projections were essentially unchanged, so we retained the simpler specification and interpret the remaining spatial structure as reflecting factors such as heterogeneous surveillance quality, vector control, or socio-environmental differences not fully captured by the static covariates.

Extrapolation and clamping tests showed that only a small fraction of projected future climate values fell outside the historical ranges used to train the GAM. When these values were clamped to the historical range, national malaria incidence projections changed only slightly, indicating that projections are not strongly driven by extrapolation into unobserved climate space and are therefore reasonably robust within the range of climate conditions expected over the next several decades.

Several limitations should be noted. Routine DHIS2 data capture only a subset of all clinical malaria episodes in children under 5. In high-transmission West African settings, community-based and

modelled estimates generally indicate substantially higher under-5 malaria incidence than the ≈30 cases per 1,000 children per year observed in DHIS2 for Togo - for example a study in Ghana using rapid diagnostic tests found a prevalence of 27.8% (with 95% CI: 25.8% - 29.91%) in children under 5 (Ejigu & Wencheko, 2021). This implies that many episodes are either not treated in facilities reporting to DHIS2 or are not coded as malaria in the Health Management Information System (HMIS). As for diarrhoea, we therefore treat DHIS2 malaria counts as a relative indicator of temporal and spatial variation rather than a complete tally of true burden. Heterogeneity in reporting completeness, diagnostic practices, and access to care across prefectures and over time may further bias absolute incidence levels and contribute to the residual spatial structure seen in the model.

DHIS2 case reporting quality varies across prefectures and over time, so under-reporting or differential diagnostic effort may bias absolute incidence levels and contribute to spatial residual structure. The model describes average monthly risk at prefecture level rather than short-lived localised outbreaks (e.g., those potentially linked to extreme rainfall or flooding), and static covariates (e.g. wealth, travel time, bednets) are prefecture-level aggregates that do not capture within-prefecture heterogeneity. Residual temporal and spatial autocorrelation suggest the presence of unmeasured or imperfectly measured processes such as vector control, health-system performance, ecological gradients or human mobility. Projections also assume stationarity of the climate–malaria associations and keep vulnerability factors fixed over time, so behavioural or infrastructural adaptation (for example improved nets, IRS or strengthened primary care) is not modelled. As a result, the outputs should be interpreted as projected changes in incidence rates per unit population under a changing climate with all else being held equal, not as full burden estimates. The estimates remain subject to multiple sources of uncertainty arising from data quality, observational coverage, model specification and downscaled CMIP6 climate inputs, although our methodology (ensemble averaging and variance propagation) help to mitigate some of these issues.

Discussion

Taken together, the malaria model results are consistent with a transmission system in which under-5 incidence responds nonlinearly to multiple dimensions of climate, with distinct contributions from current and lagged conditions. The clearest and most precisely estimated effects are for lagged heat, humidity and diurnal temperature range, with evidence that high mean temperatures become limiting. Months with more very hot days (p95), higher relative humidity and larger day–night temperature ranges one month earlier are associated with elevated incidence, consistent with warm, humid conditions favouring mosquito survival and parasite development. In contrast, once these variables are included, total rainfall and the frequency of extreme rainfall days show only small, statistically uncertain associations with malaria, suggesting that broad-scale moisture availability may matter less than the specific combination of heat and humidity captured by these metrics. The negative associations observed for mean temperature in both the current and previous month support a picture in which many locations are already near or above the thermal optimum for transmission, so additional warming tends to push conditions into a less favourable range even while short-term hot and humid episodes remain important.

For projections, the model indicates moderate overall declines (around 5–10%) in under-5 malaria incidence under future climate across the three northern priority regions, but with important spatial and temporal heterogeneity. In the near term, some elevated areas of Centrale are projected to experience slight increases in incidence (up to about 5%), reflecting warming towards more favourable thermal conditions, although these increases do not persist to mid-century in either SSP, consistent with long-term warming eventually constraining transmission even in highlands. At the same time, the ensemble retains a non-trivial possibility of near-term and mid-century increases in parts of the northern regions, underscoring that climate change may still exacerbate malaria risk locally even as national-scale incidence trends downward. Seasonally, the model reproduces the strong baseline pattern of low incidence in February–March and a pronounced peak in the late rainy and early dry season (around August–September). Under future climate scenarios this basic pattern is preserved, but the early part of the season is increasingly suppressed, and the late-season peak becomes relatively more pronounced, particularly by mid-century under SSP5. Overall, climate change is projected to further concentrate transmission into cooler, higher-elevation parts of the north in the near term, while reducing incidence elsewhere and subtly reshaping the timing and intensity of the seasonal peak. This pattern of modest climate-driven change in overall risk, coupled with spatially heterogeneous responses, is

consistent with regional mechanistic projections from the Vector-transmission Model (VECTRI)[3] and related models, which also suggest limited net change in transmission in Togo by mid-century under both moderate and high emissions pathways (Fall et al., 2023). Our finding that cooler high-elevation areas may experience slight short-term increases aligns with these studies' identification of transitional zones where warming temporarily moves conditions closer to optimal EIR. More generally, these results support earlier work implying that climate change in Togo is unlikely to uniformly amplify transmission but may alter the timing and concentration of peak-season risk (Fall et al., 2023; van der Deure et al., 2025).

Despite the clearer and more precisely estimated climate effects, most static vulnerability covariates showed only weak and statistically uncertain associations with malaria incidence at prefecture level. The main exception was physical access to healthcare: a one–standard deviation increase in motorised travel time to the nearest health facility (≈12 minutes) was associated with roughly 15% higher incidence, suggesting that limited access to diagnosis and treatment remains an important structural amplifier of malaria risk. Wealth and housing quality showed protective tendencies, with higher mean wealth and better housing associated with lower incidence, whereas mean education and treated bednet coverage displayed small positive coefficients that were not statistically significant. These counter-intuitive patterns for education and bednets likely reflect residual confounding and surveillance artefacts, for example intensified intervention delivery and better detection in historically high-burden prefectures. Taken together, the results suggest that, in this dataset, health-system access emerges as the most consistent vulnerability signal, while other socioeconomic indicators probably interact with unmeasured differences in care-seeking, intervention targeting, and reporting quality, leading to weaker and more context-dependent associations.

5.3.2 Diarrhoea

Model training

A total of 154,161 reported under-5 diarrhoea cases were included from DHIS2 spanning January 2018 to August 2025. Of the prefectures with sufficient coverage (N=27/39) (none in Maritime, which was dropped for this analysis), the mean national incidence was 2.9 cases per 1,000 children under 5 per year over the complete years from 2018-2024. No clear increasing or declining national trend over the study period was observed. Spatially, diarrhoea burden was heterogeneous across the country, with higher average incidence in Kara followed by Savanes (Figure 45).

[3] The Vector-borne disease Community model of ICTP (VECTRI) is a process-based malaria transmission model that simulates how temperature and rainfall influence mosquito populations, parasite development, and malaria transmission dynamics. It is widely used to assess climate-driven changes in malaria risk under future climate scenarios.

Figure 45 - Mean incidence rate (+/- 1 SD) of diarrhoea per 1000 children under 5 per region averaged across the years 2018-2024. The dashed line is the national mean incidence rate over the same period.

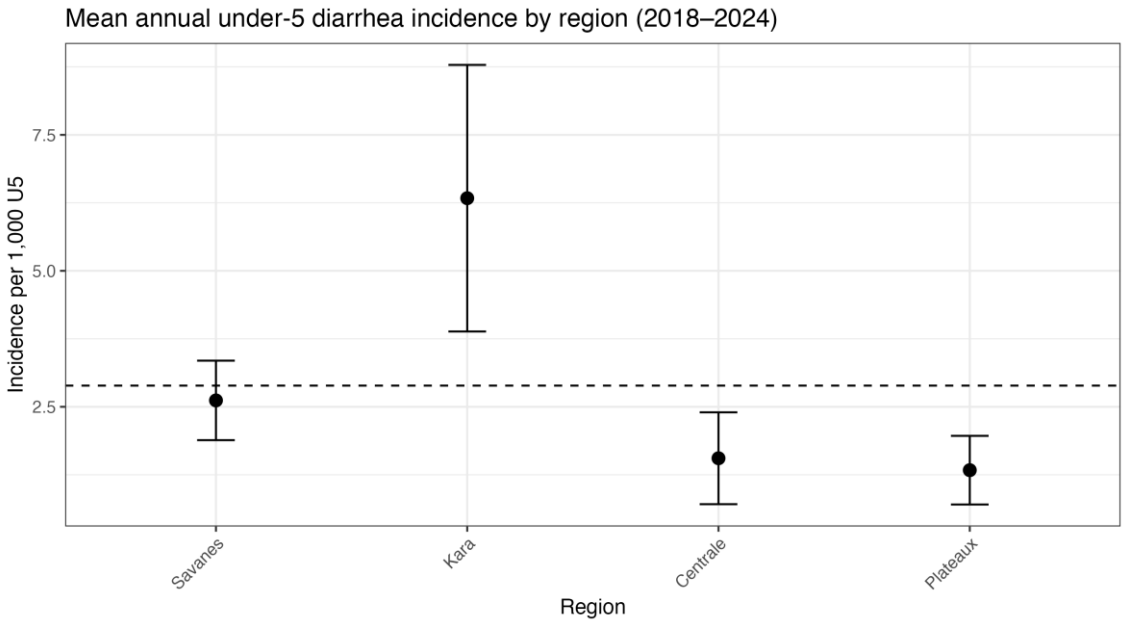

(Source: Own elaboration)

The final diarrhoea model explained 56.7% of the variation in diarrheal incidence patterns over the training period. The model detected some seasonality observed in the data, but this was far less evident than for the malaria model. In the temporal hold-out validation, the mean correlation between predicted and observed under-5 diarrhoea cases nationally was 0.80, with a median error (RMSE) of approximately 3.4 cases and a median prediction bias of around –1.0 cases per 1000 U5 population (Figure 46). Across prefectures, median temporal correlation in the hold-out period was far lower at 0.27 (median RMSE 1.5 and median bias –0.1 cases per 1,000 U5), indicating considerable predictive skill capturing overall national trends but with relatively poorer prediction accuracy at the prefecture level. In the validation test, the model was unable to predict the unusually high number of cases occurring in 2023.

Figure 46 - Temporal model validation showing observed vs predicted national diarrheal incidence (cases per 1,000 children under 5). The final GAM was refitted using only the first half of the time series (2018–2021) (dotted vertical line) and used to predict the hold-out period (2022–2025). In the hold-out years, the correlation between observed and predicted incidence was 0.80 at the national level, and the median prefecture-level correlation was 0.27.

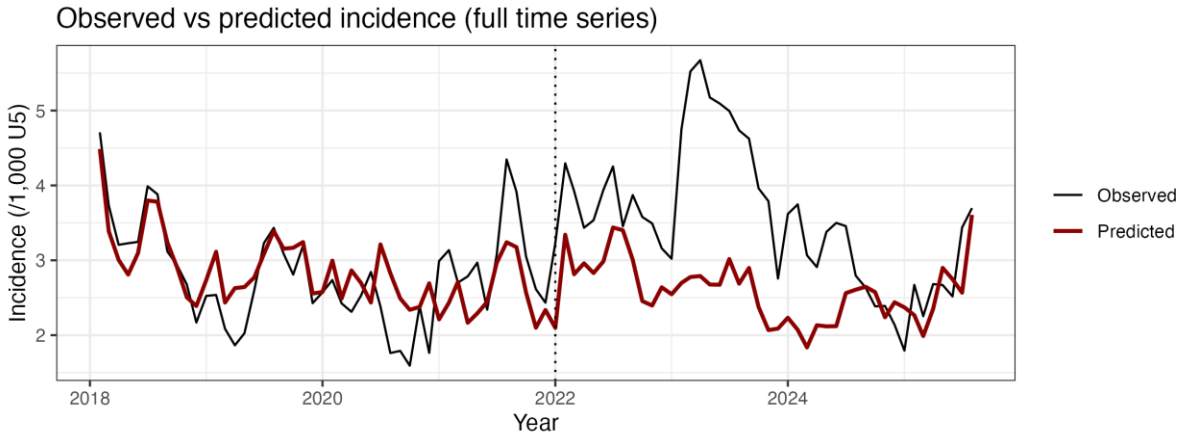

(Source: Own elaboration)

Climate effects

The model indicated strong positive associations between rainfall and diarrhoeal incidence. Both contemporaneous and lag-1 total precipitation increased incidence, suggesting that wetter conditions particularly in the preceding month are important drivers of diarrhoeal risk. Extreme rainfall was retained in the model and showed a weak positive but marginal association (IRR CIs overlap 1).

In contrast, temperature-related variables generally showed protective associations. A 1-SD increase in lag-1 mean temperature is linked to an estimated 15–20% lower incidence (IRR ≈ 0.8–0.85), with a relatively tight CI, and higher relative humidity is associated with around a 10–20% reduction in incidence (IRR ≈ 0.8–0.9), although the CI is wider here and crosses unity. Hot days ≥P95 show a smaller but still noticeable protective effect (≈ 5–10% lower incidence, IRR just below 0.95).

Overall, these results highlight precipitation (especially at a one-month lag, with minor contributions from very wet days) as the dominant climatic risk factor for childhood diarrhoea in this setting, while warmer and more humid conditions, and periods with more hot days, tend to reduce diarrhoeal burden.

Figure 47 - Partial climate effects from the GAM. Estimated percentage change in under-5 diarrheal incidence versus the top four most influential climate variables (raw units), holding other covariates at typical values. Solid lines show effects in the same month and dashed lines 1-month lagged effects; shaded bands are 95% CIs. Rugs indicate the distribution of observed climate values, with dotted vertical lines marking the minimum and maximum observed range in training data; curves are truncated to this range ±10% to limit extrapolation

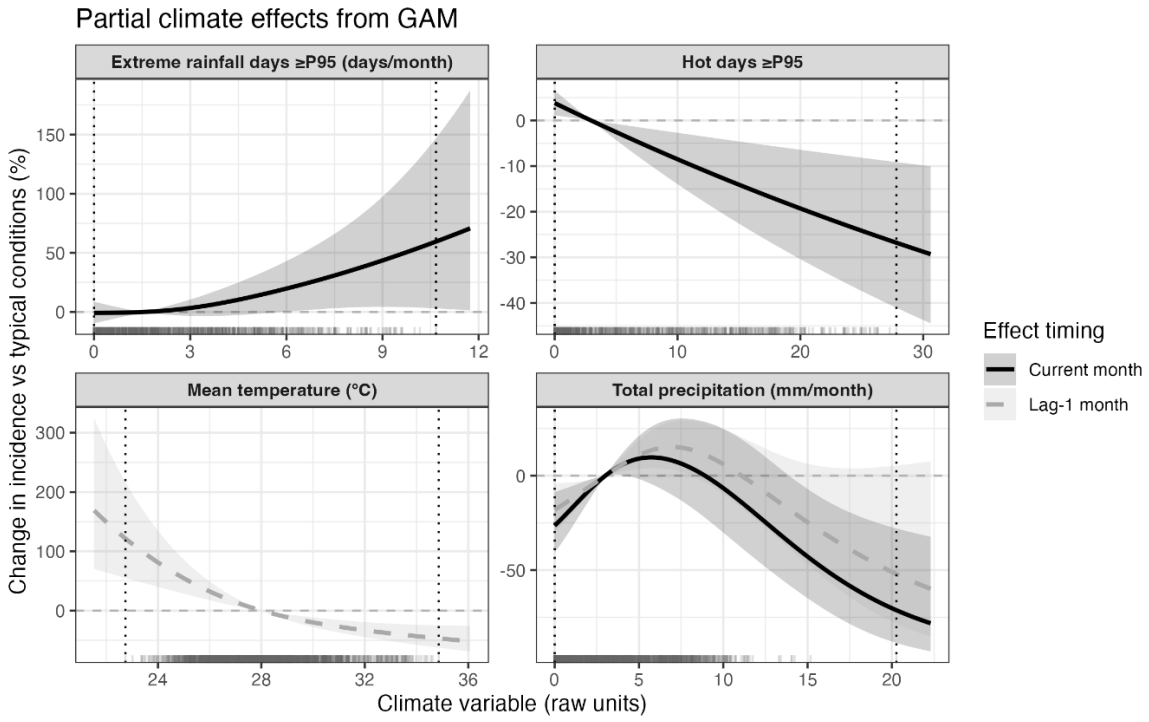

(Source: Own elaboration)

Vulnerability factors

The static covariates showed broadly plausible but mostly modest associations with under-5 diarrhoea incidence. A 1 SD higher exclusive breastfeeding coverage (≈ +13.7 units) was associated with about an 18% lower incidence (IRR = 0.82; 95% CI ≈ 35% lower to 4% higher), and a 1 SD higher improved toilet coverage (≈ +10.3 units) with about a 20% lower incidence (IRR = 0.80; 95% CI ≈ 41% lower to 7% higher); both suggest protective effects but remain borderline, as their confidence intervals include 1. Improved water coverage showed no clear association, corresponding to only about a 7% higher incidence per 1 SD increase (IRR = 1.07; 95% CI ≈ 14% lower to 34% higher). In contrast, a 1 SD

increase in travel time to motorised health care/transport (≈ +10.2 minutes) was associated with a 27% lower reported incidence (IRR = 0.73; 95% CI ≈ 43% lower to 6% lower), a statistically significant inverse association that likely reflects under-ascertainment in more remote areas rather than a truly protective effect. Finally, a 1 SD higher mean number of under-5 children per household (≈ +0.29 on the mean-U5 scale) was linked to roughly a 32% higher incidence (IRR = 1.32; 95% CI ≈ 3% to 69% higher).

Future projections

As for malaria, projections for diarrhoeal diseases had relatively wide confidence intervals when full uncertainty (parametric plus inter-model variability) was considered, but a similar and slightly stronger overall decline than for malaria was projected. The ensemble mean of the projections suggest there has already been a slight decline in suitability across the three priority regions since 1981-2000 (Figure 48). This was projected to continue in the near-term (2021-2040) and to mid-century (2041-2060) and similarly for both SSPs. As for malaria, given the uncertainty, a non-trivial potential (up to 20% probability) for future increases in incidence in the near-term remains, although this declines steadily by mid-century (Figure 48, Figure 49). Although still considered unlikely by the model, increases were slightly more likely in Kara and Centrale regions than Savanes.

Figure 48 - Projected changes in diarrheal incidence in children under 5 years in the priority regions. Points are ensemble mean values relative to the 2001-2020 period mean (dashed line). Error bars are 95% CIs.

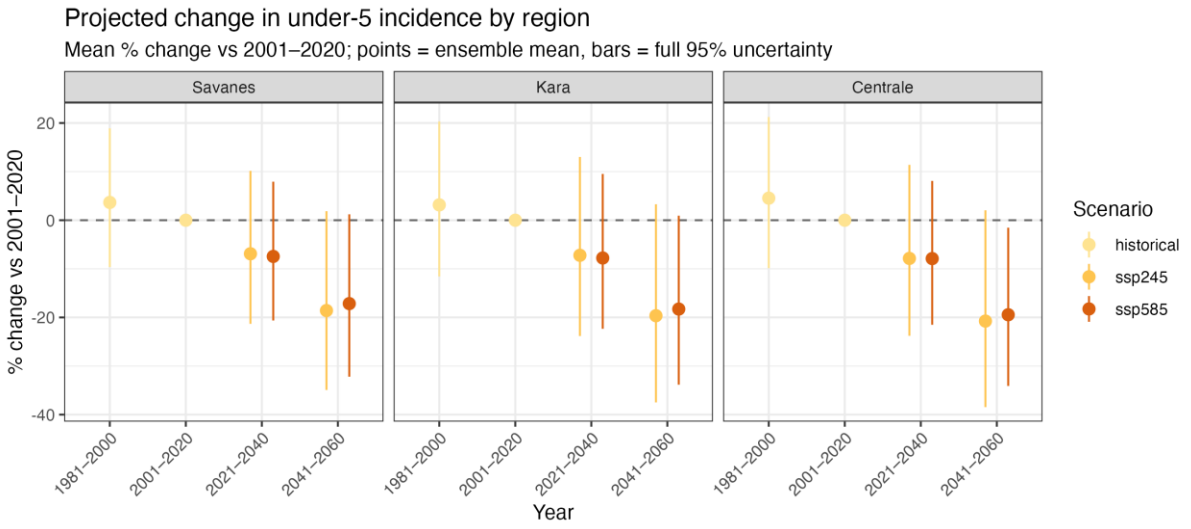

(Source: Own elaboration)

Figure 49 - Projected spatio-temporal changes in diarrheal incidence in children under 5 years in the priority regions by prefecture.

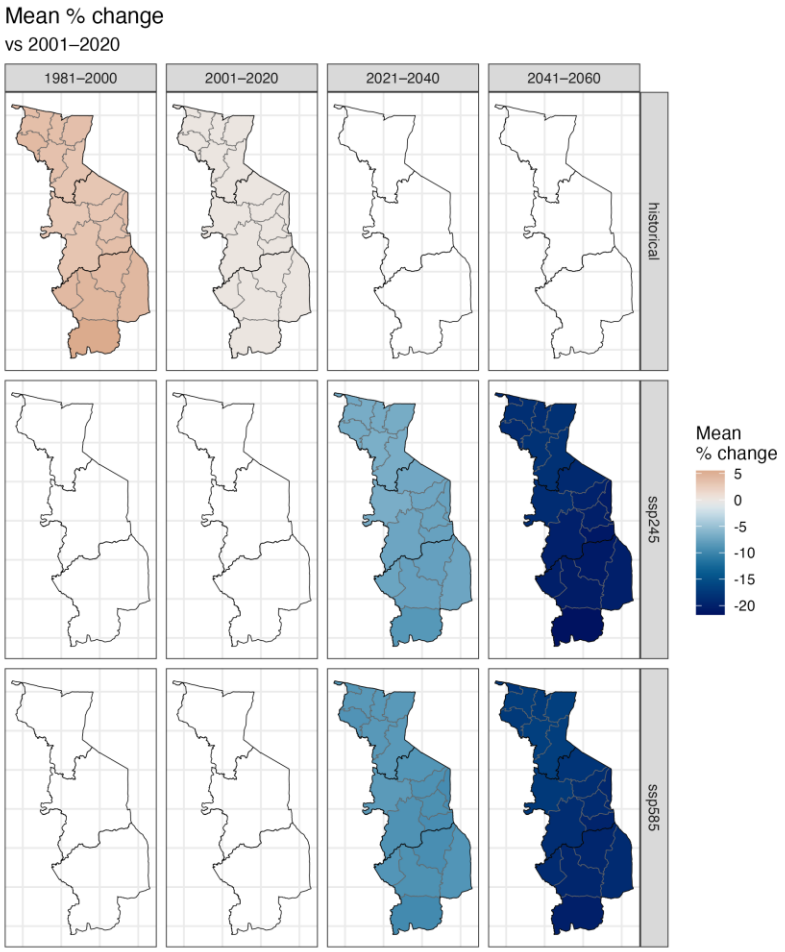

(Source: Own elaboration)

In all three northern regions, the projections show a broadly consistent seasonal pattern of under-5 diarrhoea in northern Togo that is consistent but more pronounced than in the training data. The models suggest incidence peaks during the warmer early part of the rainy season and reduced incidence in the late wet/dry season. In the DHIS data this appears as moderate positive anomalies in about March–July, and slightly earlier in Centrale and Kara compared to Savanes. Negative anomalies from roughly September–November. Across future time slices and both SSPs, the timing and shape of the seasonal cycle suggests slightly elevated incidence in shoulder periods and declines during the peak, particularly in SSP2-4.5. Overall, the model suggests declines in peak periods but increases in the off-season and the suggestion of a slight delay in seasonality by mid-century.

Figure 50 - Projected seasonal changes in diarrheal incidence in children under 5 years in the priority regions by prefecture.

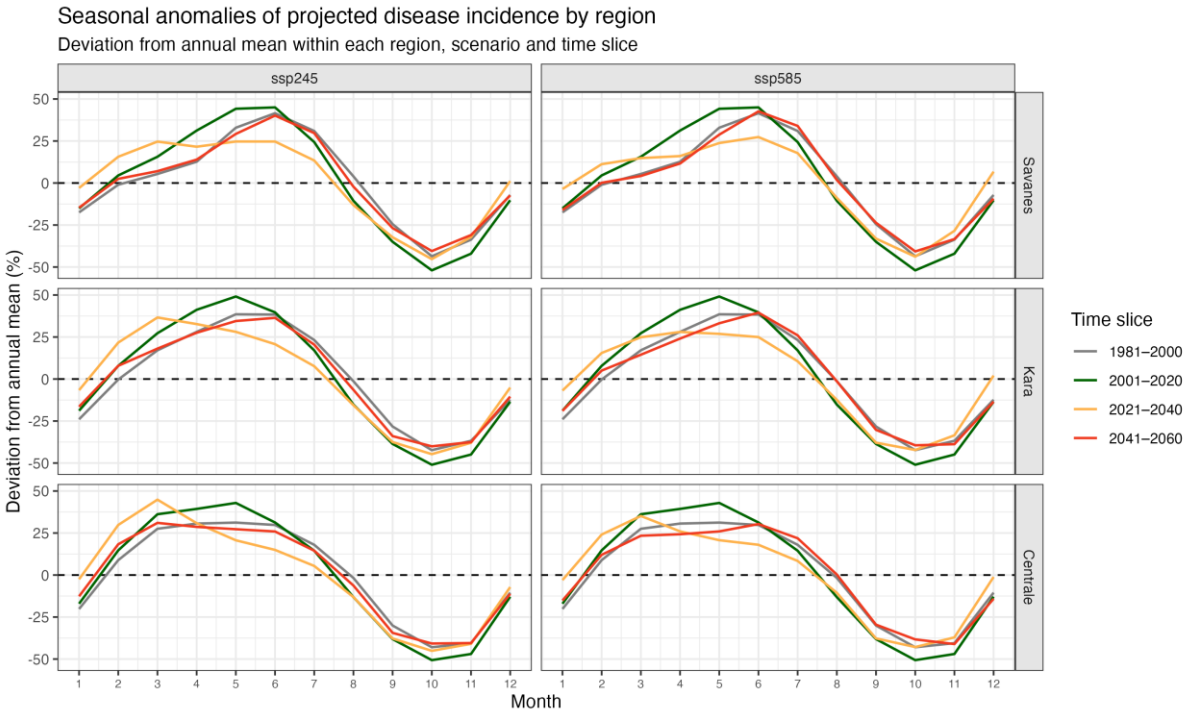

(Source: Own elaboration)

Model checks and limitations

As with the malaria model, diagnostics suggested that the chosen basis dimensions were generally adequate and no adjustments were made to the starting values (k=5).

Residual temporal autocorrelation at short lags was evident, with median lag-1 autocorrelation across prefectures of 0.66 (range 0.25–0.85) that decayed at higher lags, similar to the pattern seen for malaria. This indicates some remaining short-term dependence (e.g. local transmission dynamics, reporting artefacts), but explicitly adding an AR(1) structure did not materially change climate effect estimates or improve information criteria, so we retained the more parsimonious GAM for projections. Any remaining temporal dependence may slightly understate uncertainty at monthly scales but is unlikely to bias longer-term climate–incidence associations.

Mean deviance residuals showed significant positive spatial structure (Moran's I = 0.28, expected –0.04, p = 0.011), suggesting unmeasured spatially structured determinants. An alternative specification including a thin-plate spline over prefecture centroids achieved very similar deviance explained and information criteria and only marginally reduced spatial autocorrelation (Moran's I = 0.26, p = 0.017). Climate–diarrhoea smooths and projections were almost unchanged, so we again retained the simpler model and interpret the remaining spatial signal as reflecting unmodelled factors such as health system performance, ecological context or data quality.

For diarrhoea, the extrapolation and clamping checks gave very similar reassurance to those for malaria.

Several other limitations mirror those of the malaria analysis but with diarrhoea-specific nuances. Routine DHIS2 data capture only a small fraction of all diarrhoeal episodes. Community-based and modelled estimates from West Africa suggest around 2–3 episodes per child-year (≈2,000–3,000 per 1,000 children annually), whereas DHIS2 reports around 2–3 diarrhoea cases per 1,000 children (Walker et al., 2013). This large discrepancy likely reflects limited care-seeking, use of non-DHIS2 providers, and under-recording. As such, we must interpret DHIS2 counts as a relative signal for timing and spatial patterns rather than a complete measure of true incidence.

Furthermore, DHIS2 reporting quality for under-5 diarrhoeal cases likely varies across prefectures and over time, so under-ascertainment, changes in coding practice or rotavirus vaccine rollout may affect or bias absolute incidence levels and contribute to residual spatial structure. The model captures average monthly risk at prefecture level and cannot be relied upon to resolve short-lived, highly local outbreaks that may follow intense rainfall or flooding events, although a signal of heavy rain events was detected as a positive contributor. Vulnerability covariates (e.g. wealth, access to care, travel time, housing quality, WASH-related proxies) are static prefecture-level aggregates and do not represent within-prefecture heterogeneity. As with malaria, residual temporal and spatial autocorrelation suggests unmeasured or imperfectly measured processes such as local health-system performance, water and sanitation infrastructure, or population movement. Projections assume that climate–diarrhoea relationships remain stationary and that vulnerability factors do not change over time, so they should be interpreted as projected changes in incidence rates under a changing climate with other drivers held constant, rather than full burden trajectories that include adaptation (e.g. improved WASH, vaccination, or strengthened primary care).

Discussion

Taken together, the climate associations are consistent with a system in which under-5 diarrhoea risk in northern Togo is primarily rainfall-driven, modulated by temperature and humidity. Total precipitation in both the current and preceding month shows clear positive associations with incidence, indicating that wetter conditions—particularly in the month before cases occur—are an important driver of risk, likely via increased contamination of surface water, latrines and household environments. Extreme rainfall days were retained in the model but contribute only a weak, marginally positive signal, suggesting that more routine wet conditions matter more than rare, very intense events. In contrast, temperature-related variables generally display protective effects: warmer and more humid lag-1 conditions, and periods with more hot days, are associated with modest reductions in diarrhoeal incidence. This pattern is consistent with reduced environmental survival of many enteric pathogens under hotter, more evaporative conditions, and with shifts in water sources and behaviours during hot–dry spells. As for malaria, some of these patterns likely also capture broader seasonal processes (e.g. changes in health-seeking, food security, or circulation of other infections) that covary with climate.

For projections, the model indicates an overall long-term decline in climate-driven diarrhoeal incidence, slightly stronger than for malaria, but with substantial uncertainty. The ensemble suggests that suitability has already decreased modestly since the 1981–2000 baseline across the three northern regions and is projected to continue declining through 2021–2040 and 2041–2060 under both SSP2-4.5 and SSP5-8.5. Nonetheless, there remains a non-trivial probability (up to ~20% in some locations) of near-term increases, particularly in Kara and Centrale, even though this probability diminishes by mid-century. Seasonally, the model reproduces and sharpens the observed pattern of diarrhoea peaking in the warmer early rainy season (roughly March–July, slightly earlier in Centrale and Kara than Savanes) and decreasing in the late wet and early dry months (around September–November). Looking ahead, the seasonal cycle remains recognisable but shifts subtly: peak-season incidence is projected to decline, while shoulder periods become relatively more prominent and the peak timing appears to be slightly delayed by mid-century. Overall, climate change is expected to reduce peak diarrhoeal burden but may sustain or even increase off-season risk, implying that health systems may face a longer but less intense diarrhoea season.

Static WASH and demographic covariates behave broadly as expected but with mostly modest and imprecise effects. Higher exclusive breastfeeding coverage and improved toilet access both show protective tendencies—on the order of 15–20% lower incidence per standard deviation—although their confidence intervals overlap the null, indicating that these effects are suggestive rather than definitive. Improved water coverage shows no clear association with reported incidence, which may reflect heterogeneous water quality within the “improved” category or the importance of non-water pathways (e.g. food and person-to-person transmission). In contrast, greater travel time to motorised health care or transport is associated with substantially lower recorded diarrhoea incidence, a statistically significant inverse relationship that almost certainly reflects under-ascertainment and lower care-seeking in more remote prefectures rather than genuinely reduced risk. Finally, prefectures with more young children per household show markedly higher incidence (around one-third higher per standard deviation), consistent with greater within-household exposure and transmission among closely interacting siblings sharing the same WASH and caregiving environment. Together, these findings emphasise that observed diarrhoea patterns are shaped not only by climate and WASH but also by health-system

access and demographic structure, and that care must be taken to interpret HMIS-based trends in light of potential reporting and access biases.

5.3.3 Preterm birth

Model training

A total of 46,453 preterm births occurred between January 2018 and December 2024, corresponding to the period over which the PTB models were developed, validated, and finalised. The mean incidence nationally was 34.6 preterm births per 1000 live births per year. There was an indication of a slight increasing trend over the study period (32.1 per 1000 live births in 2018 to 35.7 per 1000 live births in 2024) at the country-level with a peak in 2021 (38.5 per 1000 live births). The linear trend was however not significant (p=0.25). Incidence varied by prefecture, but there was no clear difference between the incidence value between regions, which all convened around the national average (Figure 51)

Figure 51 Mean incidence rate (+/- 1 SD) of preterm birth per 1000 live births per region averaged across the years 2018-2024. The dashed line is the national mean incidence rate over the same period.

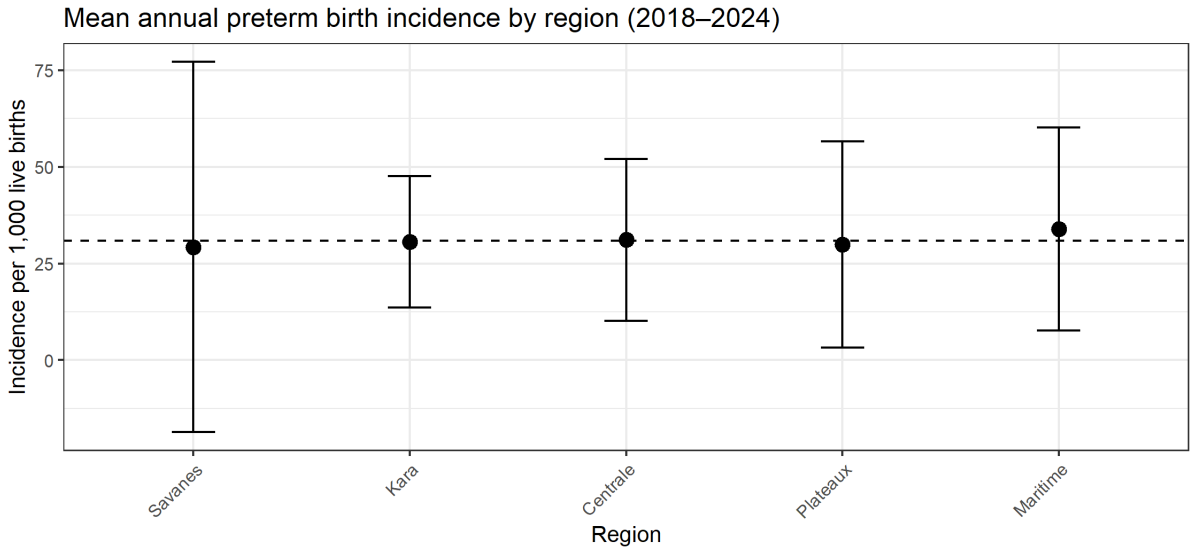

(Source: Own elaboration)

The prefecture-specific DLNM models explained a median of 37.1% (range: 13.8–65.5%) of the within-prefecture variation in monthly preterm birth rates. This level of fit is reasonable for PTB, a multifactorial outcome driven by individual-level clinical and obstetric factors (e.g. hypertensive disorders, multiple gestation, infection) that cannot be captured in monthly prefecture-level aggregates. The models nonetheless reproduced the broad temporal patterning needed to estimate stable exposure-lag-response relationships for meta-analysis.

Climate effects

The random-effects meta-analysis was conducted on 36 of the 39 prefectures. Three prefectures were excluded because monthly PTB counts were missing (assumed 0) for more than 10 months during the study period. Pooled, national exposure-lag-response function indicated an increased cumulative risk of PTB associated with heatwave exposure over lags 0-8 months before delivery. The cumulative IRR for pregnancies experiencing any heatwave, compared with non-heatwave pregnancies, was 1.20 (95% CI: 1.05-1.37) (Figure 52). Lag-specific IRRs were modest (around 1.02), but generally elevated, with strongest evidence at 1-month (1.02, 95% CI: 1.00-1.05), 2-month (1.02, 95% CI: 1.00-1.04), 3-month (1.02, 95% CI: 1.00-1.04), 6-month (1.02, 95% CI: 1.00-1.03) and 7-month lags (1.02, 95% CI: 1.00-1.04) (Figure 52). Best Linear Unbiased Prediction (BLUPs) estimates for the cumulative effect over lags 0-8 were mapped by prefecture (Figure 59) Figure 59 Percent change in preterm birth risk

associated with heatwave hazards across gestational lags (0-8 months), by prefecture. Values represent the cumulative heatwave effect from the prefecture-specific time-series models, expressed as percent change in risk ((IRR − 1) × 100). Greyed prefectures were excluded from the meta-analysis due to insufficient data quality (NA counts).and did not show a consistent North-South gradient. Prefecture-specific lag-response functions are shown in Annex 1 in **Error! Reference source not found.Error! Reference source not found.**.

Figure 52 - Exposure-response (cumulative lag 0-8) and lag-response plots for the relationship between heatwaves and preterm birth by prefecture; main analysis and sensitivity analyses. Sensitivity analysis 1 restricted flexibility in the lag-response relationship (cubic spline with 1 knot), Sensitivity 2 excluded NA/0 PTB counts, Sensitivity 3 did not control for relative humidity, Sensitivity 4 fitted the meta-regression on all 39 prefectures, and Sensitivity 5 removed prefectures highlighted as being different to the majority and highly influential (Tchaoudjo, Cinkasse, Oti-Sud, Tchamba, Agou, Est-mono, Toto, Golfe) in the meta-analysis.

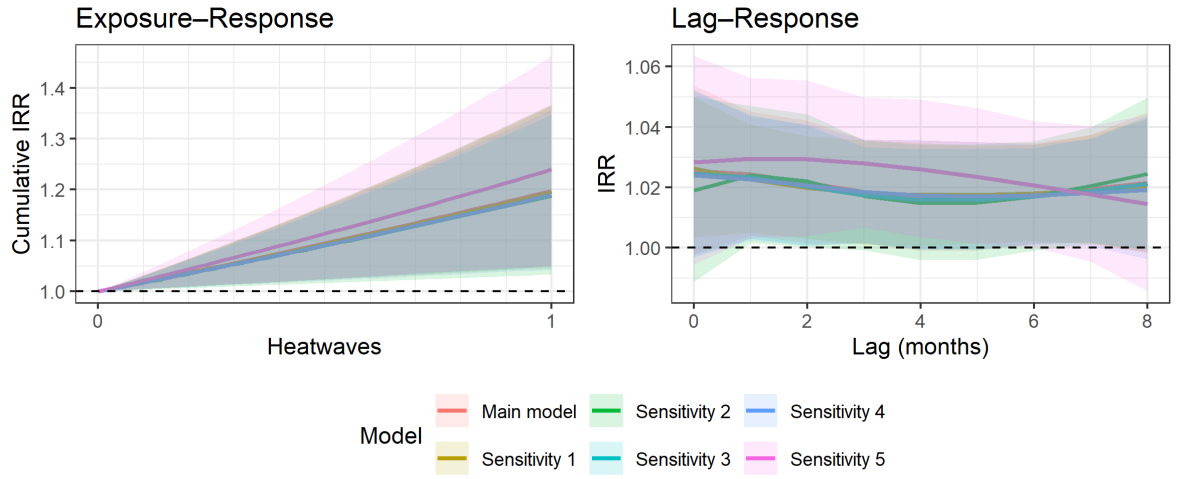

(Source: Own elaboration)

Vulnerability factors

Stratified analyses showed modest differences in cumulative heatwave-PTB associations across prefecture-level vulnerability factors (Appendix 1, **Error! Reference source not found.**Figure 61). Prefectures with lower maternal education had a cumulative IRR of 1.30 (95% CI: 1.07-1.58) compared with 1.11 (95% CI: 0.89-1.37) in higher-education areas. For A/C coverage, the IRR was 1.29 (95% CI: 1.00-1.67) in lower-coverage areas versus 1.15 (95% CI: 0.98-1.36) in higher-coverage areas. Lower household wealth corresponded to an IRR of 1.28 (95% CI: 1.04-1.57), compared with 1.14 (95% CI: 0.95-1.37) for higher wealth. Differences for ANC attendance (1.15; 95% CI: 0.97-1.37 vs 1.21; 95% CI: 0.96-1.53) and adolescent motherhood (1.17; 95% CI: 0.99-1.39 vs 1.22; 95% CI: 0.94-1.59) were small and overlapping. Across all factors, confidence intervals overlapped substantially, and meta-regression provided no evidence of significant effect modification (all $p > 0.10$). Overall, the prefecture-level vulnerability indicators did not materially alter the cumulative heatwave–PTB association.

Future projections

Heatwaves already contribute to PTBs in northern Togo. The attributable fraction (AF) represents the share of PTBs attributable to heatwave exposure during pregnancy (delivery month and preceding eight months). During the recent historical period (2001-2020), this burden was modest, but meaningful: 1.3% (0.1%-3.5%) of PTBs in Centrale, 1.7% (0.2%-3.8%) in Kara, and 1.8% (0.2%-4.1%) in Savanes were attributable to heatwaves.

Differences in AFs across Centrale, Kara and Savanes reflect differences in the proportion of PTBs attributable to heatwaves, rather than differences in underlying PTB incidence. The AF isolates the

heat-related component of risk and is therefore distinct from observed PTB incidence, which is shaped by many non-climatic factors including obstetric care, maternal health, and reporting practices.

AFs rise in both future periods and scenarios. By 2021-2040, AFs increase to 1.7% (0.2%-4.4%), 2.2% (0.3%-5.0%), and 2.4% (0.4%-5.3%) in Centrale, Kara, and Savanes under SSP2-4.5, and to 1.8% (0.1%-4.7%), 2.4% (0.3%-5.6%), and 2.7% (0.4%-6.1%) under SSP5-8.5. By 2041–2060, AFs roughly double (or more) compared with 2001-2020, reaching 2.8% (0.4%-6.3%) in Centrale, 3.6% (1.2%-7.3%) in Kara, and 3.8% (1.5%-7.9%) in Savanes under SSP2-4.5, and 3.3% (0.1%-7.5%), 4.0% (0.3%-8.4%), and 4.5% (1.1%-8.8%) under SSP5-8.5.

When expressed as percentage change relative to 2001-2020 (Figure 53), increases are large and broadly consistent across regions. By 2041-2060 under SSP2-4.5, AFs rise by 114.8% (33.2%-184.8%) in Centrale, 116.7% (64.9%-166.6%) in Kara, and 117.9% (74.1%-149.4%) in Savanes. Under SSP5-8.5, the corresponding increases are 144.3% (-73.0%-337.9%), 129.7% (-43.5%-255.6%), and 155.2% (15.2%-259.9%).

Figure 53 - Projected changes in heatwave-attributable preterm births by region. Points show ensemble mean percent change in attributable fraction relative to 2001–2020 (SSP2 baseline; dashed line), with 95% uncertainty intervals.

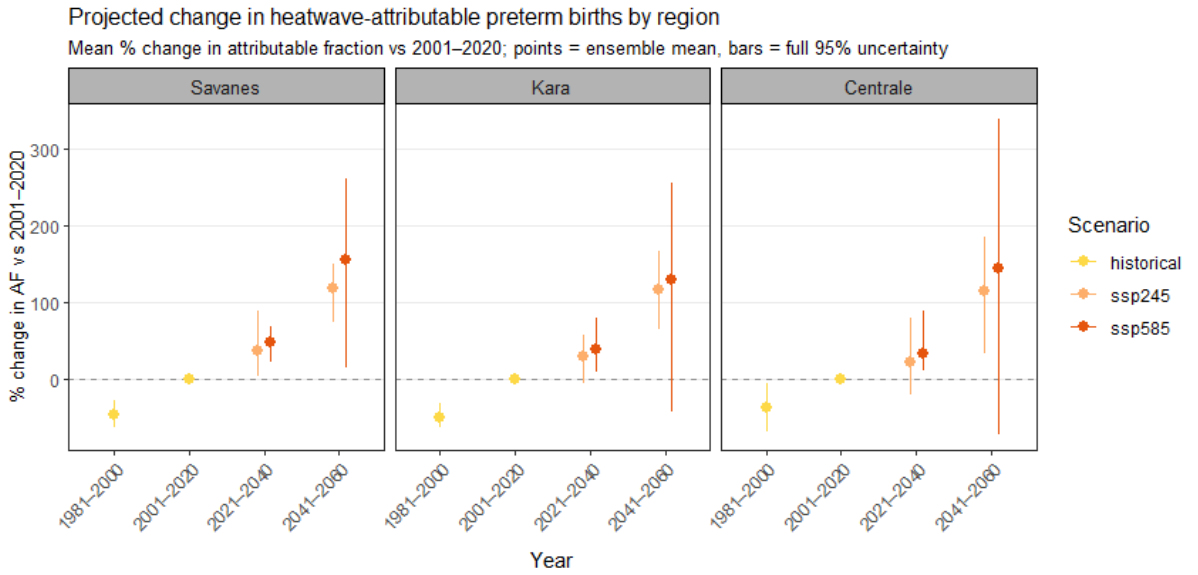

(Source: Own elaboration)

Figure 54 shows that nearly all prefectures experience positive increases in AF under both scenarios. In 2021-2040, most prefectures show moderate rises, with slightly larger increases appearing more frequently under SSP5-8.5. By 2041-2060, strong positive changes occur across almost all prefectures. Some of the largest increases appear in parts of Kara and Savanes, but overall, the pattern is one of a broad, region-wide rise, with no sharp spatial contrasts. This mirrors the regional averages in Figure 53.

Figure 54 Projected spatio-temporal changes in the heatwave-attributable fraction of preterm birth in the priority regions by prefecture.

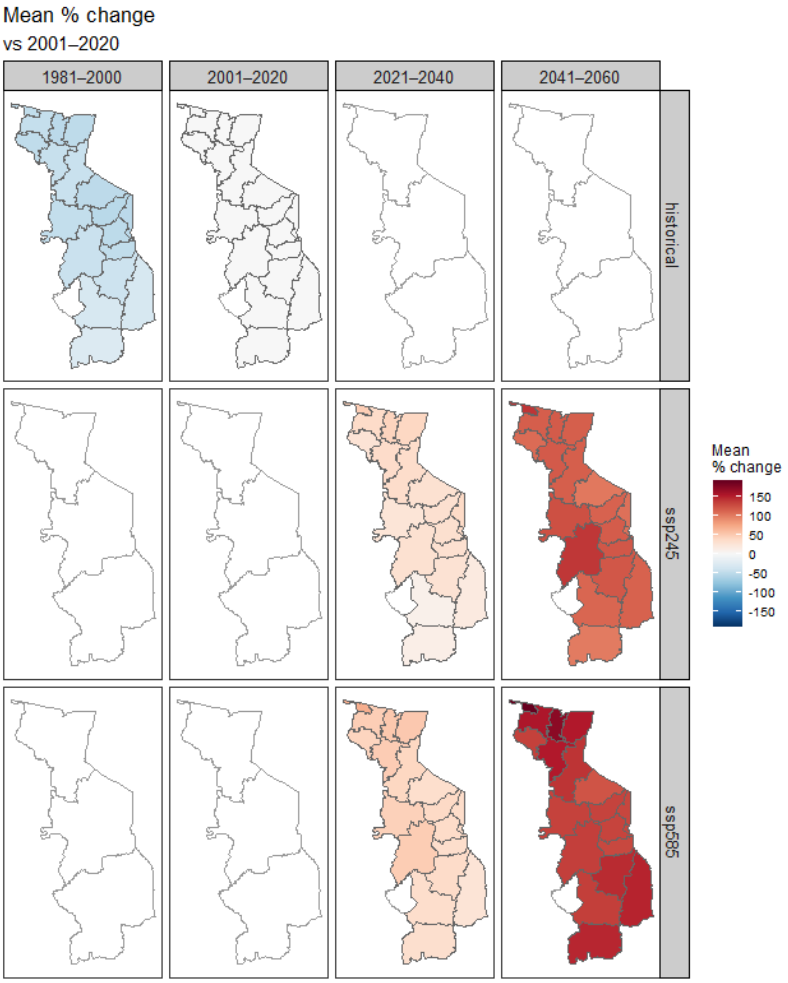

(Source: Own elaboration)

Before moving to incidence-based metrics, it is important to note that although heat exposure is greater under SSP5-8.5, absolute burdens are smaller because births decline much more rapidly in this scenario (see Appendix 1, Figure 62. In other words, SSP5-8.5 produces fewer heat-attributable PTBs not because the risk is lower, but because far fewer babies are born, overshadowing the rising effects of heat.

To move from proportional to absolute risk, incidence projections are reported per 1,000 live births. While DHIS2 reports a much lower PTB incidence (≈3.5%), consistent with substantial under-ascertainment, projections assume a baseline PTB rate of 13% (aligned with regional epidemiological estimates) to avoid underestimating absolute future burden.

By 2041-2060, heatwave-attributable incidence per 1,000 live births rises to 3.6 (0.6-8.1) and 4.3 (0.1-9.8) in Centrale, 4.3 (1.4-8.6) and 4.9 (0.4-10.3) in Kara, and 4.4 (1.7-9.0) and 5.2 (1.2-10.2) in Savanes under SSP2-4.5 and SSP5-8.5, respectively. These represent substantial increases compared with 2001–2020. For example, 120.3% (115.2%-138.0%) and 149.9% (128.0%-249.5%) in Savanes. Toward the end of the projection period, the two scenarios begin to diverge: incidence continues to rise under both, but SSP5-8.5 increases more steeply in the late 2050s, widening the gap relative to SSP2-4.5 Figure 55.

Figure 55: Projected incidence of preterm births attributable to heatwaves per 1,000 live births. Lines show ensemble mean projections, and shaded ribbons represent 95% uncertainty intervals combining climate-model and epidemiological uncertainty.

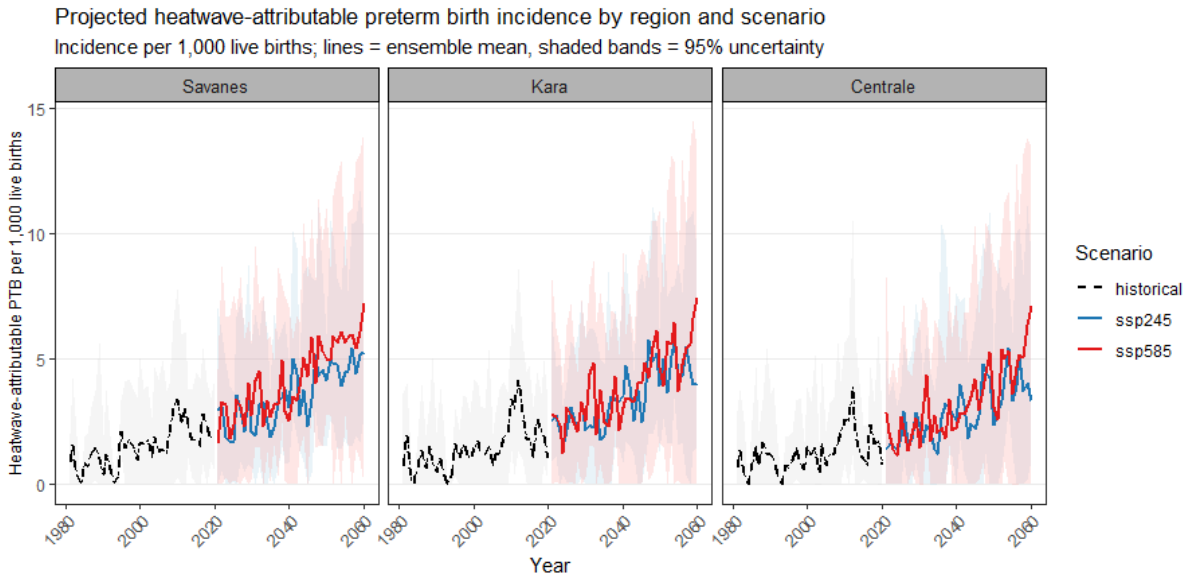

(Source: Own elaboration)

Validation and limitations

Residual diagnostics from the prefecture-specific regression models showed no evidence of major misspecification. Partial autocorrelation plots did not reveal concerning lagged structure, suggesting that short-term dependence was limited after accounting for the spline terms. For the second-stage meta-analysis, quantile-quantile plots indicated no strong deviations from normality of the prefecture-specific estimates. Although between-prefecture heterogeneity was low, BLUPs still reveal modest spatial variation around a broadly shared national heat-PTB response.

Baujat plots highlighted a few prefectures whose estimates differed from the overall pattern and exerted disproportionately high influence on the pooled estimate. Sensitivity analyses excluding these prefectures, as well as analyses that altered key modelling choices (including reducing lag–response flexibility, removing humidity adjustment, or omitting months with 0/NA counts), produced estimates that were aligned with the main model. Re-fitting the meta-analysis with all 39 prefectures yielded comparable results, suggesting that the pooled lag-response function was not overly sensitive to any individual modelling decision (Figure 52).

Sensitivity analyses replacing the Togo-specific multi-lag effect estimates with a pooled global odds ratio for heatwaves in late pregnancy produced slightly higher attributable fractions (e.g. AF in Savanes under SSP2, 2041–2060: 3.8% vs 4.6%) but preserved the overall spatial and temporal patterns of the projections (Appendix 1, Figure 63 and Figure 64). Similarly, projections run under a counterfactual scenario in which births were held constant at 2022 levels yielded incidence and AF trajectories that closely matched the main results, confirming that the projected increase in heat-attributable risk is not an artefact of demographic assumptions. Together, these checks indicate that both the epidemiological effect estimates and the projection engine are stable with respect to reasonable variations in modelling choices.

Several limitations of the DHIS2 data should be acknowledged. Firstly, there is potential for outcome misclassification. The system does not document how gestational age is measured, or how PTBs are classified, making accuracy of PTB reporting uncertain. The national PTB rate observed in DHIS2 (Jan 2018 - Dec 2024) was around 3.5%, which is substantially lower than earlier estimates for Togo (13.3% in 2010) (Blencowe et al., 2012) As recent estimates showed little change over time (2010-2020) in neighbouring countries (Benin, Nigeria, and West Africa as a whole) (Ohuma et al., 2023), we assume Togo PTB rates have not dropped significantly in recent decades. This implies that DHIS2 is likely capturing only a subset of PTBs – possibly those with shorter gestational lengths – and the heat effects

may therefore pertain to a narrower subset of PTB phenotypes. Secondly, birth-related data was only available at a monthly temporal resolution, making it impossible to confirm precisely whether each heatwave preceded the births assigned to it. The multi-month lag structure mitigates this to some extent. Monthly-prefectural level analyses also prevent an accurate representation of the preterm birth burden in specific population groups. Prefecture-level vulnerability indicators do not represent individual-level conditions and may themselves reflect a mix of social, environmental and health-system characteristics. The projections therefore reflect climate-related changes in PTB risk under current patterns of vulnerability, rather than modelling how vulnerability might itself evolve.

Additional limitations apply to the projections. Baseline PTB rates were held constant over time, so potential improvements or deteriorations in obstetric care were not represented. Future heat-PTB relationships were assumed to be stationary, meaning that behavioural or infrastructural adaptations (e.g. improved cooling, heat-health preparedness or expanded antenatal care) were not modelled and could attenuate future impacts. The use of a binary heatwave indicator captured the occurrence, but not the duration or intensity, of extreme heat. Although future fertility and live birth trajectories from SSP2-4.5 and SSP5-8.5 were fully integrated into the projections, uncertainty around those demographic projections was not propagated. Likewise, uncertainty related to baseline PTB under-reporting and future changes in registry completeness was not included. As with all climate–health projections, the estimates should therefore be interpreted as changes in PTB risk under evolving climate exposures, holding other determinants constant, rather than as forecasts of the full future burden.

Discussion

Taken together, the results indicate that preterm birth in northern Togo is a climate-sensitive outcome driven primarily by cumulative heat exposure across pregnancy, rather than by short-term or seasonally concentrated effects. In contrast to malaria and diarrhoea, where climate influences operate through ecological and environmental pathways that vary strongly across space and time, the heat-PTB association reflects a long exposure window spanning much of gestation. Lag-specific effects are individually small, but their persistence across multiple months leads to a measurable cumulative increase in risk.

This interpretation is consistent with emerging evidence from other low-income settings. In Johannesburg, South Africa, exposure to high environmental temperatures in very early pregnancy has been associated with a substantially increased risk of preeclampsia at childbirth (Part et al., 2022). Hypertensive disorders of pregnancy are a recognised risk factor for both spontaneous and medically indicated preterm birth, suggesting one plausible pathway through which early and sustained heat exposure may contribute to PTB risk.

Unlike malaria and diarrhoea, where future climate change is projected to redistribute risk spatially or alter seasonal patterns, projected heat-attributable PTB risk increases consistently across prefectures under both emissions pathways. The absence of pronounced spatial gradients and the low between-prefecture heterogeneity suggest that heat exposure during pregnancy acts as a pervasive physiological stressor, rather than one confined to specific ecological or socio-environmental contexts. Prefecture-level vulnerability indicators showed little evidence of effect modification, implying that while socioeconomic conditions shape overall maternal and neonatal health, they do not strongly alter the relative impact of heatwaves on PTB risk at this spatial scale. However, the use of monthly, prefecture-level DHIS2 data may have limited our ability to detect finer-grained heterogeneity in vulnerability.

Projection results further highlight the distinction between relative and absolute burden. Attributable fractions rise more steeply under SSP5-8.5, reflecting greater heat exposure, yet absolute numbers of heat-attributable PTBs are lower than under SSP2-4.5 because projected fertility declines more rapidly. If future live births do not decrease as strongly as assumed under SSP2-4.5 or SSP5-8.5, absolute heat-attributable burdens would be higher than those projected here. This reinforces the value of reporting AFs and incidence alongside absolute counts and clarifies that differences in AF across regions reflect variation in the proportion of PTBs attributable to heat, rather than differences in underlying PTB incidence.

Overall, the findings suggest that climate change is likely to amplify an already widespread heat-related risk for PTB, rather than concentrate risk in particular locations or seasons. This contrasts with malaria and diarrhoea, where climate change reshapes when and where risk is highest. For PTB, the results

instead point to adaptation needs that cut across geographic and socioeconomic boundaries, including reducing maternal heat exposure and strengthening heat-aware antenatal and delivery care. As heatwaves become more frequent and prolonged, such measures are likely to be important across northern Togo, not only in areas traditionally identified as most vulnerable. Improvements in routine PTB surveillance, including clear documentation of gestational age assessment and consistent classification of PTB, would substantially strengthen future analyses. Finer temporal resolution data (daily or weekly) would also allow more precise alignment of heat exposure with critical windows of pregnancy.

5.4 Synthesis and interpretation of key results

Synthesis of Stage 1 and Stage 2 Risk Assessments

The two-stage assessment was designed so that Stage 1 provides a broad, screening-level picture of climate–health risk using the IPCC Hazard–Exposure–Vulnerability framework, while Stage 2 uses epidemiological models to quantify climate–health relationships and project future incidence. Taken together, they offer a consistent and mutually reinforcing view of climate-sensitive health risks in Togo, but also highlight important nuances that are not visible from risk mapping alone.

Malaria

In Stage 1, malaria risk was driven by changes in the length of the transmission season (LTS), the concentration of under-5 children, and structural vulnerabilities such as low wealth, poor housing, low ITN coverage and long travel times to care. This screening exercise highlighted the three northern regions, especially parts of Centrale and Kara, as areas where climate suitability is increasing or remaining high, where large, exposed populations live, and where socioeconomic and health-system vulnerabilities remain substantial.

Stage 2 modelling broadly confirms and refines this picture. The GAM results show that malaria incidence in under-5 children is most strongly associated with hot, humid and thermally variable conditions at a one-month lag, while very high mean temperatures tend to be limiting. Projections suggest gradual declines in incidence in already hot lowland and northern areas, but possible increases or slower declines in cooler, higher-elevation parts of the centre of the country as they warm towards more suitable thermal conditions. This aligns with the Stage 1 LTS results, which indicated that climate suitability has already expanded or remained stable in certain elevated zones while contracting elsewhere.

On the vulnerability side, Stage 1 identified poor access to care, low wealth and poorer housing quality as key contributors to malaria risk. Stage 2 finds that longer motorised travel time to health facilities is associated with higher malaria incidence, and that wealth and housing show weakly protective trends, even if not always statistically precise. This suggests that the structural vulnerability pattern from Stage 1 is directionally consistent with the model-based evidence: climate signals matter, but their impact is modulated by health-system reach and household conditions. Together, the two stages point to highland and fringe areas of the north and centre as emerging foci where climate suitability, exposed under-5 populations and access-related vulnerabilities intersect.

Diarrhoeal disease
For diarrhoeal disease, Stage 1 distinguished two hazard pathways: “wet contamination” (extreme rainfall days) and “hot–dry” (compound heat and very low rainfall), alongside high under-5 exposure and WASH-related vulnerabilities (household crowding, low exclusive breastfeeding, unimproved water and sanitation, poor access to care). This produced a map where northern prefectures with increasing heavy rainfall and persistent WASH deficits emerged as high-risk areas.

Stage 2 modelling supports the central role of rainfall but offers a more nuanced view of temperature and seasonality. The GAM shows that total precipitation (especially at a one-month lag) is positively associated with diarrhoea incidence, consistent with the wet-contamination pathway, while warmer conditions and periods with more hot days show generally protective associations, potentially reflecting reduced environmental survival of enteric pathogens and changes in water use during hot–dry periods. Projections indicate a long-term climate-driven decline in diarrhoeal incidence, slightly stronger than for

malaria, but with non-trivial probabilities of increases in some prefectures and seasons, particularly in Kara and Centrale and during the early rainy season.

The WASH- and crowding-related vulnerabilities from Stage 1 also align with Stage 2 findings: exclusive breastfeeding and improved toilets show modestly protective but imprecise effects, while household crowding of under-5s is clearly associated with higher incidence. The inverse association between travel time and reported diarrhoea, interpreted as under-ascertainment in remote areas, reinforces the Stage 1 concern that limitations in access and reporting can mask true risk. Overall, Stage 1 highlights where diarrhoeal risk is structurally high due to WASH and crowding, while Stage 2 shows that wet months in these settings remain hazardous, even if overall climate trends may lower average incidence. Together, they suggest that WASH and surveillance strengthening in wet-season–prone northern prefectures remain essential adaptation priorities, despite projected declines.

Heat-related preterm birth

Stage 1 risk mapping for preterm birth combined changes in heatwave frequency, the concentration of live births, and vulnerability factors related to wealth, maternal education, adolescent motherhood, A/C coverage and timely ANC. This produced a pattern where the three northern regions, with both rising heat extremes and constrained adaptive capacity, stood out as priority areas for maternal and neonatal heat risk.

Stage 2 epidemiological modelling confirms that heatwaves already increase PTB risk and that this burden will grow under future climate change. The meta-analysis shows that heatwaves contribute small effects in multiple months of pregnancy (lags 0-8), which accumulate to produce an overall ~20% relative increase in PTB risk. Current heatwave-attributable fractions are modest (about 1–2% of PTBs in the northern regions), but roughly double or more by mid-century, reaching 3–4.5% under both SSP2-4.5 and SSP5-8.5, with increases spread across nearly all prefectures.

In contrast to malaria and diarrhoea, Stage 2 finds only modest and statistically non-significant differences in heatwave–PTB effects by wealth, education, A/C coverage, ANC or adolescent motherhood. This implies that, while these factors are important for overall maternal–child health, heatwave-related PTB risk is relatively widespread rather than tightly concentrated in specific vulnerability strata. Combined with the Stage 1 hazard maps, this indicates that rising heatwaves will increase PTB risk broadly across northern Togo, with only limited evidence that current prefecture-level vulnerability indicators markedly amplify or attenuate this effect. The synthesis therefore underlines heat-related PTB as a highly climate-sensitive outcome where adaptation (cooling, antenatal heat–health measures, facility preparedness) will be essential even in areas not flagged as the most socioeconomically vulnerable.

Overall synthesis

Together, the two stages support a coherent climate risk and adaptation message: climate change is reshaping health risks in Togo. Hazards are evolving (longer malaria seasons in some highlands, more frequent heatwaves), exposures remain high in children and pregnant women, and underlying vulnerabilities in WASH, housing and health-system access persist. Stage 1 tells us where these ingredients currently co-occur; Stage 2 tells us how strongly and in what direction climate is likely to shift disease incidence over the coming decades.

This integrated evidence base provides a robust foundation for prioritising northern regions for health-focused climate adaptation, targeting highland and fringe areas for malaria surveillance and vector control, focusing WASH and diarrhoea prevention on wet-season and crowded settings, and mainstreaming heat–health protection into maternal and newborn care across northern Togo.

6. Adaptation approach

In terms of the IPCC concepts, adaptation is defined as the process of adjustment in natural or human systems in response to actual or expected climate and its effects, in order to moderate harm or exploit beneficial opportunities. This chapter provides recommendations for adaptations that could reduce the risk posed from the health outcomes discussed in previous chapters. These adaptation measures relate to the exposure and vulnerability factors also discussed in previous chapters. The overall aim of these measures is to reduce vulnerability by influencing the environmental vulnerability in exposed groups, strengthen existing services and increase existing protective coverage.

The objective of these measures is to strengthen the resilience of Togo's national health systems and vulnerable communities to climate-sensitive health outcomes. This shall be achieved by developing climate-resilient health systems and implementing adaptation activities at the health facility and community level.

Implications for adaptation – Malaria

From an adaptation perspective, the key message is that modest net declines in climate suitability do not remove malaria risk in northern Togo. Instead, they redistribute it in space and time. The synthesis shows that short periods of hot, humid and thermally variable conditions, particularly at a one-month lag, will continue to drive transmission, while some cooler highland and fringe areas may become relatively more suitable as they warm. These results are consistent with other recent studies examining the implications of climate change for malaria impacts in children in Sub-Saharan Africa (Symons et al., 2025).

Adaptation planning therefore needs to anticipate more concentrated transmission in specific places and seasons, rather than a uniform decline. Surveillance and vector-control efforts should be adjusted so that preventive measures (ITN distribution, IRS, chemoprevention where relevant) are in place before the late–rainy / early–dry season peak, with particular attention to higher-elevation where risk may emerge or expand. This argues for more flexible, climate-informed micro-planning rather than fixed campaign timings based only on historical patterns. Surveillance needs to be enhanced by establishing sentinel sites to track disease trends and intervention effectiveness under changing climatic conditions.

As part of adaptation efforts, malaria prevention and control measures will help reduce vulnerability to climate-sensitive health risks. Potential key actions include supporting malaria vaccine distribution within an integrated vector management framework, installing mosquito screens on doors and windows in high-risk areas, and strengthening diagnostic capacity through rapid tests and improved laboratory services.

The vulnerability analyses emphasise that health-system access is a central adaptation lever. Longer travel times to health facilities are associated with higher malaria incidence, and under-ascertainment is likely in the most remote areas. Priority actions include reducing geographical and financial barriers to effective diagnosis and treatment (e.g. outreach, community health workers, upgraded peripheral facilities). They also encompass strengthening routine surveillance to reliably detect shifts in incidence and seasonality. Further it should be ensured that new or expanding high-risk areas are incorporated into routine vector-control programmes.

At household and community level, population growth, mobility, uneven housing quality and patchy vector-control coverage will shape how climate signals translate into actual burden. Even small climate-driven increases in suitability in highland or newly receptive areas could produce substantial case increases if baseline immunity is low and primary care is weak. Conversely, in areas where climate becomes less favourable, maintaining strong intervention coverage will be important to consolidate potential gains and prevent resurgence.

Finally, the projections reflect only the climate component of malaria risk under an "all else equal" assumption. If health systems and vector-control delivery are strained, even small climatic shifts could exacerbate underlying vulnerabilities; conversely, continued scale-up of ITNs, IRS, diagnostics, treatment and vaccines could offset or outweigh climate effects. Climate adaptation for malaria in northern Togo should therefore prioritise aspects including strengthened, flexible vector-control programmes; improved surveillance and diagnostic coverage, especially in emerging high-risk and

hard-to-reach areas; reduced access barriers to care; and, potentially, climate-informed communication campaigns or alert systems that integrate climatic indicators to anticipate periods and places of heightened transmission. Also, targeted communication for vulnerable groups such as pregnant women and caregivers of young children and mass campaigns can promote awareness, uptake of interventions, and sustained adaptive behaviours.

Implications for adaptation – Diarrhoea

For diarrhoeal disease, the models indicate that wetter months and heavy rainfall events remain the main climate drivers of risk, even though overall climate trends point to a gradual decline in incidence. This means that climate change may lower average diarrhoeal burden but still leave children in northern Togo highly vulnerable to rain-driven spikes, especially in settings with weak WASH and health systems.

Adaptation measures therefore need to focus less on the long-term mean decline and more on managing wet-season and extreme-event risk. Priority actions could include investing in flood- and drought-resilient WASH infrastructure (water supply, drainage, and sanitation that can withstand heavy rainfall and dry spells); protecting water quality during wet seasons (e.g. safe storage, point-of-use treatment, rapid repair of damaged infrastructure); and integrating rainfall and flood information into outbreak preparedness, and medicinal supply management.

The vulnerability profile points strongly to structural WASH deficits and crowding as persistent drivers of diarrhoea burden. Exclusive breastfeeding and improved toilets appear modestly protective, while the number of young children per household is clearly associated with higher incidence. This suggests that climate-informed adaptation should reinforce aspects such as behavioural interventions (exclusive breastfeeding promotion, safe food and water handling, and handwashing campaigns); reduction of overcrowding where feasible (e.g. housing and shelter programmes, especially in informal or displaced settings); and targeting WASH upgrades and hygiene promotion to high-burden, high-crowding prefectures identified in Stage 1.

The counter-intuitive finding of lower reported diarrhoea with longer travel times likely reflects under-ascertainment in remote communities. For adaptation, this underscores the need to extend surveillance and service reach (e.g. community-based reporting, mobile clinics) so that climate–diarrhoea relationships and emerging risks in remote areas are not missed, and improved data streams can lead to increased capacity for analysis and forecasting.

Given the wider evidence, climate shocks including floods, localised heavy rainfall and drought-related WASH failures, are still likely to trigger outbreaks that are missed in relatively coarse monthly prefecture averages. Our results should not be interpreted as evidence that extremes are unimportant, but rather as a reminder of data limitations. Improving diagnostic specificity, routine data quality and spatial resolution will be important both for better risk assessment and for more targeted adaptation (e.g. distinguishing bacterial vs viral diarrhoeas with different climate sensitivities).

Overall, climate adaptation for diarrhoeal disease in northern Togo should prioritise resilient WASH systems, reduction of household crowding and exposure, climate-smart surveillance, and strong outbreak preparedness. Community-level WASH behaviour changes sustained promotion of exclusive breastfeeding, and strategies to maintain safe water and sanitation are no regret adaptation strategies that will pay off during wet seasons and climate extremes, help buffer climate-related variability and reduce the overall burden of childhood diarrhoea.

To reduce climate-sensitive diarrhoeal disease risks, interventions should focus on strengthening surveillance and improving community-level prevention. Sentinel sites established to monitor diarrhoeal trends and detect outbreaks early will be beneficial. Schools and kindergartens can serve as key intervention points for health education and distribution of oral rehydration salts (ORS) and zinc for prompt treatment. Cross-community coordination among schools, parents, and healthcare providers needs to be enhanced to ensure timely response and continuity of care. Infrastructure improvements may include decentralized wastewater treatment systems (DEWATS) to reduce contamination risks and adapted toilets to support menstrual health and hygiene. These measures aim to build resilience, improve health outcomes, and foster sustainable practices under changing climatic conditions.

Implications for adaptation – Preterm birth

For PTB, the key adaptation message is that heat exposure acts as a widespread and cumulative stressor across pregnancy, rather than a risk confined to a narrow gestational window, season, or location. Unlike malaria and diarrhoea, where adaptation can be targeted to particular ecological settings or periods of heightened transmission, reducing heat-related PTB risk requires lowering maternal heat exposure throughout pregnancy.

At health-system level, this points to the importance of climate-resilient maternal care environments. Passive cooling measures in health facilities – including improved ventilation, heat-reflective roofing, appropriate building materials and revegetation – can substantially reduce indoor temperatures in maternity wards, antenatal clinics and waiting areas. These adaptations reduce cumulative heat exposure during routine antenatal care as well as during periods of prolonged facility attendance later in pregnancy and represent no-regret investments under rising heat extremes.

Clinical preparedness is also relevant. Although the epidemiological analysis does not isolate specific obstetric complications, heat may exacerbate physiological stress during pregnancy and care-seeking. Ensuring the availability of heat-stable essential medicines, such as carbetocin, and strengthening logistics and medicines management systems (LMIS) to function reliably under high temperatures are therefore important components of climate-resilient maternal health services.

Community-level adaptation should focus on awareness and behavioural protection across pregnancy. Integrating heat-health messaging into antenatal care and outreach – including guidance on hydration, rest, timing of travel, and recognising heat-related symptoms – can support pregnant women to reduce avoidable exposure during heatwaves. Framing heat as a maternal health risk, rather than a routine environmental condition, is likely to be important as heatwaves become more frequent.

Finally, the findings highlight the need for strengthened analytical and modelling capacity for heat and maternal and perinatal health. Compared with malaria and diarrhoea, evidence on heat-related pregnancy outcomes remains limited, particularly in low-income settings. Building national capacity to monitor heat exposure, link climate data to maternal health outcomes, and evaluate adaptation measures will be essential for refining interventions and identifying whether particular gestational windows are more sensitive as data improve.

Overall, adaptation for heat-related PTB requires a system-wide approach that reduces maternal heat exposure across pregnancy, strengthens facility resilience, safeguards essential medicines, and improves heat-health awareness. As heat exposure during pregnancy is cumulative and widespread, protecting maternal and newborn health under climate change will depend on embedding heat protection into routine maternal care, rather than relying on narrowly targeted or season-specific interventions.

7. References

Adeboyejo, A. T. D. O. A., Yemi Adewoyin, Abisola O. Oyasiji. (2020). Spatial and demographic patterns of climate related diseases among hospitalized children in parts of

Southwest Nigeria. *Journal of Studies and Research in Human Geography*, *14*(1). https://doi.org/10.5719/hgeo.2020.141.4

Ahmed, M. S., Abubakar, M. L., Lawal, A. I., & Richifa, K. I. (2024). Influence of extreme temperature on adverse pregnancy outcomes in Kaduna State, Nigeria. *Science World Journal*, *19*(2), 409-417. https://doi.org/10.4314/swj.v19i2.17

Alize le Roux, J. C. (2025). *Climate*. Retrieved 01/12 from

Asare, E. J. L. W., Virginia E Pitzer,. (2022). Spatiotemporal Patterns of Diarrhea Incidence in Ghana and the Impact of Meteorological and Socio-Demographic Factors. *Frontiers in Epidemiology*, *2*(871232). https://doi.org/10.3389/fepid.2022.871232

Bakai, T. A., Thomas, A., Iwaz, J., Atcha-Oubou, T., Tchadjobo, T., Khanafer, N., Rabilloud, M., & Voirin, N. (2020). Changes in registered malaria cases and deaths in Togo from 2008 to 2017. *International Journal of Infectious Diseases*, *101*, 298-305. https://doi.org/https://doi.org/10.1016/j.ijid.2020.10.006

Baskett, W. A.-O., Qureshi, A. I., Shyu, D., Armer, J. M., & Shyu, C. A.-O. (2022). COVID-Specific Long-term Sequelae in Comparison to Common Viral Respiratory Infections: An Analysis of 17 487 Infected Adult Patients. *PMC*(2328-8957 (Print)).

Beck, H. E., McVicar, T. R., Vergopolan, N., Berg, A., Lutsko, N. J., Dufour, A., Zeng, Z., Jiang, X., van Dijk, A. I. J. M., & Miralles, D. G. (2023). High-resolution (1 km) Köppen-Geiger maps for 1901–2099 based on constrained CMIP6 projections. *Scientific Data*, *10*(1), 724. https://doi.org/10.1038/s41597-023-02549-6

Beck, H. E., van Dijk, A. I. J. M., Larraondo, P. R., McVicar, T. R., Pan, M., Dutra, E., & Miralles, D. G. (2022). MSWX: Global 3-Hourly 0.1° Bias-Corrected Meteorological Data Including Near-Real-Time Updates and Forecast Ensembles. *Bulletin of the American Meteorological Society*, *103*(3), E710-E732. https://doi.org/10.1175/bams-d-21-0145.1

Beck, H. E., Wood, E. F., Pan, M., Fisher, C. K., Miralles, D. G., Van Dijk, A. I. J. M., McVicar, T. R., & Adler, R. F. (2019). MSWEP v2 Global 3-hourly 0.1° precipitation: Methodology and quantitative assessment. *Bulletin of the American Meteorological Society*, *100(3)*, 473–500. https://www.gloh2o.org

Behrman RE, B. A., editors. . (2007). Sociodemographic and Community Factors Contributing to Preterm Birth. In *Preterm Birth: Causes, Consequences, and Prevention.* Institute of Medicine (US) Committee on Understanding Premature Birth and Assuring Healthy Outcomes.

Blencowe, H., Cousens S Fau - Oestergaard, M. Z., Oestergaard Mz Fau - Chou, D., Chou D Fau - Moller, A.-B., Moller Ab Fau - Narwal, R., Narwal R Fau - Adler, A., Adler A Fau - Vera Garcia, C., Vera Garcia C Fau - Rohde, S., Rohde S Fau - Say, L., Say L Fau - Lawn, J. E., & Lawn, J. E. (2012). National, regional, and worldwide estimates of preterm birth rates in the year 2010 with time trends since 1990 for selected countries: a systematic analysis and implications. (1474-547X (Electronic)). https://doi.org/10.1016/S0140-6736(12)60820-4

Brimicombe, C., Conway, F., Portela, A., Lakhoo, D., Roos, N., Gao, C., Solarin, I., & Jackson, D. (2024). A scoping review on heat indices used to measure the effects of heat on maternal and perinatal health. *BMJ Public Health*, *2*(1), e000308. https://doi.org/10.1136/bmjph-2023-000308

Cann, K. F., Thomas, D. R., Salmon, R. L., Wyn-Jones, A. P., & Kay, D. (2013). Extreme water-related weather events and waterborne disease. *Epidemiol Infect*, *141*(4), 671-686. https://doi.org/10.1017/S0950268812001653

Carlton, E. J., Eisenberg, J. N., Goldstick, J., Cevallos, W., Trostle, J., & Levy, K. (2014). Heavy rainfall events and diarrhea incidence: the role of social and environmental factors. *Am J Epidemiol*, *179*(3), 344-352. https://doi.org/10.1093/aje/kwt279

Carlton, E. J., Woster, A. P., DeWitt, P., Goldstein, R. S., & Levy, K. (2016). A systematic review and meta-analysis of ambient temperature and diarrhoeal diseases. *International Journal of Epidemiology*, *45*(1), 117-130. https://doi.org/10.1093/ije/dyv296

Chersich, M. A.-O., Pham, M. D., Areal, A., Haghighi, M. M., Manyuchi, A., Swift, C. P., Wernecke, B., Robinson, M., Hetem, R., Boeckmann, M., & Hajat, S. (2022). Associations between high temperatures in pregnancy and risk of preterm birth, low birth weight, and stillbirths: systematic review and meta-analysis. *The BMJ*(1756-1833 (Electronic)).

Colón-González, F. J., Sewe, M. O., Tompkins, A. M., Sjödin, H., Casallas, A., Rocklöv, J., Caminade, C., & Lowe, R. (2021). Projecting the risk of mosquito-borne diseases in a warmer and more populated world: a multi-model, multi-scenario intercomparison modelling study. *The Lancet Planetary Health*, *5*(7), e404-e414. https://doi.org/10.1016/S2542-5196(21)00132-7

Colston, J. M. B. F., Malena K. Nong, Pavel Chernyavskiy, Navya Annapareddy, Venkataraman Lakshmi, Margaret N. Kosek. (2024). Spatial variation in housing construction material in low- and middle-income countries: A Bayesian spatial prediction model of a key infectious diseases risk factor and social determinant of health. *PLOS Global Public Health*, *4*(12). https://doi.org/https://doi.org/10.1371/journal.pgph.0003338

CREWS. (2025). *Climate Risk and Early Warning Systems: Togo*. Retrieved 8th December from

Del Carretto, M. A.-O., Godin, A. A.-O., Neves, D. A.-O., Paixão, E. S., Wan, K., Pescarini, J., Ferreira, A., Cortes, T. A.-O., Smeeth, L., Barreto, M. L., Brickley, E. B., & Part, C. A.-O. (2025). Short-term ambient heat exposure and low APGAR score in newborns: A time-stratified case-crossover analysis in São Paulo state, Brazil (2013-2019). *PLOS Global Public Health*(2767-3375 (Electronic)). https://doi.org/10.1371/journal.pgph.0004557

DHIS2. (2025). *DHIS2 Togo*. Retrieved 8th December from https://togo.dhis2.org/

https://doi.org/https://doi.org/10.5067/MODIS/MOD13A3.061

Djaman, K. V. S., Daran Rudnick, Komlan Koudahe, Suat Irkmak (2017). Spatial and Temporal Variation in Precipitation in Togo. *International Journal of Hydrology*, *1*(4). https://doi.org/10.15406/ijh.2017.01.00019

Dunn, G., & Johnson, G. D. (2018). The geo-spatial distribution of childhood diarrheal disease in West Africa, 2008–2013: A covariate-adjusted cluster analysis. *Spatial and Spatio-temporal Epidemiology*, *26*, 127-141. https://doi.org/https://doi.org/10.1016/j.sste.2018.06.005

Ejigu, B. A., & Wencheko, E. (2021). Spatial Prevalence and Determinants of Malaria among under-five Children in Ghana. *medRxiv*, 2021.2003.2012.21253436. https://doi.org/10.1101/2021.03.12.21253436

Exchange, H. D. (2025). *Togo Healthsites*. Retrieved 23/10/2025 from

Fall, P., Diouf, I., Deme, A., Diouf, S., Sene, D., Sultan, B., & Janicot, S. (2023). Enhancing Understanding of the Impact of Climate Change on Malaria in West Africa Using the Vector-Borne Disease Community Model of the International Center for Theoretical Physics (VECTRI) and the Bias-Corrected Phase 6 Coupled Model Intercomparison Project Data (CMIP6). *Microbiology Research*, *14*(4), 2148-2180.

Flückiger, M., & Ludwig, M. (2022). Temperature and risk of diarrhoea among children in Sub-Saharan Africa. *World Development*, *160*, 106070. https://doi.org/https://doi.org/10.1016/j.worlddev.2022.106070

GADM. (2022). *Database of Global Administrative Areas (GADM), version 4.1*. Retrieved 8th December from www.gadm.org

Gaston, R. T., & Ramroop, S. (2020). Prevalence of and factors associated with malaria in children under five years of age in Malawi, using malaria indicator survey data. *Heliyon*, *6*(5). https://doi.org/10.1016/j.heliyon.2020.e03946

Geremew, G., Cumming, O., Haddis, A., Freeman, M. C., & Ambelu, A. (2024). Rainfall and Temperature Influences on Childhood Diarrhea and the Effect Modification Role of Water and Sanitation Conditions: A Systematic Review and Meta-Analysis. *International Journal of Environmental Research and Public Health*, *21*(7), 823. https://www.mdpi.com/1660-4601/21/7/823

GIZ. (2021). *Les besoins émergents des prestations du système de la santé dû aux changements climatiques au Togo (Rapport ProSanté).*

GIZ, D. G. f. i. Z. G. G. *Feasibility Study*.

GIZ, D. G. f. I. Z. G. G. (2024). *Concept Note*.

Helsel, D. R. R. M. H., Karen R. Ryberg, Stacey A. Archfield, Edward J. Gilroy. (2020). Statistical Methods in Water Resources. *USGS*. https://doi.org/https://doi.org/10.3133/tm4A3

Ilori, O. W., & Adeyewa, D. Z. (2025). Projected changes in extreme rainfall events over West Africa and its sub-regions: a multi-scenario climate analysis. *Meteorology and Atmospheric Physics*, *137*(4). https://doi.org/10.1007/s00703-025-01081-z

INSEED. (2022). *Résultats définitifs du RGPH-5 de Novembre 2022*. https://inseed.tg/resultats-definitifs-du-rgph-5-novembre-2022/

Institute for Health Metrics and Evaluation. (2023). *GBD Results* (https://doi.org/https://ghdx.healthdata.org/gbd-2023

Kimario, A. A., Mahmoud, A., Thomas, J. A., Mallilah, B. P., Mlay, P. S., Olomi, G., & Mmbaga, B. (2024). Service availability and readiness to provide maternal and newborn healthcare

services in Kilimanjaro region, Tanzania: a cross sectional study. *BMJ Open*, *14*(12), e086275. https://doi.org/10.1136/bmjopen-2024-086275
Koffi Djaman, V. S., Daran Rudnick, Komlan Koudahe, Suat Irkmak (2017). Spatial and Temporal Variation in Precipitation in Togo. *International Journal of Hydrology*, *1*(4). https://doi.org/10.15406/ijh.2017.01.00019
Komba, E. B. R. T. B. a. D. A. I. (2024). Contributions of time, temperature and humidity on the biting behaviour of anopheles funestus at Lupiro village in Morogoro, Tanzania. *Acta Entomology and Zoology*, *5*(2), 47-53. https://doi.org/10.33545/27080013.2024.v5.i2a.155
Kombate, G., Kone, I., Douti, B., Soubeiga, K. A.-M., Grobbee, D. E., & van der Sande, M. A. B. (2024). Malaria risk mapping among children under five in Togo. *Scientific Reports*, *14*(1), 8213. https://doi.org/10.1038/s41598-024-58287-1
Kombate, G. A.-O., Gmakouba, W., Scott, S., Azianu, K. A., Ekouevi, D. K., & van der Sande, M. A. B. (2022). Regional heterogeneity of malaria prevalence and associated risk factors among children under five in Togo: evidence from a national malaria indicators survey. (1475-2875 (Electronic)).
Kouakou, Y. E. K. E. B., Yao Anicet Zouzou, Guéladio Cissé, Brama Koné. (2024). Methodological framework for assessing malaria risk associated with climate change in Côte d'Ivoire. *Geospatial Health*, *19*(2). https://doi.org/https://doi.org/10.4081/gh.2024.1285
Kyu, H. H., Vongpradith, A., Dominguez, R.-M. V., Ma, J., Albertson, S. B., Novotney, A., Khalil, I. A., Troeger, C. E., Doxey, M. C., Ledesma, J. R., Sirota, S. B., Bender, R. G., Swetschinski, L. R., Cunningham, M., Spearman, S., Abate, Y. H., Abd Al Magied, A. H. A., Abd ElHafeez, S., Abdoun, M.,…Murray, C. J. L. (2025). Global, regional, and national age-sex-specific burden of diarrhoeal diseases, their risk factors, and aetiologies, 1990–2021, for 204 countries and territories: a systematic analysis for the Global Burden of Disease Study 2021. *The Lancet Infectious Diseases*, *25*(5), 519-536. https://doi.org/10.1016/S1473-3099(24)00691-1
Lakhoo, D. A.-O., Brink, N. A.-O., Radebe, L., Craig, M. A.-O., Pham, M. D., Haghighi, M. M., Wise, A., Solarin, I., Luchters, S., Maimela, G., & Chersich, M. A.-O. (2025). A systematic review and meta-analysis of heat exposure impacts on maternal, fetal and neonatal health. *Nature*(1546-170X (Electronic)).
Levesque, J.-F., Harris, M. F., & Russell, G. (2013). Patient-centred access to health care: conceptualising access at the interface of health systems and populations. *International Journal for Equity in Health*, *12*(1), 18. https://doi.org/10.1186/1475-9276-12-18
Levy, K., Woster, A. P., Goldstein, R. S., & Carlton, E. J. (2016). Untangling the Impacts of Climate Change on Waterborne Diseases: a Systematic Review of Relationships between Diarrheal Diseases and Temperature, Rainfall, Flooding, and Drought. *Environmental Science and Technology*(1520-5851 (Electronic)).
Li-Maloney, C., Wagar, K. E., Tetzlaff, E. J., & Kenny, G. P. (2025). Pregnancy and extreme heat events: A rapid review of evidence related to health outcomes, risk factors and interventions. *Women and Birth*, *38*(4), 101931. https://doi.org/https://doi.org/10.1016/j.wombi.2025.101931
McElroy, S., Ilango, S., Dimitrova, A., Gershunov, A., & Benmarhnia, T. (2021). Extreme heat, preterm birth, and stillbirth: A global analysis across 14 lower-middle income countries. *Environment International*(1873-6750 (Electronic)). https://doi.org/10.1016/j.envint.2021.106902
Megersa, D. M., & Luo, X.-S. (2025). Effects of Climate Change on Malaria Risk to Human Health: A Review. *Atmosphere*, *16*(1), 71.
MERF. (2018). *Plan National d'Adaptation aux Changements Climatiques du Togo (PNACC)*.
Miller, A. G., Miller-Petrie, M. K., Williams, R. B., Klohmann, C., O'Neill, B., Hess, J., & Levy, K. (2025). Projections of climate change-attributable diarrhea burden: a systematic review. *Environmental Research Letters*, *20*(5). https://doi.org/10.1088/1748-9326/adccd8
Muñoz Sabater, J. (2019). *ERA5-Land monthly averaged data from 1950 to present.* (https://doi.org/10.24381/cds.68d2bb30
Ohuma, E. O., Moller, A. B., Bradley, E., Chakwera, S., Hussain-Alkhateeb, L., Lewin, A., Okwaraji, Y. B., Mahanani, W. R., Johansson, E. W., Lavin, T., Fernandez, D. E., Domínguez, G. G., de Costa, A., Cresswell, J. A., Krasevec, J., Lawn, J. E., Blencowe, H., Requejo, J., & Moran, A. C. (2023). National, regional, and global estimates of preterm birth in 2020, with trends from 2010: a systematic analysis. *The Lancet*(1474-547X (Electronic)).
Part, C., le Roux, J., Chersich, M., Sawry, S., Filippi, V., Roos, N., Fairlie, L., Nakstad, B., de Bont, J., Ljungman, P., Stafoggia, M., Kovats, S., Luchters, S., & Hajat, S. (2022). Ambient temperature during pregnancy and risk of maternal hypertensive disorders: A time-to-event

study in Johannesburg, South Africa. *Environmental Research*, *212*, 113596. https://doi.org/https://doi.org/10.1016/j.envres.2022.113596
Perez-Saez, J., Lessler, J., Lee, E. C., Luquero, F. J., Malembaka, E. B., Finger, F., Langa, J. P., Yennan, S., Zaitchik, B., & Azman, A. S. (2022). The seasonality of cholera in sub-Saharan Africa: a statistical modelling study. *Lancet Global Health*(2214-109X (Electronic)).
Pörtner, H.-O. D. C. R., M. Tignor; E.S. Poloczanska; K. Mintenbeck; A. Alegría; M. Craig, S. Langsdorf;, & (2022). *IPCC, 2022: Climate Change 2022: Impacts, Adaptation and Vulnerability. Contribution of Working Group II to the Sixth Assessment Report of the Intergovernmental Panel on Climate Change*.
PROVIDE. (2025). *Climate Risk Dashboard*. Retrieved 8th December from https://climate-risk-dashboard.iiasa.ac.at/impacts/explore
Ranjha, R., Singh, K., Baharia, R. K., Mohan, M., Anvikar, A. R., & Bharti, P. K. (2023). Age-specific malaria vulnerability and transmission reservoir among children. *Global Pediatrics*, *6*, 100085. https://doi.org/https://doi.org/10.1016/j.gpeds.2023.100085
Reddam, A., Mujtaba, M. N., Tuholske, C., Kaali, S., Ae-Ngibise, K. A., Wylie, B. J., Medgyesi, D. N., Boamah-Kaali, E., Baccarelli, A. A., Agyei, O., Chillrud, S. N., Asante, K. P., Jack, D. W., Lee, A. G., & Abubakari, S. W. (2025). Prenatal exposure to heat and humidity and infant birth size in Ghana. *Environ Res*, *266*, 120557. https://doi.org/10.1016/j.envres.2024.120557
Republic Togelese. (2017). *PLAN NATIONAL DE DEVELOPPEMENT SANITAIRE 2017-2022*. Togo
Romanello, M., Walawender, M., Hsu, S. C., Moskeland, A., Palmeiro-Silva, Y., Scamman, D., Ali, Z., Ameli, N., Angelova, D., Ayeb-Karlsson, S., Basart, S., Beagley, J., Beggs, P. J., Blanco-Villafuerte, L., Cai, W., Callaghan, M., Campbell-Lendrum, D., Chambers, J. D., Chicmana-Zapata, V.,…Costello, A. (2024). The 2024 report of the Lancet Countdown on health and climate change: facing record-breaking threats from delayed action. (1474-547X (Electronic)).
Schantz-Dunn, J. F. N., Nawal M ; Nour, N. M,. (2009). Malaria and pregnancy: a global health perspective. *Obstetrics & Gynecology*, *2*(3), 186-192.
Schmuck, H. S. K., Claire Belluard, Olga Bassong. (2019). *Final Report: Assessment of Climate Change-related Risks and Vulnerabilities in the Health Sector in Togo*.
Sow, M., Dixon, R. D., Diakhaté, M., Guichard, F., Couvreux, F., & Gaye, A. T. (2025). Contribution From the Occurrence and Intensity of Wet Days to the West African Rainfall Variability in CMIP6 Models. *Geophysical Research Letters*, *52*(21). https://doi.org/10.1029/2024gl110022
Ssempiira, J., Kasirye, I., Kissa, J., Nambuusi, B., Mukooyo, E., Opigo, J., Makumbi, F., Kasasa, S., & Vounatsou, P. (2018). Measuring health facility readiness and its effects on severe malaria outcomes in Uganda. *Scientific Reports*, *8*(1), 17928. https://doi.org/10.1038/s41598-018-36249-8
Symons, T. L., Moran, A., Balzarolo, A., Vargas, C., Robertson, M., Lubinda, J., Saddler, A., McPhail, M., Harris, J., Rozier, J., Browne, A., Amratia, P., Bertozzi-Villa, A., Bhatt, S., Cameron, E., Golding, N., Smith, D. L., Noor, A. M., Rumisha, S. F.,…Gething, P. W. (2025). Projected ecological and disruptive impacts of climate change on malaria in Africa. *medRxiv*, 2025.2002.2011.25322113. https://doi.org/10.1101/2025.02.11.25322113
Taguela, T. N., Akinsanola, A. A., Adeliyi, T. E., Rhoades, A., & Nazarian, R. H. (2025). Understanding drivers and uncertainty in projected African precipitation. *npj Climate and Atmospheric Science*, *8*(1). https://doi.org/10.1038/s41612-025-01123-8
Tano, A. R., Bouo, F.-X. D. B., Kouamé, J. K., Tchétché, Y., Zézé, S. D., & Ouattara, B. (2023). Rainfall Variability and Trends in West Africa. *Atmospheric and Climate Sciences*, *13*(01), 72-83. https://doi.org/10.4236/acs.2023.131006
TCCiP. (2025). *Shared Socioeconomic Pathway Introduction*. Retrieved 17th December from https://tccip.ncdr.nat.gov.tw/ds_02_06_ar6_eng.aspx
The Climate Hazards Group. (2018). *Climate Hazards Group InfraRed Precipitation with Station data (CHIRPS): Quasi-global daily satellite and observation based precipitation estimates over land. Climate Hazard Group* (https://catalogue.ceda.ac.uk/uuid/4e53c2aee3fe44e7aa107c163696d2e7
The DHS Program. (2017). *Togo: Malaria Indicator Survey (MIS), 2017* (
The World Factbook. (2025). *Togo*. CIA. Retrieved 23/10/2025 from
Thomas, A. A.-O., Bakai, T. A., Atcha-Oubou, T., Tchadjobo, T., Rabilloud, M., & Voirin, N. (2024). Exploring malaria prediction models in Togo: a time series forecasting by health district and target group. *BMJ Open*(2044-6055 (Electronic)).
Thomas, A. T. A. B., Tinah Atcha-Oubou, Tchassama Tchadjobo, Nicolas Voirin,. (2020). Implementation of a malaria sentinel surveillance system in Togo: a pilot study. *Malaria Journal*, *19*(330). https://doi.org/https://doi.org/10.1186/s12936-020-03399-y

Thrasher, B., Wang, W., Michaelis, A., & Nemani, R. (2022). *The NASA Earth Exchange (NEX) Global Daily Downscaled Projections (GDDP) dataset (NEX-GDDP-CMIP6). NASA Center for Climate Simulation.* (https://doi.org/10.7917/OFSG3345
United Nations Office for West Africa and the Sahel. (2025). *Map*. United Nations. Retrieved 17/10/2025 from
van der Deure, T. A.-O., Nogués-Bravo, D. A.-O., Njotto, L. A.-O., & Stensgaard, A. A.-O. (2025). Climate Change Favors African Malaria Vector Mosquitoes. (1365-2486 (Electronic)).
Walker, C. L. F., Rudan, I., Liu, L., Nair, H., Theodoratou, E., Bhutta, Z. A., O'Brien, K. L., Campbell, H., & Black, R. E. (2013). Global burden of childhood pneumonia and diarrhoea. (1474-547X (Electronic)). https://doi.org/http://dx.doi.org/10.1016/

S0140-6736(13)60222-6
Wang, Y.-Y., Li, Q., Guo, Y., Zhou, H., Wang, Q.-M., Shen, H.-P., Zhang, Y.-P., Yan, D.-H., Li, S., Chen, G., Zhou, S., He, Y., Yang, Y., Peng, Z.-Q., Wang, H.-J., & Ma, X. (2020). Ambient temperature and the risk of preterm birth: A national birth cohort study in the mainland China. *Environment International*, *142*, 105851. https://doi.org/https://doi.org/10.1016/j.envint.2020.105851
WBG. (2022). *Domestic private health expenditure (% of current health expenditure) – Togo* (
Weiss, D. J., Nelson, A., Vargas-Ruiz, C. A., Gligorić, K., Bavadekar, S., Gabrilovich, E., Bertozzi-Villa, A., Rozier, J., Gibson, H. S., Shekel, T., Kamath, C., Lieber, A., Schulman, K., Shao, Y., Qarkaxhija, V., Nandi, A. K., Keddie, S. H., Rumisha, S., Amratia, P.,…Gething, P. W. (2020). Global maps of travel time to healthcare facilities. *Nature Medicine*, *26*(12), 1835-1838. https://doi.org/10.1038/s41591-020-1059-1
Worede, E. A.-O., Malede, A., Feleke, H., Abere, G., Demeke, E. A., & Azanaw, J. (2025). Prevalence of diarrheal diseases and associated factors among under five children in Africa: A meta-analysis. *PLOS Global Health*(1932-6203 (Electronic)). https://doi.org/https://doi.org/10.1371/journal.pone.0326501
World Bank Group. (2024). *Poverty & Equity Brief Togo*. Retrieved 24 Sept from
World Bank Group. (2025). *Climate Change Knowledge Portal - Country Overview*. Retrieved 21 November from
World Health Organization. (2024). *World Malaria Report 2024*.
World Health Organization. (2025a). *Diarrhoeal disease*. Retrieved 19/11/2025 from
World Health Organization. (2025b). *Global health estimates: Leading causes of DALYs*. World Health Organization. Retrieved 17th October 2025 from
World Health Organization. (2025c). *Togo: Country Overview*. Retrieved 15 October 2025 from
World Health Organization. (2025d). *World malaria report 2025: addressing the threat of antimalarial drug resistance.* (ISBN 978-92-4-011782-2).
World Health Organization, U. N. C. s. F. (2025). *Progress on household drinking water, sanitation and hygiene 2000–2024: special focus on inequalities*. https://cdn.who.int/media/docs/default-source/wash-documents/wash-coverage/jmp/jmp-2025-wash-households-lowres-launch.pdf?sfvrsn=12ccab42_3&download=true
Worldpop. (2020). *The spatial distribution of population in 2020 with country total adjusted to match the corresponding UNPD estimate, Togo*. Retrieved December 5 from
Yu, W., Guo, M., Li, G., Li, W., Cao, Y., Hu, K., Wang, H., Ma, W., Zhao, Q., Li, L., & Yan, J. (2025). Compound drought and heatwave events and childhood diarrhea: current impacts and future risk in low- and middle-income countries. *Environ Int*, *203*, 109792. https://doi.org/10.1016/j.envint.2025.109792
Yusa, A., Berry, P., J, J. C., Ogden, N., Bonsal, B., Stewart, R., & Waldick, R. (2015). Climate Change, Drought and Human Health in Canada. *Int J Environ Res Public Health*, *12*(7), 8359-8412. https://doi.org/10.3390/ijerph120708359
Zebisch, M. K. R., Massimiliano Pittore, Uta Fritsch,, Sophie Rose Fruchter, S. K., Thomas Schinko, Edward Sparkes,, & Michael Hagenlocher, S. S., and Jess L. Delvis. (2023). Climate Risk Sourcebook. In. Bonn and Eschborn, Germany: Deutsche Gesellschaft für Internationale Zusammenarbeit (GIZ) GmbH.

8. Appendix 1

Literature review search strategy

1: TI=("climate" near/4 ("benefit*" or "co-benefit*")) or AB=("climate" near/4 ("benefit*" or "co-benefit*"))

2: TI=(("health*" or "well-being" or "wellbeing" or "morbidity" or "mortality" or "disease*" OR "illness*" OR "infection*" OR "DALY*" OR "life year*" OR "QALY*" OR "death*" OR ("life" NEAR/2 "satisf*") OR "wellness" OR "quality of life" OR "QOL" OR "food-borne" OR "vector*" or "water-borne" or injur* or "trauma*") not "soil") or AB=(("health*" or "well-being" or "wellbeing" or "morbidity" or "mortality" or "disease*" OR "illness*" OR "infection*" OR "DALY*" OR "life year*" OR "QALY*" OR "death*" OR ("life" NEAR/2 "satisf*") OR "wellness" OR "quality of life" OR "QOL" OR "food-borne" OR "vector*" or "water-borne" or injur* or "trauma*") not "soil")

3: TI=("respiratory" or "cardiovascular" or "cardio-vascular" or "stroke" or "cerebrovascular" or "cerebro-vascular" or ("circulatory" NEAR/1 disorder*) or "diabetes" or "zoonoses" or "cholera" or "vibrio cholerae" or "malaria" or "plasmodium" or "dengue" or "rift-valley fever" or "yellow fever" or "leishmaniasis" or "leishmania" or "diarrheal" or "haemorrhagic fever" or "hemorrhagic fever" or "ebola" or "ebolavirus" or "leptospirosis" or "weil disease" or "leptospira" or "west nile fever" or "west nile virus" or "anthrax" or "bacillus anthracis" or "schistosomiasis" or "schistosoma" or "trypanosomiasis" or "chagas" or "trypanosoma" or "salmonellosis" or "salmonella" or "giardiasis" or "giardia" or "cryptosporidiosis" or "cryptosporidium" or "e coli" or "Escherichia coli" or "campylobacter" or "pre-term birth*" or "premature birth*" or "premature labor" or "premature labour" or "low birthweight" or "low birth-weight" or "heat stroke" or "heat stress" or "malnutrition" or "stunting" or "wasting" or "depression" or "depressive" or "anxiety" or "eco-anxiety" or "eco-distress" or "mosquito*" or "culicidae" or "ticks") or AB=("respiratory" or "cardiovascular" or "cardio-vascular" or "stroke" or "cerebrovascular" or "cerebro-vascular" or ("circulatory" NEAR/1 disorder*) or "diabetes" or "zoonoses" or "cholera" or "vibrio cholerae" or "malaria" or "plasmodium" or "dengue" or "rift-valley fever" or "yellow fever" or "leishmaniasis" or "leishmania" or "diarrheal" or "haemorrhagic fever" or "hemorrhagic fever" or "ebola" or "ebolavirus" or "leptospirosis" or "weil disease" or "leptospira" or "west nile fever" or "west nile virus" or "anthrax" or "bacillus anthracis" or "schistosomiasis" or "schistosoma" or "trypanosomiasis" or "chagas" or "trypanosoma" or "salmonellosis" or "salmonella" or "giardiasis" or "giardia" or "cryptosporidiosis" or "cryptosporidium" or "e coli" or "Escherichia coli" or "campylobacter" or "pre-term birth*" or "premature birth*" or "premature labor" or "premature labour" or "low birthweight" or "low birth-weight" or "heat stroke" or "heat stress" or "malnutrition" or "stunting" or "wasting" or "depression" or "depressive" or "anxiety" or "eco-anxiety" or "eco-distress" or "mosquito*" or "culicidae" or "ticks")

4: TI=(("climate" or "climactic") near/2 (change$ or "changing" or variab* or disrupt* or hazard* or impact* or vulnerab* or function* or "extreme" or catastroph* or emergenc* or shift* or dynamic* or sensitiv* or sustainab* or anomal* or effect$ or "induced" or parameter* or driver$ or cause*)) OR AB=(("climate" or "climactic") near/2 (change$ or "changing" or variab* or disrupt* or hazard* or impact* or vulnerab* or function* or "extreme" or catastroph* or emergenc* or shift* or dynamic* or sensitiv* or sustainab* or anomal* or effect$ or "induced" or parameter* or driver$ or cause*))

5: TI=("environmental" near/1 (cause* or "induced" or parameter* or driver$)) or AB=("environmental" near/1 (cause* or "induced" or parameter* or driver$))

6: TI=("global tipping point$") or AB=("global tipping point$")

7: TI=(("global" or planet* or "world" or climat* or "earth" or "worldwide" or "world-wide" or ocean*) near/1 ("heating" or "warming" or temperature*)) or AB=(("global" or planet* or "world" or climat* or "earth" or "worldwide" or "world-wide" or ocean*) near/1 ("heating" or "warming" or temperature*)) Results: 111697

8: TI=(("ambient" or "mean" or "average" or "rising" or "change$") near/1 temperature$) or AB=(("ambient" or "mean" or "average" or "rising" or "change$") near/1 temperature$)

9: TI=((temperature$ or "cold" or "heat" or "hot" or "relative humidity" or "thermal") near/4 ("extreme" or elevate* or "irregular" or "intense" or "rising" or "reduced" or pattern* or anomal* or "global")) or AB=((temperature$ or "cold" or "heat" or "hot" or "relative humidity" or "thermal") near/4 ("extreme" or elevate* or "irregular" or "intense" or "rising" or "reduced" or pattern* or anomal* or "global"))

10: TI=(ENSO or "el nino-southern oscillation") or AB=(ENSO or "el nino-southern oscillation")

11: TI=("thermal threshold$") or AB=("thermal threshold$")

12: TI=(heatwave$ or "heat-wave$") or AB=(heatwave$ or "heat-wave$") Results: 13696

13: TI=(coldwave$ or "cold-wave$") or AB=(coldwave$ or "cold-wave$") Results: 667

14: TI=("thermal environ*" or "heat-island*") or AB=("thermal environ*" or "heat-island*")

15: TI=(("sea-level" or "sea level") near/5 (rise$ or "rising" or change$ or "changing")) or AB=(("sea-level" or "sea level") near/5 (rise$ or "rising" or change$ or "changing"))

16: TI=((rain* or "precipitation") near/4 ("extreme" or elevate$ or "heavy" or "elevating" or "irregular" or "intense" or "reduced" or pattern* or anomal*)) or AB=((rain* or "precipitation") near/4 ("extreme" or elevate$ or "heavy" or "elevating" or "irregular" or "intense" or "reduced" or pattern* or anomal*)) Results: 66517

17: TI=drought$ or AB=drought$

18: TI=(flood* or ("land" near/2 inundat*)) or AB=(flood* or ("land" near/2 inundat*))

19: TI=(cyclone$ or hurricane$ or storm*) or AB=(cyclone$ or hurricane$ or storm*)

20: TI=(("tide" or "tidal" or "sea" or ocean*) near/2 ("surge" or "surges")) or AB=(("tide" or "tidal" or "sea" or ocean*) near/2 ("surge" or "surges"))

21: TI=windstorm$ or AB=windstorm$

22: TI=landslide$ or AB=landslide$

23: TI=mudslide$ or AB=mudslide$

24: TI=(wildfire$ or "wild-fire$" or bushfire$ or "bush-fire$") or AB=(wildfire$ or "wild-fire$" or bushfire$ or "bush-fire$")

25: TI=((fire$ or "burnt" or "inferno" or "conflagration") near/2 (change* or variab* or "extreme" or "expand" or "expansion" or "intense" or elevate$ or increas* or catastroph* or emergenc* or shift* or dynamic* or frequen* or "more")) or AB=((fire$ or "burnt" or "inferno" or "conflagration") near/2 (change* or variab* or "extreme" or "expand" or "expansion" or "intense" or elevate$ or increas* or catastroph* or emergenc* or shift* or dynamic* or frequen* or "more"))

26: TI=(("water" near/2 (salin* or salt* or "brackish")) or "saltwater" or "salin* intrusion") or AB=(("water" near/2 (salin* or salt* or "brackish")) or "saltwater" or "salin* intrusion")

27: TI=(("water" or "freshwater") near/1 (insecur* or "scarcity" or "scarce" or environment$ or shortage$ or "source" or availabl* or "inadequate access" or "inadequate" or "lack or resource$" or "stress")) or AB=(("water" or "freshwater") near/1 (insecur* or "scarcity" or "scarce" or environment$ or shortage$ or "source" or availabl* or "inadequate access" or "inadequate" or "lack or resource$" or "stress"))

28: TI=("West* Africa" or Benin or Dahomey or "Burkina Faso" or "Burkina Fasso" or Ghana or "Gold Coast" or (Guinea not ("New Guinea" or "Guinea Pig*" or "Guinea Fowl" or "Equatorial Guinea")) or "Guinea-Bissau" or "Portuguese Guinea" or "Ivory Coast" or "Cote d'Ivoire" or "Cote dIvoire" or Nigeria or Togo or "Togolese Republic" or Togoland) or AB=("West* Africa" or Benin or Dahomey or "Burkina Faso" or "Burkina Fasso" or "Upper Volta" or Ghana or "Gold Coast" or (Guinea not ("New Guinea" or "Guinea Pig*" or "Guinea Fowl" or "Equatorial Guinea")) or "Guinea-Bissau" or "Portuguese Guinea" or "Ivory Coast" or "Cote d'Ivoire" or "Cote dIvoire" or Nigeria or Togo or "Togolese Republic" or Togoland)

29: #1 OR #2 OR #3

30: #27 OR #26 OR #25 OR #24 OR #23 OR #22 OR #21 OR #20 OR #19 OR #18 OR #17 OR #16 OR #15 OR #14 OR #13 OR #12 OR #11 OR #10 OR #9 OR #8 OR #7 OR #6 OR #5 OR #4 Results: 1572550

31: #30 AND #29 AND #28

32: #31 AND (LA==("ENGLISH"))

Results:
Medline: 1384
Embase: 1871
Global Health: 3466
Africa-Wide Information: 1566
GreenFILE: 298
Web of Science: 2220
Scopus: 3622

Summary of climate, health, demographic and socio-economic data sets

Table 7: Summary of climate, health, demographic, and socio-economic data sets

	Data type	Source and description	Coverage and notes	Weblink
1	Historical observed climate datasets	Multi-Source Weather dataset (MSWX)	Daily data, 1980 – a few months before present) Spatial resolution 0.1° (~11 km at equator)	https://www.gloh2o.org/mswx/
		The Multi-Source Weighted-Ensemble Precipitation dataset (MSWEP)	Daily data, Spatial resolution 0.1°	MSWEP - GloH2O
		The European Centre for Medium-Range Weather Forecasts (ECMWF) Reanalysis v5 – Land dataset (ERA5-Land)	Daily data, Spatial resolution 0.1°	https://cds.climate.copernicus.eu/datasets/reanalysis-era5-land-monthly-means?tab=overview
		The Climate Hazards Group InfraRed Precipitation with Station dataset (CHIRPS)	Daily data, Spatial resolution 0.05°	https://catalogue.ceda.ac.uk/uuid/4e53c2aee3fe44e7aa107c163696d2e7
2	Future climate projections	NASA NEX-GDDP-CMIP6 5 GCMs including GFDL-ESM4, IPSL-CM6A-LR, MPI-ESM1-2-HR, MRI-ESM2-0, and UKESM1-0-LL	Daily data, Spatial resolution 0.25 degree (~28km at equator), 'historical experiments' (1950-2014), 'scenario experiments' (2015-2100) of SSP2-4.5 (middle of the road) and SSP5-8.5 (fossil-fuelled development).	https://www.nasa.gov/nasa-earth-exchange-nex/gddp/downscaled-climate-projections-nex-gddp-cmip6/
3	Health data	District Health Information system (DHIS2)	Malaria, diarrhoea and live birth cases at the prefecture level and at a monthly resolution, covering the period from January 2018 to August 2025	https://togo.dhis2.org/
		Malaria Indicator Survey (MIS) 2017	children aged 0–5 years with key malaria biomarker variables and other specified socioeconomic and environmental covariates.	https://dhsprogram.com/methodology/survey/survey-display-497.cfm
4	Demographic data	National Institute of Statistics and Economic and Demographic Studies (INSEED) Census 2022	Population estimates at the prefecture level, both overall and for specific demographic subgroups (e.g., children under 5 years of age, women of reproductive age)	https://inseed.tg/resultats-definitifs-du-rgph-5-novembre-2022/
5	Healthcare access data	Malaria Atlas Project (MAP) 2020	Estimates of travel time in minutes to the nearest facility using motorised vehicles, 1km spatial resolution, averaged across prefectures	https://malariaatlas.org

6	Housing data	Demographic and Health surveys (DHS) and Multiple Indicator Cluster surveys (MICS) (Colston et al., 2024)	0.05 decimal degree resolution, values averaged over prefectures, coverage of improved walls, floors and roofs was averaged to produce a composite improved housing index.	https://dhsprogram.com/ and https://mics.unicef.org/surveys
7	Socio-economic data	National Institute of Statistics and Economic and Demographic Studies (INSEED) Census 2022	proportions of selected vulnerability indicators e.g., access to air conditioning, use of improved drinking water sources, household size, improved toilet facilities, etc.	https://inseed.tg/resultats-definitifs-du-rgph-5-novembre-2022/
		Malaria Indicator Survey (MIS) 2017	Mean wealth score, caregiver education, by prefecture	https://dhsprogram.com/methodology/survey/survey-display-497.cfm
8	Administrative Boundary	The Global Administrative Areas Database (GADM)	Shape files with a base grid of 0.1° (approx. 11x11km at the equator) for various administrative levels including canton, prefecture, and region	www.gadm.org

(Source: Own elaboration)

Table 8 Summary of vulnerability indicators by causal pathway and health outcome

Health outcome	Pathway	Potential indicators
Malaria	Socio-economic factors	Caregiver education, Wealth/Income, Ethnicity, Migrant status, religion
	Healthcare access	Access to malaria testing, early diagnosis and treatment, Community health worker distribution, Distance to clinics or hospitals
	Vector control strategies	Coverage of insecticide-treated bed nets (ITNs), Coverage and frequency of indoor residual spraying (IRS), Insecticide resistance management, Larval source management (drainage, elimination of breeding sites)
	Living conditions	Proximity to mosquito breeding sites (stagnant water, irrigation, wetlands), Housing quality and conditions, Rural residence, Local environmental features (e.g. deforestation), Water storage practices, Access to air-conditioning and fans, ownership of livestock and agriculture
	Individual child factors	Nutritional status (malnutrition, stunting), Immunity level (low immunity or low prior exposure), Co-morbidities (e.g., anaemia, HIV)
Diarrhoeal disease	Socio-economic factors	Caregiver education, Wealth/Income, Ethnicity, Migrant status
	Healthcare access	Timely access to primary healthcare, Availability of routine child immunisations, Distance to health facilities
	Water, Health and Sanitation (WASH) facilities	Access to safe drinking water (improved and protected sources, treatment), Reliable water supply, Access to functional latrines/toilets and safe disposal of faeces (improved facilities), Availability of handwashing facilities

	Living conditions	Household overcrowding (e.g. of children under 5 years), High population density, Rural residence, Built environment (informal settlements, flood-prone housing), Household water storage practices, Food storage and preparation (e.g. refrigeration), Proximity to waste, industrial discharge or flood-affected zones
	Individual child factors	Infancy, Nutritional status (stunting, wasting, micronutrient deficiencies), Exclusive breastfeeding, Vaccination status (e.g. rotavirus), Co-morbidities (HIV, recurrent respiratory infections, anaemia)
Preterm birth	Socio-economic factors	Maternal education, Wealth/Income, Ethnicity, Occupation
	Healthcare access	Timely antenatal care access, hospital access, Community health worker distribution, Distance to clinics or hospitals
	Living conditions	Urban heat island, rural residence, A/C or fan access, Neighbourhood green space, Housing quality
	Individual maternal factors	Age (young or old), Body Mass Index (BMI), Smoking, Alcohol use, Parity, Co-morbidities (e.g. hypertension, gestational diabetes)

Indicators highlighted in bold were selected for Stage 1 risk assessments.

(Source: Own elaboration)

Figure 56 Sensitivity analysis for Malaria risk assessment. A) Vulnerability factors were weighted equally; B) Weights were applied to household wealth (0.10), caregiver education (0.25), treated bednet ownership (0.30), housing quality (0.15), and motorised travel time to healthcare (0.20); C) A higher weighting was applied to treated bednet ownership (0.50) while other vulnerability factors were each weighted 0.125.

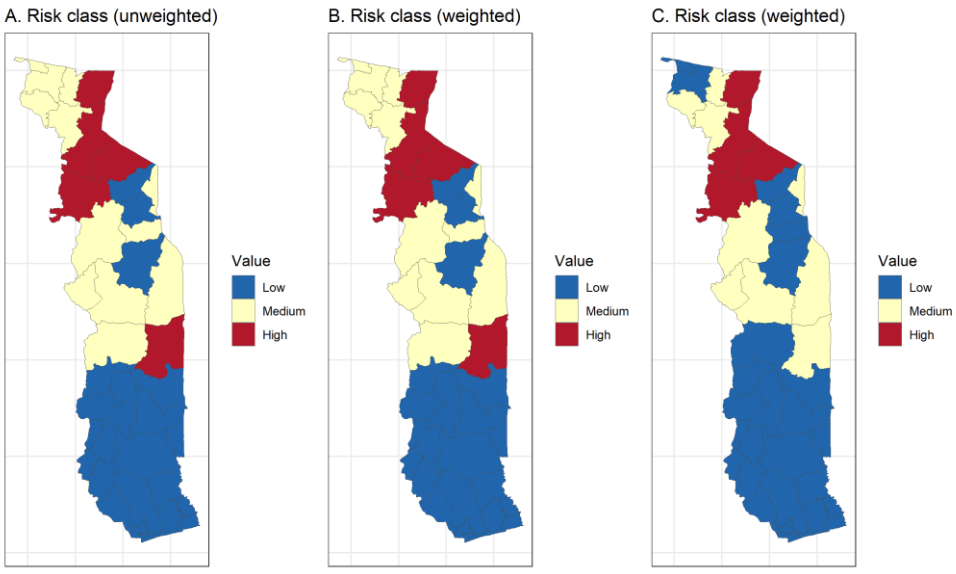

(Source: Own elaboration)

Figure 57 Sensitivity analysis for Diarrhoeal disease risk assessment. A) Vulnerability factors were weighted equally; B) Weights were applied to exclusive breastfeeding (0.25), improved water access (0.30), improved sanitation (0.15), motorised travel time to healthcare (0.20), and under-5 household crowding (0.10); C) A higher weighting was applied to improved water access (0.50), while other vulnerability factors were each weighted 0.125.

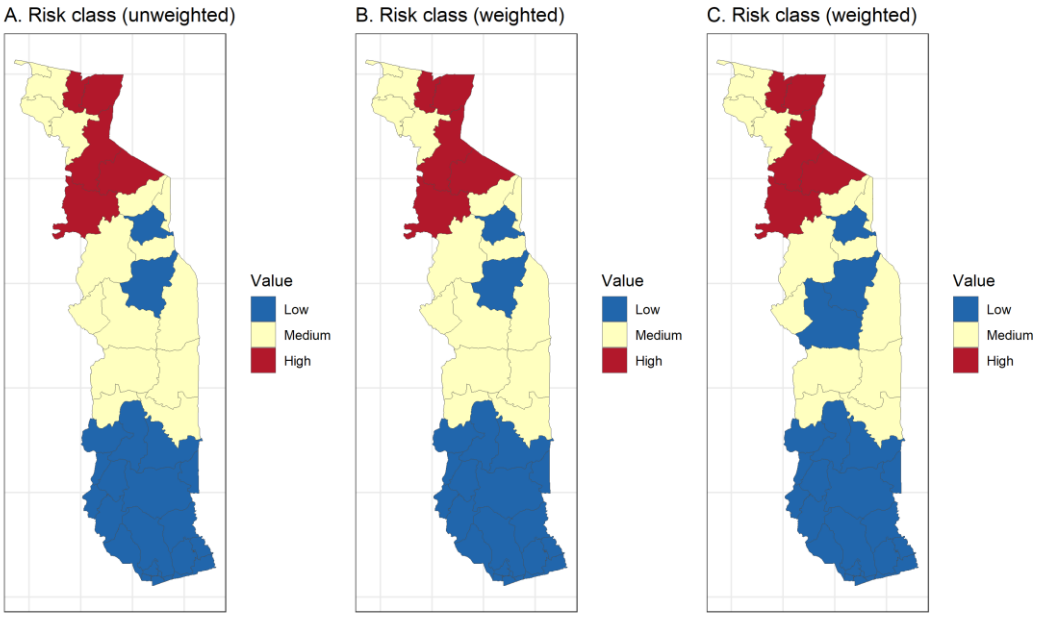

(Source: Own elaboration)

Figure 58 Sensitivity analysis for Preterm birth risk assessment. A) Vulnerability factors were weighted equally; B) Weights were applied to household wealth (0.15), first-trimester antenatal care attendance (0.30), adolescent motherhood (0.20), air-conditioning access (0.25), and mothers with no formal

education (0.10); C) A higher weighting was applied to first-trimester antenatal care attendance (0.50), while other vulnerability factors were each weighted 0.125.

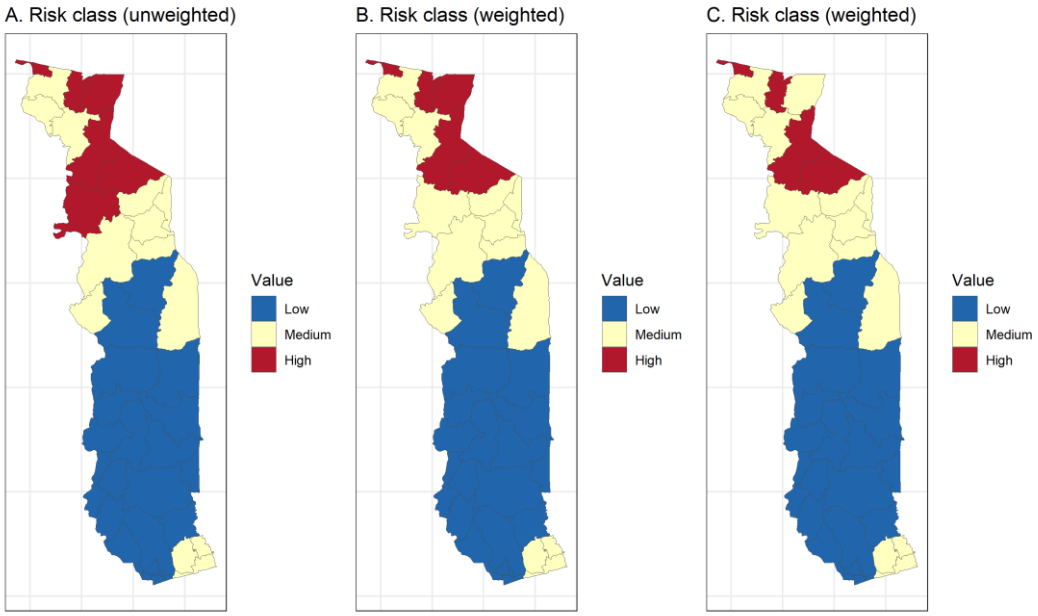

(Source: Own elaboration)

Figure 59 Percent change in preterm birth risk associated with heatwave hazards across gestational lags (0-8 months), by prefecture. Values represent the cumulative heatwave effect from the prefecture-specific time-series models, expressed as percent change in risk ((IRR − 1) × 100). Greyed prefectures were excluded from the meta-analysis due to insufficient data quality (NA counts).

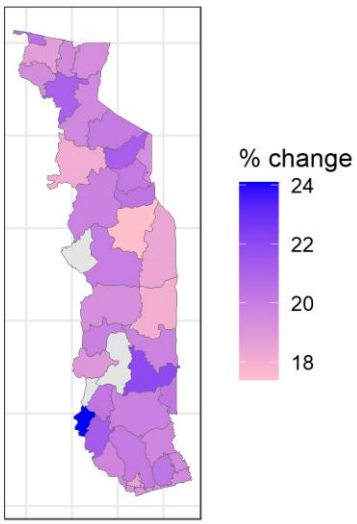

(Source: Own elaboration)

Figure 60 - Best Linear Unbiased Prediction (BLUP) lag-response plots for the relationship between heatwaves and preterm birth by prefecture

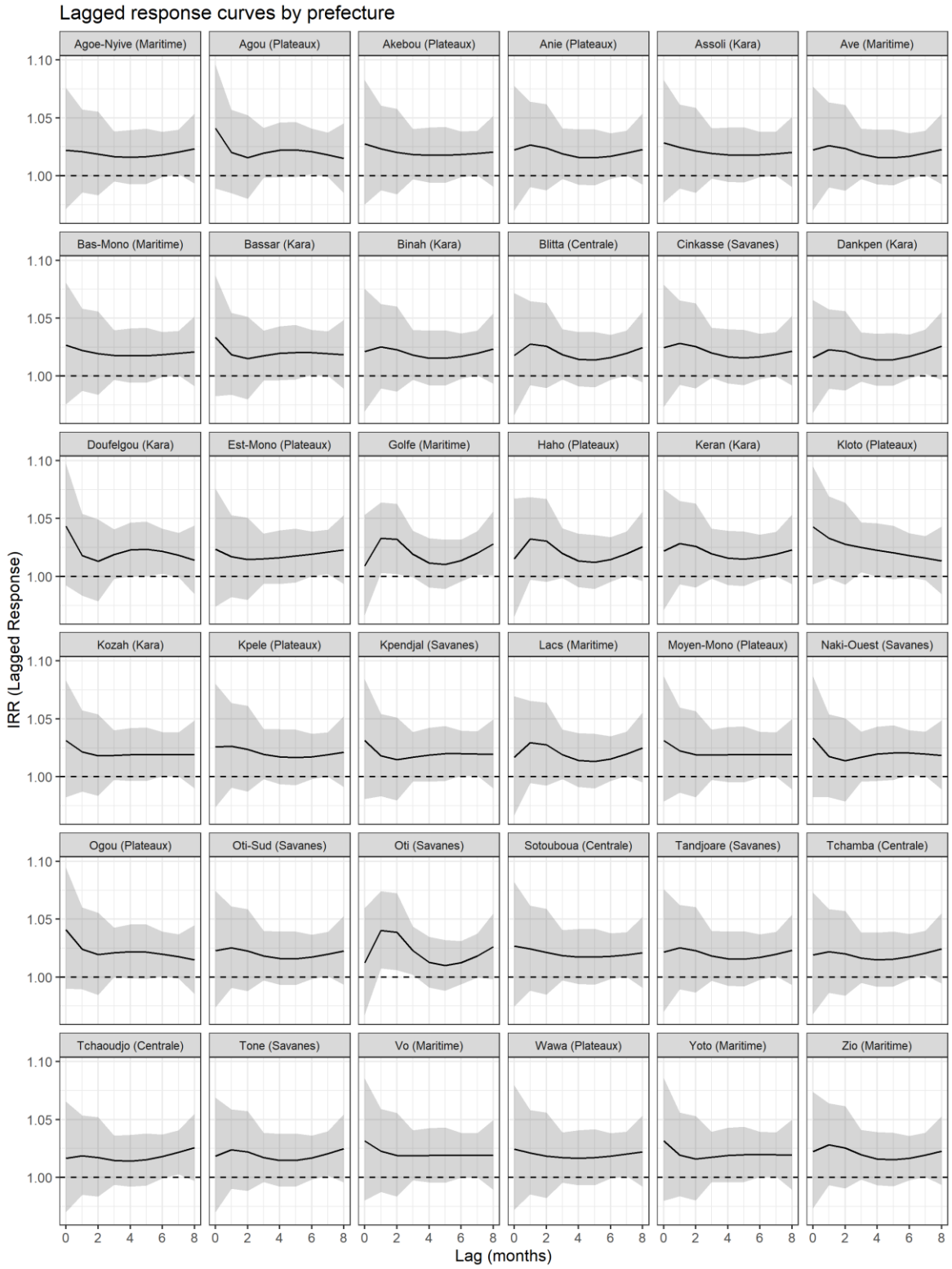

(Source: Own elaboration)

Figure 61 - Cumulative association between heatwave exposure during pregnancy and preterm birth, stratified by prefecture-level vulnerability factors. Points show cumulative incidence rate ratios (IRRs), representing the combined effect of heatwave exposure across gestational lags 0–8 months. Error bars denote 95% confidence intervals.

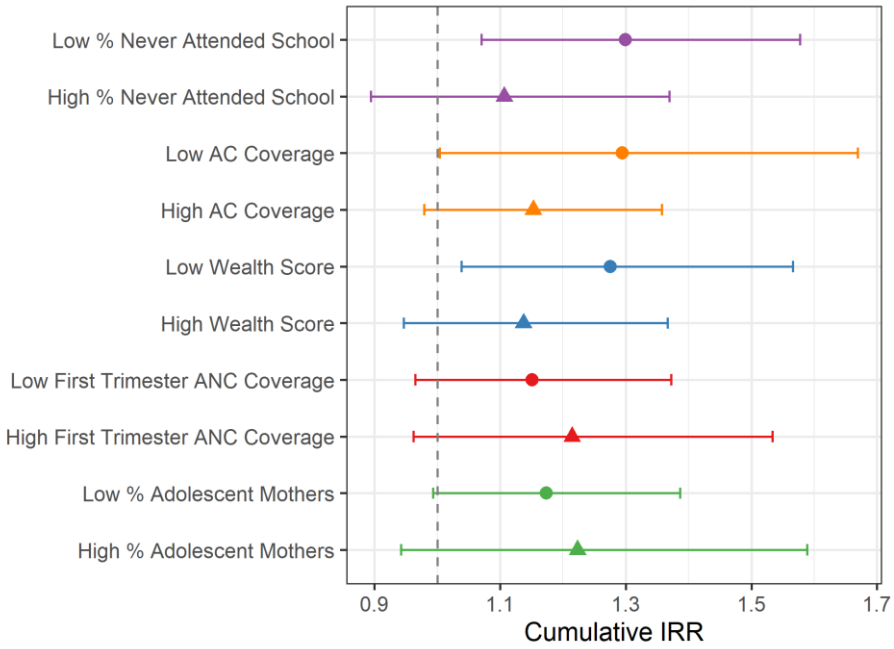

(Source: Own elaboration)

Figure 62 National live births in Togo, 1981–2060, from UN WPP projections (dashed line) and SSP2/SSP5 scenario-specific projections. WPP provides national projections to 2100 (shown for comparison, but not used in future projections). SSP2-4.5 and SSP5-8.5 trajectories diverge after 2021 because they incorporate scenario-specific fertility pathways.

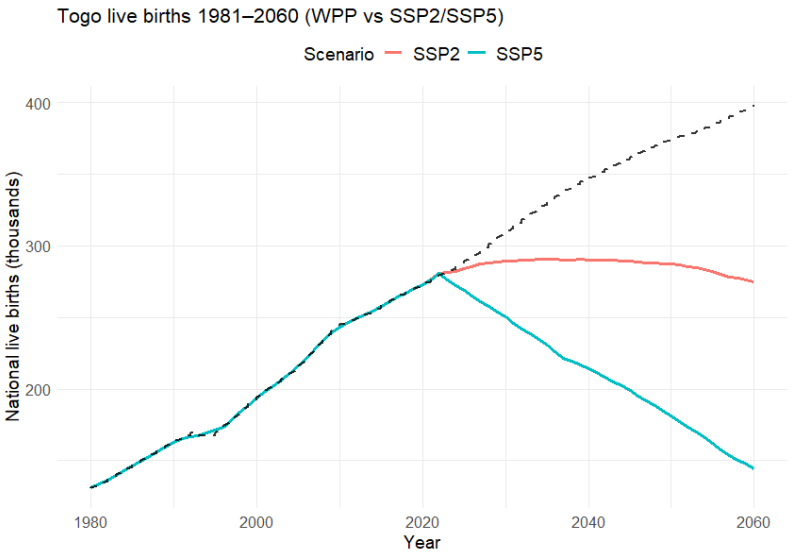

(Source, Own Elaboration)

Figure 63 – Sensitivity analysis: projected change in heatwave-attributable preterm births by region using a global lag-0 heatwave–PTB effect

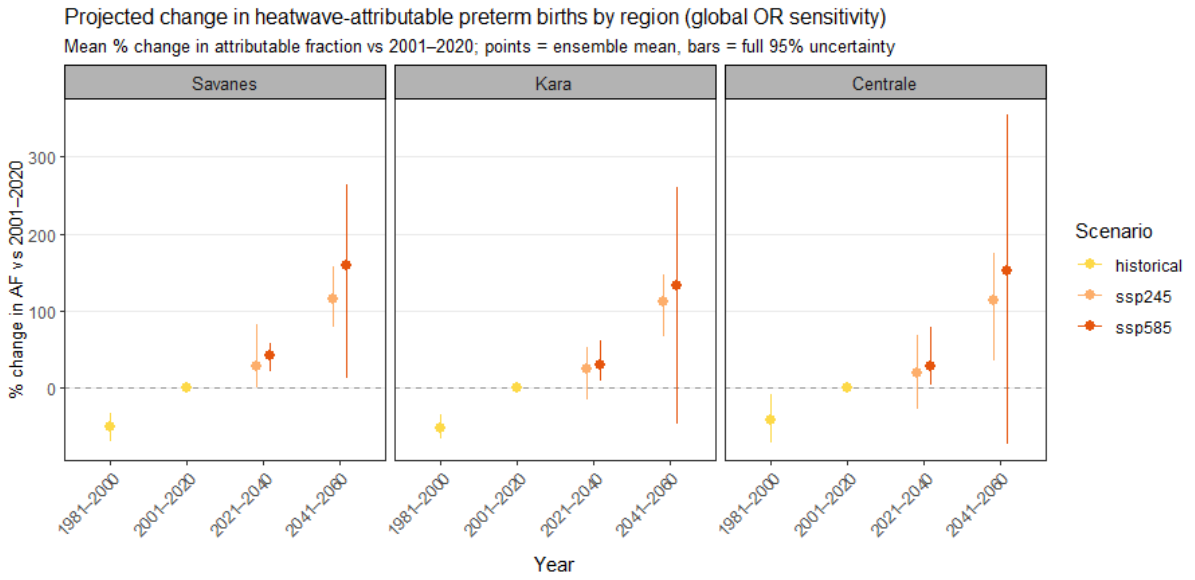

(Source: Own Elaboration)

Figure 64 Sensitivity analysis: mean % change in heatwave-attributable preterm births by prefecture relative to 2001–2020, using a global lag-0 heatwave-PTB effect

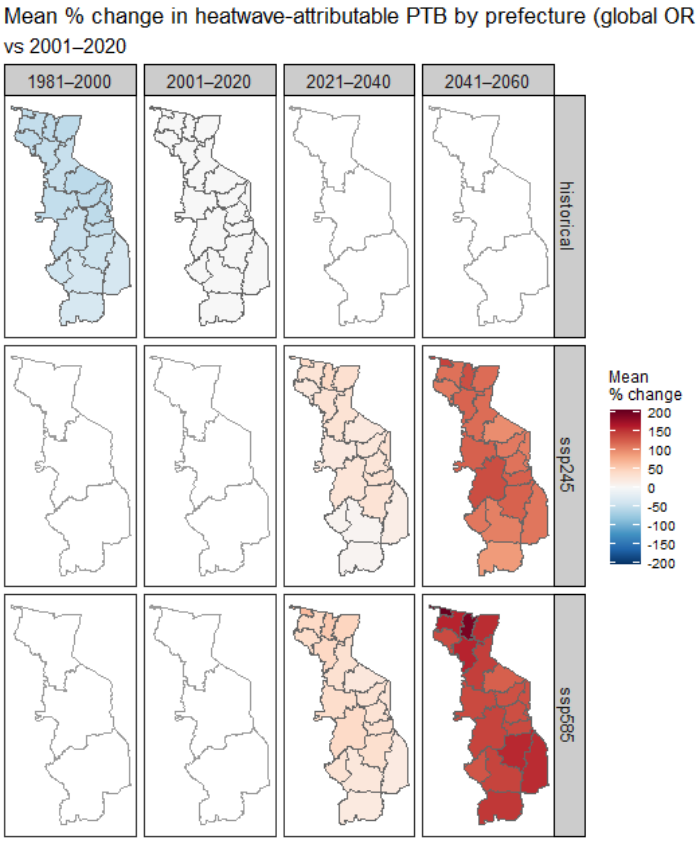

(Source: Own elaboration)

9. Appendix 2

Figure 65 - MSWX trends tests

region_order	var_order	Variable	Region	1981–2000				2001–2024				1981–2024			
				mk_tau	mk_p	sen_slope	change/decad	mk_tau	mk_p	sen_slope	change/decad	mk_tau	mk_p	sen_slope	change/decade
	1	Maximum temperature	Savanes	-0,326	0,048	-0,023	-0,225	0,319	0,031	0,027	0,268	0,249	0,017	0,012	0,122
	2		Kara	-0,158	0,347	-0,016		0,514	0	0,04	0,403	0,347	0,001	0,014	0,135
	3		Centre	-0,105	0,538	-0,006		0,594	0	0,044	0,436	0,459	0	0,022	0,219
	4		Plateaux	-0,074	0,673	-0,004		0,696	0	0,049	0,489	0,552	0	0,026	0,262
	5		Maritime	0,074	0,673	0,007		0,681	0	0,042	0,42	0,619	0	0,027	0,27
	1	Mean temperature	Savanes	-0,032	0,871	-0,002		0,42	0,004	0,027	0,272	0,499	0	0,02	0,199
	2		Kara	0,042	0,82	0,005		0,616	0	0,036	0,361	0,571	0	0,022	0,217
	3		Centre	0,126	0,456	0,005		0,725	0	0,04	0,404	0,63	0	0,025	0,254
	4		Plateaux	0,168	0,315	0,009		0,739	0	0,045	0,445	0,674	0	0,029	0,29
	5		Maritime	0,232	0,163	0,012		0,703	0	0,043	0,426	0,677	0	0,026	0,263
	1	Minimum temperature	Savanes	0,032	0,871	0,002		0,645	0	0,047	0,469	0,579	0	0,028	0,28
	2		Kara	0,158	0,347	0,008		0,739	0	0,052	0,52	0,619	0	0,024	0,243
	3		Centre	0,179	0,284	0,011		0,688	0	0,046	0,46	0,628	0	0,025	0,247
	4		Plateaux	0,253	0,127	0,012		0,623	0	0,044	0,439	0,666	0	0,028	0,28
	5		Maritime	0,326	0,048	0,016	0,159	0,645	0	0,041	0,415	0,693	0	0,029	0,289
	1	Precipitation	Savanes	0,105	0,538	0,009		0,232	0,118	0,017		-0,038	0,723	-0,001	
	2		Kara	0,137	0,417	0,016		0,029	0,862	0,002		-0,285	0,007	-0,011	-0,114
	3		Centre	-0,095	0,581	-0,007		0,087	0,568	0,006		-0,387	0	-0,017	-0,175
	4		Plateaux	-0,147	0,381	-0,02		-0,036	0,823	-0,003		-0,351	0,001	-0,022	-0,217
	5		Maritime	-0,274	0,098	-0,027		-0,036	0,823	-0,002		-0,252	0,017	-0,013	-0,13
	1	Relative Humidity	Savanes	0,284	0,086	0,126		0,225	0,13	0,069		0,349	0,001	0,069	0,691
	2		Kara	0,158	0,347	0,05		-0,232	0,118	-0,101		0,085	0,424	0,019	
	3		Centre	0,042	0,82	0,021		-0,384	0,009	-0,158	-1,581	-0,135	0,199	-0,03	
	4		Plateaux	-0,074	0,673	-0,026		-0,442	0,003	-0,121	-1,207	-0,258	0,014	-0,048	-0,479
	5		Maritime	0,021	0,922	0,003		-0,304	0,04	-0,049	-0,492	-0,18	0,087	-0,018	
	6	Extreme heat days (p95)	Savanes	-0,242	0,144	-0,052		0,362	0,014	0,052	0,522	0,146	0,166	0,014	
	6		Kara	-0,253	0,127	-0,043		0,464	0,002	0,057	0,568	0,036	0,739	0,002	
	6		Centre	-0,084	0,626	-0,031		0,551	0	0,115	1,153	0,228	0,03	0,027	0,274
	6		Plateaux	0,021	0,922	0,004		0,514	0	0,142	1,423	0,338	0,001	0,051	0,507
	6		Maritime	0,189	0,256	0,047		0,587	0	0,184	1,842	0,552	0	0,077	0,77
	7	Extreme precipitation days (p9	Savanes	0,084	0,626	0,009		0,203	0,172	0,011		0,093	0,379	0,003	
	7		Kara	0,211	0,206	0,016		0,203	0,172	0,007		0,017	0,879	0	
	7		Centre	0,179	0,284	0,012		0,065	0,673	0,004		-0,146	0,166	-0,005	
	7		Plateaux	0,021	0,922	0,001		0,232	0,118	0,019		-0,129	0,221	-0,005	
	7		Maritime	-0,242	0,144	-0,036		0,145	0,333	0,017		-0,184	0,08	-0,013	

10. Appendix 3

Figure 66 - NEX trend tests

					2015-2060			
region_order	var_order	Variable	Region	Scenario	mk_tau	mk_p	sen_slope	change/decade
1	1	Maximum temperature	Savanes	ssp245	0,797	0,000	0,038	+0.38 °C per decade
1	1		Savanes	ssp585	0,830	0,000	0,044	+0.44 °C per decade
2	1		Kara	ssp245	0,797	0,000	0,039	+0.39 °C per decade
2	1		Kara	ssp585	0,820	0,000	0,042	+0.42 °C per decade
3	1		Centre	ssp245	0,795	0,000	0,039	+0.39 °C per decade
3	1		Centre	ssp585	0,820	0,000	0,041	+0.41 °C per decade
4	1		Plateaux	ssp245	0,776	0,000	0,036	+0.36 °C per decade
4	1		Plateaux	ssp585	0,809	0,000	0,039	+0.39 °C per decade
5	1		Maritime	ssp245	0,741	0,000	0,032	+0.32 °C per decade
5	1		Maritime	ssp585	0,784	0,000	0,037	+0.37 °C per decade
1	2	Mean temperature	Savanes	ssp245	0,811	0,000	0,037	+0.37 °C per decade
1	2		Savanes	ssp585	0,863	0,000	0,046	+0.46 °C per decade
2	2		Kara	ssp245	0,828	0,000	0,039	+0.39 °C per decade
2	2		Kara	ssp585	0,859	0,000	0,049	+0.49 °C per decade
3	2		Centre	ssp245	0,828	0,000	0,039	+0.39 °C per decade
3	2		Centre	ssp585	0,853	0,000	0,049	+0.49 °C per decade
4	2		Plateaux	ssp245	0,809	0,000	0,037	+0.37 °C per decade
4	2		Plateaux	ssp585	0,845	0,000	0,046	+0.46 °C per decade
5	2		Maritime	ssp245	0,776	0,000	0,032	+0.32 °C per decade
5	2		Maritime	ssp585	0,834	0,000	0,042	+0.42 °C per decade
1	3	Minimum temperature	Savanes	ssp245	0,772	0,000	0,036	+0.36 °C per decade
1	3		Savanes	ssp585	0,836	0,000	0,050	+0.50 °C per decade
2	3		Kara	ssp245	0,814	0,000	0,038	+0.38 °C per decade
2	3		Kara	ssp585	0,851	0,000	0,055	+0.55 °C per decade
3	3		Centre	ssp245	0,809	0,000	0,040	+0.40 °C per decade
3	3		Centre	ssp585	0,867	0,000	0,057	+0.57 °C per decade
4	3		Plateaux	ssp245	0,795	0,000	0,037	+0.37 °C per decade
4	3		Plateaux	ssp585	0,861	0,000	0,053	+0.53 °C per decade
5	3		Maritime	ssp245	0,776	0,000	0,033	+0.33 °C per decade
5	3		Maritime	ssp585	0,855	0,000	0,047	+0.47 °C per decade
1	4	Precipitation	Savanes	ssp245	-0,129	0,211	-0,002	
1	4		Savanes	ssp585	0,028	0,791	0,000	
2	4		Kara	ssp245	-0,300	0,003	-0,006	-0.06 mm/day per decade
2	4		Kara	ssp585	-0,125	0,226	-0,003	
3	4		Centre	ssp245	-0,358	0,000	-0,008	-0.08 mm/day per decade
3	4		Centre	ssp585	-0,212	0,039	-0,005	-0.05 mm/day per decade
4	4		Plateaux	ssp245	-0,370	0,000	-0,008	-0.08 mm/day per decade
4	4		Plateaux	ssp585	-0,397	0,000	-0,008	-0.08 mm/day per decade
5	4		Maritime	ssp245	-0,316	0,002	-0,006	-0.06 mm/day per decade
5	4		Maritime	ssp585	-0,308	0,003	-0,007	-0.07 mm/day per decade
1	5	Relative Humidity	Savanes	ssp245	-0,277	0,007	-0,033	-0.33 % RH per decade
1	5		Savanes	ssp585	0,212	0,039	0,020	+0.20 % RH per decade
2	5		Kara	ssp245	-0,474	0,000	-0,063	-0.63 % RH per decade
2	5		Kara	ssp585	0,038	0,719	0,002	
3	5		Centre	ssp245	-0,544	0,000	-0,066	-0.66 % RH per decade
3	5		Centre	ssp585	-0,146	0,156	-0,013	
4	5		Plateaux	ssp245	-0,623	0,000	-0,056	-0.56 % RH per decade
4	5		Plateaux	ssp585	-0,186	0,069	-0,015	
5	5		Maritime	ssp245	-0,467	0,000	-0,028	-0.28 % RH per decade
5	5		Maritime	ssp585	0,055	0,596	0,004	
1	6	Extreme heat days (p95	Savanes	ssp245	0,669	0,000	0,044	+0.44 days/month per decade
1	6		Savanes	ssp585	0,768	0,000	0,065	+0.65 days/month per decade
2	6		Kara	ssp245	0,686	0,000	0,042	+0.42 days/month per decade
2	6		Kara	ssp585	0,711	0,000	0,061	+0.61 days/month per decade
3	6		Centre	ssp245	0,699	0,000	0,035	+0.35 days/month per decade
3	6		Centre	ssp585	0,662	0,000	0,054	+0.54 days/month per decade
4	6		Plateaux	ssp245	0,585	0,000	0,025	+0.25 days/month per decade
4	6		Plateaux	ssp585	0,623	0,000	0,046	+0.46 days/month per decade
5	6		Maritime	ssp245	0,508	0,000	0,030	+0.30 days/month per decade
5	6		Maritime	ssp585	0,626	0,000	0,054	+0.54 days/month per decade
1	7	Extreme precipitation da	Savanes	ssp245	0,110	0,285	0,001	
1	7		Savanes	ssp585	0,350	0,001	0,004	+0.04 days/month per decade
2	7		Kara	ssp245	-0,008	0,947	0,000	
2	7		Kara	ssp585	0,331	0,001	0,005	+0.05 days/month per decade
3	7		Centre	ssp245	-0,085	0,410	-0,001	
3	7		Centre	ssp585	0,196	0,056	0,003	
4	7		Plateaux	ssp245	-0,085	0,410	-0,001	
4	7		Plateaux	ssp585	0,039	0,712	0,001	
5	7		Maritime	ssp245	-0,009	0,940	0,000	
5	7		Maritime	ssp585	0,082	0,426	0,001	

11. Appendix 4

Figure 67 - Hazard trend tests

region_order	var_order	Disease	Hazard	Region	Scenario	2015-2060 mk_tau	mk_p	Sen	Sen per decade	Change per decade
1	1	Malaria	Malaria transmission season	Savanes	ssp245	-0,212	0,041	-0,001	-0,007	-0.38 weeks per decade
1	1			Savanes	ssp585	-0,103	0,324	0,000	-0,003	
2	1			Kara	ssp245	-0,266	0,010	-0,001	-0,009	-0.46 weeks per decade
2	1			Kara	ssp585	-0,063	0,544	0,000	-0,003	
3	1			Centre	ssp245	-0,228	0,028	-0,001	-0,008	-0.43 weeks per decade
3	1			Centre	ssp585	-0,221	0,033	-0,001	-0,010	-0.5 weeks per decade
4	1			Plateaux	ssp245	-0,288	0,005	-0,001	-0,010	-0.54 weeks per decade
4	1			Plateaux	ssp585	-0,458	0,000	-0,002	-0,021	-1.09 weeks per decade
5	1			Maritime	ssp245	-0,173	0,094	-0,001	-0,009	
5	1			Maritime	ssp585	-0,340	0,001	-0,002	-0,019	-0.98 weeks per decade
1	2	Diarrheal	Extreme precipitation days (p95)	Savanes	ssp245	0,110	0,285	0,001	0,014	
1	2			Savanes	ssp585	0,350	0,001	0,004	0,037	+0.037 days/month per decade
2	2			Kara	ssp245	-0,008	0,947	0,000	0,000	
2	2			Kara	ssp585	0,331	0,001	0,005	0,045	+0.045 days/month per decade
3	2			Centre	ssp245	-0,085	0,410	-0,001	-0,011	
3	2			Centre	ssp585	0,196	0,056	0,003	0,029	
4	2			Plateaux	ssp245	-0,085	0,410	-0,001	-0,014	
4	2			Plateaux	ssp585	0,039	0,712	0,001	0,006	
5	2			Maritime	ssp245	-0,009	0,940	0,000	-0,001	
5	2			Maritime	ssp585	0,082	0,426	0,001	0,012	
1	3		Compound hot-dry days (p95)	Savanes	ssp245	0,431	0,000	0,036	0,363	+0.363 days/month per decade
1	3			Savanes	ssp585	0,442	0,000	0,044	0,439	+0.439 days/month per decade
2	3			Kara	ssp245	0,449	0,000	0,034	0,344	+0.344 days/month per decade
2	3			Kara	ssp585	0,396	0,000	0,036	0,365	+0.365 days/month per decade
3	3			Centre	ssp245	0,430	0,000	0,027	0,274	+0.274 days/month per decade
3	3			Centre	ssp585	0,357	0,000	0,024	0,242	+0.242 days/month per decade
4	3			Plateaux	ssp245	0,239	0,020	0,013	0,127	+0.127 days/month per decade
4	3			Plateaux	ssp585	0,301	0,003	0,013	0,128	+0.128 days/month per decade
5	3			Maritime	ssp245	0,174	0,090	0,009	0,091	
5	3			Maritime	ssp585	0,331	0,001	0,016	0,160	+0.160 days/month per decade
1	4	Preterm Birth	Heatwave days (count)	Savanes	ssp245	0,639	0,000	0,019	0,191	+0.191 events/month per decade
1	4			Savanes	ssp585	0,762	0,000	0,029	0,290	+0.290 events/month per decade
2	4			Kara	ssp245	0,679	0,000	0,018	0,181	+0.181 events/month per decade
2	4			Kara	ssp585	0,717	0,000	0,027	0,269	+0.269 events/month per decade
3	4			Centre	ssp245	0,679	0,000	0,014	0,139	+0.139 events/month per decade
3	4			Centre	ssp585	0,665	0,000	0,022	0,222	+0.222 events/month per decade
4	4			Plateaux	ssp245	0,545	0,000	0,009	0,095	+0.095 events/month per decade
4	4			Plateaux	ssp585	0,610	0,000	0,018	0,179	+0.179 events/month per decade
5	4			Maritime	ssp245	0,485	0,000	0,011	0,105	+0.105 events/month per decade
5	4			Maritime	ssp585	0,618	0,000	0,022	0,219	+0.219 events/month per decade